AN IMAGE GUIDEDADAPTIVE RADIOTHERAPY STRATEGY FOR CERVIX CANCER TREATMENT

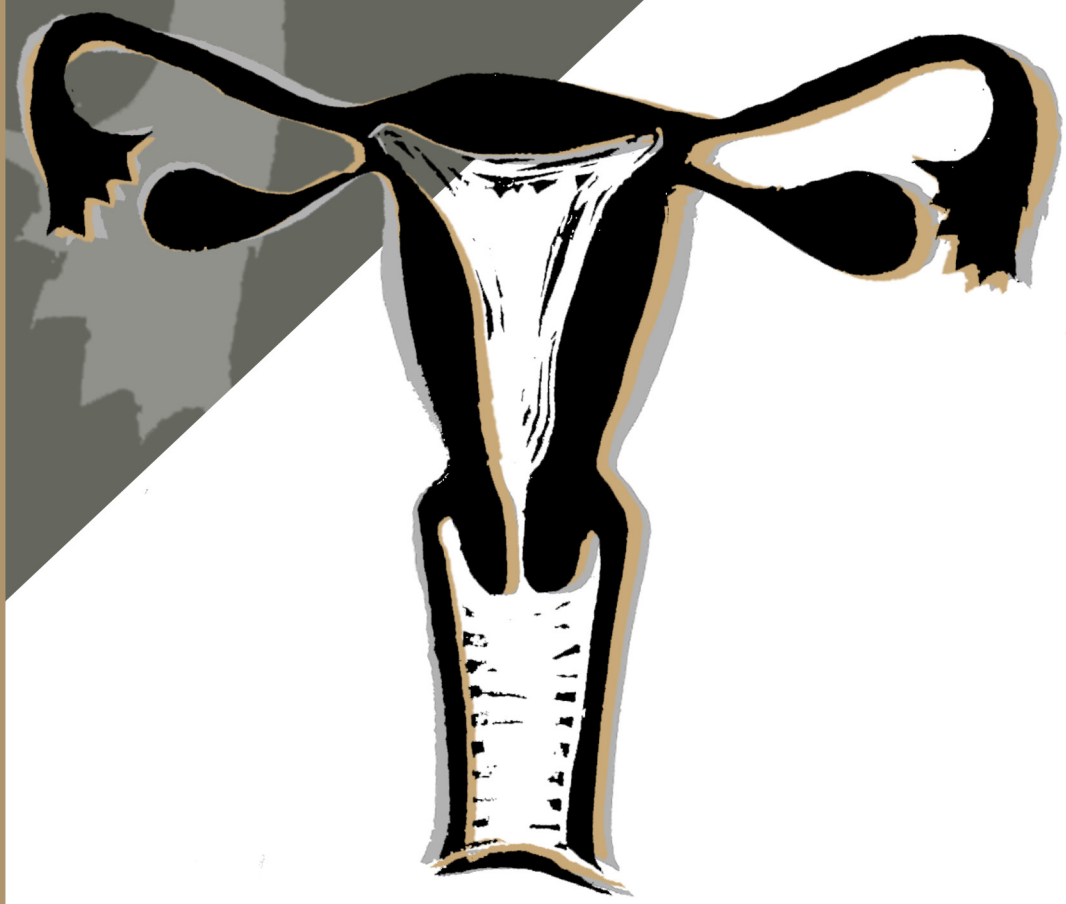

AN IMAGE GUIDED ADAPTIVE RADIOTHERAPY STRATEGY FOR CERVIX CANCER TREATMENT

Based on Equivalent Uniform Dose

FHJ O'REILLY

AN IMAGE GUIDED ADAPTIVE RADIOTHERAPY STRATEGY FOR CERVIX CANCER TREATMENT BASED ON EQUIVALENT UNIFORM DOSE

BY

Frederika Hendrika Jacoba O'Reilly

Thesis submitted to comply with the requirements for the Ph.D. (Medical Physics) degree in the Faculty of Health Sciences at the University of the Free State

Promoter: Dr. W Shaw

Co-Promoter: Dr. FCP du Plessis

Department of Medical Physics

November 2021

DECLARATION

AUTHOR: Frederika Hendrika Jacoba O'Reilly

DEGREE: PhD

TITLE: AN IMAGE GUIDED ADAPTIVE RADIOTHERAPY STRATEGY FOR CERVIX CANCER TREATMENT BASED ON EQUIVALENT UNIFORM DOSE

Submission date: 30 November 2021

I, Frederika O'Reilly, declare that the thesis that I herewith submit for the Doctoral Degree in Medical Physics at the University of the Free State, is my independent effort and had not previously been submitted for a degree at another University/faculty.

TABLE OF CONTENTS

Glossary

3DCRT - 3-dimensional conformal radiotherapy

ART - adaptive radiotherapy

BT - brachytherapy

CIL – common iliac left

CIR – common iliac right

CTV - clinical target volume

CT - computed tomography

CBCT - cone beam CT

CoVP – coverage probability planning

DIR - deformable image registration

DVH – dose volume histogram

EB – empty bladder

EBRT - external beam radiotherapy

EIL - external iliac left

EIR - external iliac right

FB – full bladder

FIGO - International Federation of Gynecology and Obstetrics

FDG-PET/CT - fluorodeoxyglucose positron computed tomography

FM – fixed margins

HR-CTV - High-Risk Clinical Target Volume

HPV - high-risk human papillomavirus

HIV - human immunodeficiency virus

IGABT - image-guided adaptive brachytherapy

IIL – internal iliac left

IIR – internal iliac right

IMRT - intensity-modulated radiotherapy

ITV - Internal target volume

LACC - locally advanced cervical cancer

LMIC - low-middle-income country

MRI - magnetic resonance imaging

MVCB – megavolt cone beam

MOD – margin of the day

MC - Monte Carlo

MRgART - MR-guided adaptive radiotherapy

nCTV - nodal CTV

OAR – Organs at risk

OBTL – obturator left

OBTR – obturator right

OP - occupancy probability

PRV - Planning organ at risk volumes

PTV - planning target volume

POTD - plan-of-the-day

PreSac - presacral

pCTV - primary CTV

QA - quality assurance

ICRU - The International Commission on Radiation Units and Measurements

TPS - treatment planning system

VOI - volume of interest

VMAT - volumetric-modulated arc therapy

Abstract

Aim: This study aims to develop an image-guided adaptive strategy to compensate for temporal effects of tumour shrinkage and organ motion in cervix cancer treatment based on the equivalent uniform dose (EUD). The strategy should be flexible enough to retain a minimum workload system.

Materials and Methods: Patients receiving radical radiotherapy treatment for cervix cancer with daily pre-treatment CBCT imaging were included in this retrospective study. A thorough investigation of bladder volume variation and its influence on primary and nodal tumor motion using both empty and full bladder protocols during cervix cancer RT was performed. 6 treatment strategies; fixed margins (7, 10, 15, and 20 mm), offline and online adaptive ART strategies, an ITV approach, variable margin (VBM) and coverage probability (CoVP) strategy were simulated for both groups. Planning strategies were scored based on the equivalent uniform and dose volume histogram parameters.

Results and Discussion: Although empty bladder volumes were more reproducible no significant difference in movement between EB and FB patients was observed. Our study confirmed dosimetric advantages in bladder and small bowel sparing when a full bladder protocol is used. Occupancy probability maps were used to quantify primary and nodal movement. The best target coverage and OAR sparing were seen when online and offline adaptive strategies were used. Fixed margins <10 mm caused underdosages in most patients. Although adequate target coverage was noted for the ITV and VBM strategy, OAR sparing was inferior. CovP planning resulted in dosimetric outcomes similar and even better than the online strategy.

Conclusion: Considering bladder volume reproducibility and protocol executability, an empty bladder protocol appears simpler in our department. However, variations in target shape and position cannot be attributed to bladder filling alone. The EUD can be used as a quick and reliable way of scoring treatment plans. Based on EUD metrics this study demonstrated that a personalized on-line adaptive strategy is most effective to account for target motion and deformation, yielding sufficient target coverage with adequate OAR sparing.

Keywords: Image guided adaptive radiotherapy, equivalent uniform dose, cervical cancer, external beam radiotherapy, treatment planning, coverage probability.

Chapter 1: Introduction

1.1 Background

1.1.1 Global cervical cancer burden

Tears and tribulations. Two emotions that we associate with the word cancer daily. Even more severe is the plight of women in low and middle-income countries when it comes to the dire situation regarding cervical cancer. It is the second most common female cancer worldwide with approximately 90% of deaths occurring in low- and middle-income countries [1]. By 2030 the number of new cancer cases is expected to increase more than 80% in low-income countries, double the rate expected in high-income countries [2]. In developed countries, preventative measures such as effective screening and vaccination programs enabling early diagnosis and treatment are in place increasing the inequality in burden between women in these countries in contrast to women in resource-limited settings.

The link between high-risk human papillomavirus (HPV) and cervical carcinoma has become well established and more than 99% of pre-cancerous lesions and cervical carcinomas can be attributed to HPV [3,4]. Effective screening permits the early detection and treatment of pre-cancerous lesions which can prevent up to 80% of cervical cancers. Limited accessibility to preventative measures and the increased burden of untreated human immunodeficiency virus (HIV) infections in developing countries makes the diagnosis of cervical cancer challenging and cause late-stage disease, which requires treatment such as surgery, radiotherapy, and chemotherapy.

1.1.2 Treatment options for cervical cancer

Radiotherapy remains the cornerstone for the treatment of cervical cancer. The choice for treatment of cervical cancer depends on the stage of the disease. Early-stage cervical cancer such as the International Federation of Gynecology and Obstetrics (FIGO) stage IB-IIA can be treated with radical surgery or radiotherapy with no difference in effectiveness [5]. The

standard treatment for locally advanced cervical cancer is generally a combined modality approach of radiotherapy and chemotherapy yielding an increase of 6% overall and disease-free survival at 10 years post-treatment [6,7]. Typical dose prescriptions range from 45 Gy in 25 fractions once daily to 50.4 Gy in 28 fractions or 50 Gy in 25 fractions for advanced-stage disease. A local control rate, even in advanced disease, of >90-95% is achievable when external beam radiotherapy (EBRT) and chemotherapy are combined with image-guided adaptive brachytherapy (IGABT). Using the combined treatment approach of brachytherapy (BT) and EBRT has been associated with improved treatment outcomes. A local failure rate of 48% was found when doses of up to 70 Gy were delivered using only EBRT techniques.[8] Utilizing brachytherapy (BT) ensures that the main tumor can be boosted with doses > 80Gy while maintaining OAR tolerances especially in smaller tumor volumes and symmetric disease.[9, 10]

1.2 External beam Radiotherapy (EBRT)

1.2.1 Evolution of radiotherapy

In the last three decades, significant advances in EBRT techniques have been seen, allowing definitive radiation delivery to the target while minimizing dose to surrounding organs at risk (OARs). The advent of volumetric imaging has enabled a shift from 2-dimensional (2D) to 3-dimensional conformal radiotherapy (3DCRT) techniques. The next generation of 3DCRT, intensity-modulated radiotherapy (IMRT) and volumetric-modulated arc therapy (VMAT), allowed even higher conformal treatment delivery. In addition, VMAT offers several advantages including faster treatment time, fewer monitor units, and dosimetric advantages for the rectum V40 (volume of the rectum receiving 40 Gy) [11]. These high-precision techniques offer greater tumoricidal dose while minimizing treatment-related toxicities [12,13,14,15]. Published and active prospective trials involving advanced radiation therapy techniques in cervical cancer including; TIME-C[16], PARCER[17], INTERTECC[18] , and EMBRACE II[19] found significant improvement in gastrointestinal, genitourinary, and hematological toxicities. The benefits of IMRT are however strongly diminished using large population-based margins that account for treatment uncertainties[20–23]. Currently, no data are confirming that IMRT improves disease-specific survival or overall survival over 2D/3D techniques. Therefore, care must be taken to account for and reduce treatment uncertainties to maximize clinical

outcome[24]. The key in EBRT improvement lies in the development of strategies and techniques to reduce large margins and therefore acute and late toxicities, while still delivering a tumoricidal dose. Image-guided radiotherapy (IGRT) is a vital tool to minimize treatment uncertainties, avoid geometrical misses and reduce treatment margins.

1.2.2 Image-guided Radiotherapy (IGRT)

In the era of modern targeted radiotherapy, geometrical accuracy is critical for the safe application of highly conformal techniques. Before the start of treatment, imaging plays an integral part in the diagnosis, prognosis, and assessment of biological properties of tumours and healthy tissues aiding in the decision making of a suitable treatment strategy. Computed tomography (CT), magnetic resonance imaging (MRI), and fluorodeoxyglucose positron computed tomography (FDG-PET/CT) are generally the imaging modalities of choice during pre-treatment evaluation with regards to staging and treatment planning [25,26]. MRI provides the best soft tissue discrimination within the pelvis and is considered the golden standard for determining soft tissue and parametrial invasion in advanced stages of cervical cancer [27]. PET/CT is recommended for the assessment of nodal involvement as well as distant metastases and adds additional information regarding physiological movement and biological characteristics of tumours [28]. A CT scan with the patient immobilized in the treatment position is generally used for delineation of tumour volumes and treatment planning. Despite advanced radiotherapy techniques, geometric uncertainties persist with delineation most arguably the largest [29,30]. Registering MRI images to planning the CT scan offers high spatial resolution, high sensitivity to detect all involved tissues, and high specificity to spare surrounding normal tissues. Combining these imaging modalities ensures an accurate definition of the target volume and a reduction in delineation uncertainty[31].

Correct positioning of the patient at the time of treatment is an integral part of the radiotherapy process for the safe delivery of treatment to the intended target. Various technologies for online 2D/3D imaging such as kV x-ray, cone beam CT (CBCT), or megavolt (MVCB) are currently used for in-room image guidance. On-board images are fused with planning images to quantify and correct set-up errors and assess organ motion and deformation [19,32]. IGRT techniques using CBCT images registered to bone are effective to minimize and correct translational shifts but are limited with regards to increased image noise

and soft tissue visualization [33,34]. Additionally, it poses an extra dose burden increasing the risk of both deterministic effects to organs at risk (OARs) and stochastic effects [35]. Although MRI has been the recommended imaging modality in brachytherapy, CBCT is still routinely used in RT for cervical cancer. The potential of MRI in the EBRT part of treatment, not only for delineation but also for image-guidance, is undeniable and confirmed by the excellent results that have been achieved in brachytherapy through MR-guidance [36,37]. The uterus and cervix are prone to large inter-and intrafraction motion and tumour regression of up to 60-80% can be expected for cervical cancer. The superior soft tissue contrast of MR-guided radiotherapy (MRgRT) can be exploited to accurately detect these large and complex movements as well as tumour shrinkage with the potential to reduce toxicity and escalate dose to the target volume [27,33,38]. Hybrid MR-linear accelerator systems offer onboard real-time visualization of both geometric and anatomical changes on an intra- and inter-fraction basis making it the most suitable imaging modality for RT. This imaging information can be used to quantify changes occurring between- and within a treatment fraction and reoptimize the treatment plan accordingly [39,40].

1.2.3 Image-guided Adaptive Radiotherapy (IGART)

Traditionally margins are added to the clinical target volume (CTV) to account for uncertainties as a result of set-up errors, organ motion, and deformation. Margins of up to 3 cm are necessary to account for the large, complex, and patient-specific cervix-uterus movements [41,42]. The benefit of high-precision techniques such as IMRT is diminished using such large margins. Yan et al.[43] proposed adaptive radiotherapy (ART) to maintain the therapeutic window in the presence of anatomical changes. An imaging feedback loop is used to adapt a plan to patient-specific changes unaccounted for in the initial plan. ART can be used to address systematic (weight, tumor, and organ geometric and biological response) and random (bladder filling, peristaltic motion, and respiration) anatomical changes occurring over various time scales ranging from seconds to minutes to days [39,40]. Adaptation approaches can be separated into offline, online, and real-time strategies. Offline ART occurs between treatment fractions and mostly addresses systematic changes occurring during treatment. Random changes occurring over a shorter period such as daily variation of organ motion can be accounted for through online adaptation performed before each treatment

fraction. Therefore, both systematic and random changes can be accounted for through online adaptation but it comes at the cost of increased workload, imaging, and dose to the patient [44]. Variations that occur within a treatment fraction can be accounted for by real-time ART. MR-guided adaptive radiotherapy (MRgART) is a clinically feasible option for implementation of daily online re-planning using imaging with superior soft tissue contrast with no extra dose to the patient [45–48]. Due to the substantial organ motion in the pelvis and significant regression of cervical cancer, ART offers a promising outcome for these patients [27,38].

Most linear accelerators are equipped with a CBCT system which is sufficient for the implementation of off- and online adaptive strategies. A plan-of-the-day (POTD) strategy is considered a more feasible online ART approach. This approach is based on a plan selection strategy from a library of plans obtained before treatment to account for expected anatomical changes such as bladder filling [19,38,49,50]. Triggered adaptation refers to plan re-optimization based on a certain threshold being exceeded. Adapting a plan due to significant weight loss is an example of geometrically triggered offline adaptation. Plan adaptation can also be triggered by dosimetrically significant anatomical changes guided by imaging [51]. Imaging a patient before or during each treatment fraction allows for the correction of both systematic and random anatomical changes. However, online adaptation is still challenging because it requires superior image quality, robust algorithms to perform automatic delineation, rapid re-planning, plan review, and patient-specific quality assurance which makes it resource and time intensive [38,52]. ART has benefits but these need to be balanced with workflow and efficiency. The dosimetric benefit in patients with limited motion may not be worth the increased clinical effort.

1.3 Uncertainties in Radiotherapy

To fully realize the potential of high precision treatment techniques, uncertainties during treatment delivery must be compensated for. The first step in implementing any form of conformal treatment should be to determine these uncertainties preferably with data from the treating institution [22,29,30]. Uncertainties consist of patient setup errors (external), inter- and intra-fraction organ motion (internal), and target delineation. Generally, uncertainties are divided into systematic (same for each fraction of the treatment) and random errors (vary

from day to day). Setup errors and organ motion both have a systematic as well as a random component, while delineation errors are purely systematic [53–55].

1.3.1 Patient setup and organ motion

The International Commission on Radiation Units and Measurements (ICRU) recommends in reports 62 and 83 [56,57] that the clinical target volume (CTV) should be expanded with a safety margin to generate a planning target volume (PTV) to account for both internal and external uncertainties. The selection of margin size is a trade-off between maintaining target coverage and minimizing dose to surrounding normal tissues [58]. These safety margins can be reduced through IGRT which can be used either in an off-line or online approach. Systematic errors can be reduced to negligible values using off-line strategies (corrections between treatment fractions) while random errors require online techniques (corrections at each treatment fraction) [39,43,55].

Patient setup errors can be reduced through the use of rigid immobilization devices and setup protocols. Setup errors can be quantified and corrected by registering daily images, acquired with the patient in the treatment position, to the planning scans. Couch corrections can be performed to correct translational errors. However, rotational setup errors cannot be corrected for with most couches only able to correct one degree of these rotational movements [59]. Methods to correct for rotational errors include gantry and collimator rotations as well as the implementation of 6D repositioning devices.

Internal organ motion and tumour regression throughout treatment is a major source of uncertainty in cervical cancer. Movements are patient-specific and complex since the CTV consist of multiple structures that can move independently [19,60]. In addition to the filling status of the bladder and rectum which will influence the position and shape of the CTV, tumour regression will also cause anatomical variations. The ICRU 62 [57] recommends the use of an internal margin (IM) to account for organ motion. Inter- and intrafractional tumour and organ movement have been investigated by several groups and showed significant movement in the order of centimeters [60–62]. Quantification of these positional variations through the use of image guidance is essential in the determination of appropriate internal margins [63].

1.3.2 Delineation errors

Currently, tumour delineation is the weakest link in the delivery of accurate and precise RT. Delineation errors will affect each treatment fraction in the same way which can potentially cause a geometric miss leading to lower control rates and increased morbidity for patients [29,39,54]. Considerable interobserver variability, especially for EBRT, was described for cervical carcinoma with the largest differences in caudal and cranial CTV borders due to the inclusion of specific nodal regions [54]. Eminowicz et al. reported significant under dosages especially in the vagina, obturator, and external iliac nodes [64]. The use of different imaging modalities such as MRI and FDG-PET CT and image co-registration can be used to reduce uncertainties. Consensus guidelines and training of staff should be implemented to further reduce contouring uncertainties [65,66].

1.3.3 Error compensation

1.3.3.1 CTV-PTV margins

Defining an appropriate margin is likely the most difficult task in the IGRT process. Isotropic margins ranging from 15 – 21 mm and anisotropic margins up to 32 mm, 20 mm, and 17 mm in the anterior-posterior direction, superior-inferior, and lateral directions have been proposed in literature [22,67]. Several margin recipes accounting for systematic and random errors have been proposed in literature of which the most commonly used are the recipe derived by van Herck et al. [68]. This margin assures 90% of patients in the population will receive a minimum cumulative CTV dose of at least 95% of the prescribed dose (2.5 times the total standard deviation (SD) of the systematic error (Σ) plus 0.7 times the total SD of the random error (σ)). Stroom et al. [55] derived a margin based on coverage probability ensuring 99% of the target volume receives 95% of the prescribed dose or more ($2\Sigma + 0.7\sigma$) [29]. Because margin recipes are based on the standard deviation of errors estimated for the population the majority of patients will benefit from such an approach. However individuals, for example, patients with significant organ motion, may be penalized in terms of either under dosage of the target or collateral dose burden to critical organs [69].

Margin sizes are usually linked to the level of IGRT utilized. Daily online position verification and couch correction to reduce setup errors warrants the use of standard population-based

margins for the CTV. A margin reduction from 10 mm to 5 mm can be made for the elective nodal target volume when daily imaging, bony fusion, and couch corrections are performed [19]. Variable bladder filling scans acquired before the start of treatment are used to quantify patient-specific organ motion to determine individualized margins based on internal target motion. Daily CBCTs can further be used to exploit the benefits of individualized adaptive strategies.

1.3.3.2 Margin-less planning

Although margins ensure adequate target coverage, the PTV usually overlaps with nearby critical structures forcing the planner to compromise between maximizing target dose while minimizing OAR dose. Planning organ at risk volumes (PRVs) are used to compensate for uncertainties in OAR movement during treatment and may be useful in optimizing treatment plans [57,70]. However, the use of PRVs increases the overlap region even further. To overcome these problems numerous approaches incorporating the uncertainties into the optimization process have been suggested [69,71–73]. The distribution of uncertainties can be obtained from population statistics or multiple image instances. Probabilities are assigned to a volume indicating the likelihood of finding the target or OAR in that position. These occupancy maps represent organ motion and replace the need for static margins [74].

1.4 Planning strategies

Several strategies have been proposed to account for the substantial organ movement in the pelvic region. Organ motion is complex and patient-specific indicating the need to move away from large population-based margins and customize treatment for an individual patient. Individualizing treatment using pre-treatment image sets to define an internal target volume (ITV) is proposed as a relatively simple solution to reduce to risk of CTV under dosage [75]. In many of these approaches, a single treatment plan is used for the entire treatment ignoring anatomical changes taking place throughout treatment. Adaptive treatment strategies seek to account for these changes occurring on different time scales from seconds for cardiac motion, minutes for bladder-filling, and weeks for treatment-related changes like weight loss [39,76]. Although online strategies are the most efficient way to correct both systematic and random errors, the infrastructure necessary (computing power for fast re-planning and

quality assurance (QA)) to successfully implement these strategies is still a limitation [77]. A plan of the day approach is possibly the easiest to implement consisting of plans generated from either a single CT scan, a series of pre-treatment scans, or from CBCTs acquired during the first few treatment fractions. Offline strategies can only correct for slowly varying or systematic changes but are the most feasible option regarding current infrastructure in many treating institutions.

Online ART takes place with the patient in the treatment position and should be incorporated flawlessly into the current workflow not to prolong treatment times and consequently increase associated uncertainties. Automation of the most important steps namely re-contouring, re-planning, and QA will reduce overall implementation time as well as associated workload. Deformable image registration (DIR) is one solution frequently used in this context. Contours are propagated from the original plan which reduces the time necessary to delineate structures daily. Through the use of deformation fields dose distributions from different geometries can be warped back to the reference geometry enabling fractional dose accumulation [40]. Sobotta et al. [78] emphasized the uncertainties related to dose accumulation with deformation fields. They demonstrated the usefulness of the equivalent uniform dose (EUD) as a metric for quick scoring of treatment plans.

1.4.1 Equivalent uniform dose (EUD)

A uniform and non-uniform dose distribution are considered equivalent when they cause the same radiobiological effect [79,80]. Niemierko introduced the EUD for tumours and later extended it to a generalized EUD concept to apply to normal tissues as well [79,81]. The EUD can be used to determine the combined effect of dose distributions in different geometries yielding a worst-case scenario without the need for DIR. Lower boundaries for targets and upper boundaries for organs at risk can be computed to score a treatment plan at the fraction of the cost of full analysis [82].

1.5 Aim

This retrospective planning study aims to develop an image-guided adaptive strategy to compensate for temporal effects of tumour shrinkage and organ motion in cervix cancer treatment based on the equivalent uniform dose. The strategy should be flexible enough to retain a minimum workload system.

1.6 References

1. WHO | Cervical cancer. *WHO* (2018).
2. WHO | Key statistics. https://www.who.int/cancer/resources/keyfacts/en/.
3. Bedell, S. L., Goldstein, L. S., Goldstein, A. R. & Goldstein, A. T. Cervical Cancer Screening : Past , Present , and Future. *Sex. Med. Rev.* (2019) doi:10.1016/j.sxmr.2019.09.005.
4. Mundt, A. J. *et al.* Intensity-modulated whole pelvic radiotherapy in women with gynecologic malignancies1. *Int. J. Radiat. Oncol.* **52**, 1330–1337 (2002).
5. Landoni, F. *et al.* Randomised study of radical surgery versus radiotherapy for stage Ib-IIa cervical cancer. **350**, (1997).
6. Kirwan, J. M. *et al.* A systematic review of acute and late toxicity of concomitant chemoradiation for cervical cancer. *Radiother. Oncol.* **68**, 217–226 (2003).
7. O 'reilly, F. H. J. & Shaw, W. A dosimetric evaluation of IGART strategies for cervix cancer treatment. *Phys. Medica* **32**, 1360–1367 (2016).
8. Tanderup, K. *et al.* Adaptive Management of Cervical Cancer Radiotherapy. *Semin. Radiat. Oncol.* **20**, 121–129 (2010).
9. Karlsson, J., Dreifaldt, A.-C., Mordhorst, L. B. & Sorbe, B. Differences in outcome for cervical cancer patients treated with or without brachytherapy. *Brachytherapy* **16**, 133–140 (2017).
10. Gill, B. S. *et al.* National cancer data base analysis of radiation therapy consolidation modality for cervical cancer: The impact of new technological advancements. *Int. J. Radiat. Oncol. Biol. Phys.* **90**, 1083–1090 (2014).
11. Bai, W. *et al.* Dosimetric comparison of volumetric-modulated arc therapy and intensity-modulated radiation therapy in patients with cervical cancer: a meta-analysis. *Onco. Targets. Ther.* **11**, 7179 (2018).
12. Chan, P. *et al.* Inter- and Intrafractional Tumor and Organ Movement in Patients With Cervical Cancer Undergoing Radiotherapy: A Cinematic-MRI Point-of-Interest Study. *Int. J. Radiat. Oncol. Biol. Phys.* **70**, 1507–1515 (2008).
13. Roeske, J. C., Bonta, D., Mell, L. K., Lujan, A. E. & Mundt, A. J. A dosimetric analysis of acute gastrointestinal toxicity in women receiving intensity-modulated whole-pelvic radiation therapy. *Radiother Oncol* **69**, 201–207 (2003).

14. Portelance, L., Chao, K. S., Grigsby, P. W., Bennet, H. & Low, D. Intensity-modulated radiation therapy ({IMRT}) reduces small bowel, rectum, and bladder doses in patients with cervical cancer receiving pelvic and para-aortic irradiation. *Int. J. Radiat. Oncol. Biol. Phys.* **51**, 261–266 (2001).
15. Oh, C. E., Antes, K., Darby, M., Song, S. & Starkschall, G. Comparison of 2D conventional, 3D conformal, and intensity-modulated treatment planning techniques for patients with prostate cancer with regard to target-dose homogeneity and dose to critical, uninvolved structures. *Med. Dosim.* **24**, 255–263 (1999).
16. Klopp, A. H. *et al.* Patient-Reported Toxicity During Pelvic Intensity-Modulated Radiation Therapy: NRG Oncology–RTOG 1203. *J. Clin. Oncol.* **36**, 2538 (2018).
17. Chopra, S. *et al.* Late Toxicity After Adjuvant Conventional Radiation Versus Image-Guided Intensity-Modulated Radiotherapy for Cervical Cancer (PARCER): A Randomized Controlled Trial. *https://doi.org/10.1200/JCO.20.02530* JCO.20.02530 (2021) doi:10.1200/JCO.20.02530.
18. Huang, J., Gu, F., Ji, T., Zhao, J. & Li, G. Pelvic bone marrow sparing intensity modulated radiotherapy reduces the incidence of the hematologic toxicity of patients with cervical cancer receiving concurrent chemoradiotherapy: a single-center prospective randomized controlled trial. doi:10.1186/s13014-020-01606-3.
19. Pötter, R. *et al.* The EMBRACE II study: The outcome and prospect of two decades of evolution within the GEC-ESTRO GYN working group and the EMBRACE studies. *Clin. Transl. Radiat. Oncol.* **9**, 48–60 (2018).
20. Ahmad, R. *et al.* A margin-of-the-day online adaptive intensity-modulated radiotherapy strategy for cervical cancer provides superior treatment accuracy compared to clinically recommended margins: {A} dosimetric evaluation. *Acta Oncol* **52**, 1430–1436 (2013).
21. van de Bunt, L. *et al.* Motion and deformation of the target volumes during {IMRT} for cervical cancer: {What} margins do we need? *Radiother. Oncol.* **88**, 233–240 (2008).
22. Jadon, R. *et al.* A {Systematic} {Review} of {Organ} {Motion} and {Image}-guided {Strategies} in {External} {Beam} {Radiotherapy} for {Cervical} {Cancer}. *Clin. Oncol.* **26**, 185–196 (2014).
23. Jensen, N. B. K. *et al.* Cone beam computed tomography-based monitoring and management of target and organ motion during external beam radiotherapy in cervical

cancer. *Phys. Imaging Radiat. Oncol.* **9**, 14–20 (2018).

24. Chino, J. *et al.* Radiation Therapy for Cervical Cancer: Executive Summary of an ASTRO Clinical Practice Guideline. *Pract. Radiat. Oncol.* **10**, 220–234 (2020).
25. Kaidar-Person, O. *et al.* The role of imaging in the management of non-metastatic cervical cancer. *Med Oncol* **29**, 3389–3393 (2012).
26. Webster, A., Appelt, A. L. & Eminowicz, G. Image-Guided Radiotherapy for Pelvic Cancers : A Review of Current Evidence and Clinical Utilisation. *Clin. Oncol.* **32**, 805–816 (2020).
27. Tanderup, K. *et al.* Adaptive {Management} of {Cervical} {Cancer} {Radiotherapy}. *Semin. Radiat. Oncol.* **20**, 121–129 (2010).
28. Kusmirek, J. *et al.* PET/CT and MRI in the imaging assessment of cervical cancer. *Abdom. Imaging* **40**, 2486–2511 (2015).
29. van Herk, M. Errors and margins in radiotherapy. *Semin. Radiat. Oncol.* **14**, 52–64 (2004).
30. Bernstein, D. *et al.* An Inter-observer Study to Determine Radiotherapy Planning Target Volumes for Recurrent Gynaecological Cancer Comparing Magnetic Resonance Imaging Only With Computed Tomography-Magnetic Resonance Imaging. *Clin. Oncol.* **33**, 307–313 (2021).
31. Fonti, R., Conson, M. & Del Vecchio, S. PET/CT in radiation oncology. *Semin. Oncol.* **46**, 202–209 (2019).
32. De Los Santos, J. *et al.* Image guided radiation therapy (IGRT) technologies for radiation therapy localization and delivery. *Int. J. Radiat. Oncol. Biol. Phys.* **87**, 33–45 (2013).
33. Corradini, S. *et al.* MR-guidance in clinical reality: Current treatment challenges and future perspectives. *Radiat. Oncol.* **14**, 1–12 (2019).
34. Pollard, J. M., Wen, Z., Sadagopan, R., Wang, J. & Ibbott, G. S. The future of image-guided radiotherapy will be MR guided. *Br. J. Radiol.* **90**, (2017).
35. Stock, M., Palm, A., Altendorfer, A., Steiner, E. & Georg, D. {IGRT} induced dose burden for a variety of imaging protocols at two different anatomical sites. *Radiother. Oncol.* **102**, 355–363 (2012).
36. Pötter, R. *et al.* Clinical outcome of protocol based image ({MRI}) guided adaptive brachytherapy combined with 3D conformal radiotherapy with or without chemotherapy in patients with locally advanced cervical cancer. *Radiother Oncol* **100**,

116–123 (2011).

37. Tanderup, K. *et al.* Image Guided Adaptive Brachytherapy in cervix cancer: A new paradigm changing clinical practice and outcome. *Radiother. Oncol.* **120**, 365–369 (2016).
38. Buschmann, M. *et al.* Image guided adaptive external beam radiation therapy for cervix cancer: Evaluation of a clinically implemented plan-of-the-day technique. *Z. Med. Phys.* **28**, 184–195 (2018).
39. Sonke, J. J., Aznar, M. & Rasch, C. Adaptive Radiotherapy for Anatomical Changes. *Seminars in Radiation Oncology* vol. 29 245–257 (2019).
40. Glide-hurst, C. K. *et al.* Adaptive Radiation Therapy (ART) Strategies and Technical Considerations : A State of the ART Review From NRG Oncology. *Radiat. Oncol. Biol.* **109**, 1054–1075 (2020).
41. Tyagi, N. *et al.* Daily {Online} {Cone} {Beam} {Computed} {Tomography} to {Assess} {Interfractional} {Motion} in {Patients} {With} {Intact} {Cervical} {Cancer}. *Int. J. Radiat. Oncol.* **80**, 273–280 (2011).
42. Eminowicz, G., Rompokos, V., Stacey, C., Hall, L. & Mccormack, M. Understanding the impact of pelvic organ motion on dose delivered to target volumes during IMRT for cervical cancer. *Radiother. Oncol.* **122**, 116–121 (2017).
43. Yan, D., Vicini, F., Wong, J. & Martinez, A. Adaptive radiation therapy. *Phys Med Biol* **42**, 123–132 (1997).
44. Baum, C., Alber, M. & Nüsslin, F. [{Dosimetric} consequences of the application of a rectum hull-planning volume for treatment planning of intensity modulated radiotherapy of prostate cancer]. *Z Med Phys* **16**, 208–216 (2006).
45. Cree, A. *et al.* The Potential Value of MRI in External-Beam Radiotherapy for Cervical Cancer. *Clin. Oncol.* **30**, 737–750 (2018).
46. Intven, M. P. W. *et al.* Online adaptive MR-guided radiotherapy for rectal cancer; feasibility of the workflow on a 1.5T MR-linac: clinical implementation and initial experience. *Radiother. Oncol.* **154**, 172–178 (2021).
47. Lim, S. N. *et al.* Indications of Online Adaptive Replanning Based On Organ Deformation. *Pract. Radiat. Oncol.* **10**, e95–e102 (2020).
48. Van Timmeren, J. E. *et al.* Treatment plan quality during online adaptive re-planning. *Radiat. Oncol.* **15**, 1–11 (2020).

49. Heijkoop, S. T. *et al.* Clinical Implementation of an Online Adaptive Plan-of-the-Day Protocol for Nonrigid Motion Management in Locally Advanced Cervical Cancer IMRT. *Radiat. Oncol. Biol.* **90**, 673–679 (2014).
50. Xing, L., Siebers, J. & Keall, P. Computational Challenges for Image-Guided Radiation Therapy: Framework and Current Research. *Semin. Radiat. Oncol.* **17**, 245–257 (2007).
51. Lim, K. *et al.* Dosimetrically triggered adaptive intensity modulated radiation therapy for cervical cancer. *Int. J. Radiat. Oncol. Biol. Phys.* **90**, 147–154 (2014).
52. Schulze, D., Liang, J., Yan, D. & Zhang, T. Comparison of various online {IGRT} strategies: {The} benefits of online treatment plan re-optimization. *Radiother. Oncol.* **90**, 367–376 (2009).
53. van Herk, M. Errors and margins in radiotherapy. *Semin. Radiat. Oncol.* **14**, 52–64 (2004).
54. Segedin, B. & Petric, P. Uncertainties in target volume delineation in radiotherapy – are they relevant and what can we do about them ? **c**, (2016).
55. Stroom, J. C., de Boer, H. C. J., Huizenga, H. & Visser, A. G. Inclusion of geometrical uncertainties in radiotherapy treatment planning by means of coverage probability. *Int. J. Radiat. Oncol.* **43**, 905–919 (1999).
56. ICRU. *Prescribing, {Recording}, and {Reporting} {Photon}-beam {Intensity}-{Modulated} {Rdiation} {Therapy} ({IMRT})*. (2010).
57. S, M.-F. *ICRU Report 62*. *The British Journal of Radiology* vol. 74 (1999).
58. Gordon, J. J., Crimaldi, A. J., Hagan, M., Moore, J. & Siebers, J. V. Evaluation of clinical margins via simulation of patient setup errors in prostate IMRT treatment plans. *Med. Phys.* **34**, 202–214 (2007).
59. Zhang, X., Shan, G., Liu, J. & Wang, B. Margin evaluation of translational and rotational set - up errors in intensity modulated radiotherapy for cervical cancer. *Springerplus* (2016) doi:10.1186/s40064-016-1796-2.
60. van de Bunt, L. *et al.* Motion and deformation of the target volumes during IMRT for cervical cancer: What margins do we need? *Radiother. Oncol.* **88**, 233–240 (2008).
61. Collen, C. *et al.* Volumetric Imaging by Megavoltage Computed Tomography for Assessment of Internal Organ Motion During Radiotherapy for Cervical Cancer. *Int. J. Radiat. Oncol.* **77**, 1590–1595 (2010).
62. Quantification of intra-fraction changes during radiotherapy of cervical cancer

assessed with pre- and post-fraction Cone Beam CT scans. *Radiother. Oncol.* **117**, 536–541 (2015).

63. Taylor, A. & Powell, M. E. B. An assessment of interfractional uterine and cervical motion: {Implications} for radiotherapy target volume definition in gynaecological cancer. *Radiother. Oncol.* **88**, 250–257 (2008).
64. Eminowicz, G., Rompokos, V., Stacey, C. & McCormack, M. The dosimetric impact of target volume delineation variation for cervical cancer radiotherapy. *Radiother. Oncol.* **120**, 493–499 (2016).
65. Tanderup, K. *et al.* Adaptive {Management} of {Cervical} {Cancer} {Radiotherapy}. *Semin. Radiat. Oncol.* **20**, 121–129 (2010).
66. Lim, K. *et al.* Consensus guidelines for delineation of clinical target volume for intensity-modulated pelvic radiotherapy for the definitive treatment of cervix cancer. *Int. J. Radiat. Oncol. Biol. Phys.* **79**, 348–355 (2011).
67. Ríos, I., Vásquez, I., Cuervo, E., Garzón, Ó. & Burbano, J. Problems and solutions in IGRT for cervical cancer. *Reports of Practical Oncology and Radiotherapy* vol. 23 517–527 (2018).
68. Erk, H., Emeijer, P. E. R., Asch, C. O. E. N. R. & Ebesque, J. O. O. S. V. L. THE PROBABILITY OF CORRECT TARGET DOSAGE : DOSE-POPULATION HISTOGRAMS FOR DERIVING TREATMENT MARGINS IN RADIOTHERAPY. **47**, 1121–1135 (2000).
69. Tilly, D., Holm, Å., Grusell, E. & Ahnesjö, A. Probabilistic optimization of dose coverage in radiotherapy. *Phys. Imaging Radiat. Oncol.* **10**, 1–6 (2019).
70. McKenzie, A., Van Herk, M. & Mijnheer, B. Margins for geometric uncertainty around organs at risk in radiotherapy. *Radiother. Oncol.* **62**, 299–307 (2002).
71. Baum, C., Alber, M., Birkner, M. & Nüsslin, F. Robust treatment planning for intensity modulated radiotherapy of prostate cancer based on coverage probabilities. *Radiother. Oncol.* **78**, 27–35 (2006).
72. Witte, M. G. *et al.* IMRT optimization including random and systematic geometric errors based on the expectation of TCP and NTCP. *Med. Phys.* **34**, 3544–3555 (2007).
73. van Herk, M., Remeijer, P. & Lebesque, J. V. Inclusion of geometric uncertainties in treatment plan evaluation. *Int. J. Radiat. Oncol.* **52**, 1407–1422 (2002).
74. Sobotta, B., Söhn, M. & Alber, M. Robust optimization based upon statistical theory. *Med. Phys.* **37**, 4019–4028 (2010).

75. Rigaud, B. *et al.* CBCT-guided evolutive library for cervical adaptive IMRT. *Med. Phys.* **45**, 1379–1390 (2018).
76. Lim-Reinders, S., Keller, B. M., Al-Ward, S., Sahgal, A. & Kim, A. Online Adaptive Radiation Therapy. *Int. J. Radiat. Oncol. Biol. Phys.* **99**, 994–1003 (2017).
77. Oh, S. *et al.* Hybrid adaptive radiotherapy with on-line {MRI} in cervix cancer {IMRT}. *Radiother. Oncol.* **110**, 323–328 (2014).
78. Sobotta, B., Söhn, M., Shaw, W. & Alber, M. On expedient properties of common biological score functions for multi-modality, adaptive and 4D dose optimization. *Phys Med Biol* **56**, N123--129 (2011).
79. Niemierko, A. Reporting and analyzing dose distributions: {A} concept of equivalent uniform dose. *Med. Phys.* **24**, 103–110 (1997).
80. Wu, Q., Mohan, R., Niemierko, A. & Schmidt-Ullrich, R. Optimization of Intensity-Modulated Radiotherapy plans based on the Equivalent Uniform Dose. *Int. J. Radiat. Oncol. * Biol. * Phys.* **53**, 224–235 (2002).
81. Niemierko, A. A generalized concept of equivalent uniform dose ({EUD}) [abstract]. *Med. Phys* **26**, 1100 (1999).
82. Sobotta, B., Söhn, M., Shaw, W. & Alber, M. On expedient properties of common biological score functions for multi-modality, adaptive and 4D dose optimization. *Phys Med Biol* **56**, N123--129 (2011).

Chapter 2: Cervix cancer treatment target motion: Predicting the unpredictable in unlikely

2.1 Introduction

The standard treatment for locally advanced cervical cancer (LACC) is a combined modality approach of external beam radiotherapy (EBRT), concomitant chemotherapy, and brachytherapy (BT)[1–4]. The dose required for a 3-year local control rate of 90% is 87 Gy EQD_2 to 90% of the High-Risk Clinical Target Volume (HR-CTV) [5,6] and can be as high as 95 Gy in stage III disease[7] with combined EBRT and image-guided adaptive BT (IGABT). Although the effectiveness of this treatment approach in terms of local control and survival rate has been shown, some challenges to further reduce acute toxicity, especially in EBRT, remain [2,8,9]. Recent technological developments incorporating online adaptive Magnetic Resonance (MR) image guidance will play a significant role in normal tissue dose reduction [10,11], while highly conformal and rapid EBRT treatment techniques like volumetric arc therapy (VMAT) relying on online cone-beam computed tomography (CBCT) image guidance allow superior sparing of normal surrounding tissue. These techniques are now advocated as possible treatments of choice in this setting [12–14]. However, the reproducibility and potential benefits of these techniques are affected by complex inter- and intrafraction organ motion, tumor volume, and shape deformation as well as setup- and contour uncertainties [15–17]. Although new technologies and highly conformal treatment methods are being investigated for future implementation, population-based clinical target to planning target volume (CTV-PTV) margins is applied to compensate for uncertainties. However, to maximize the benefit, such margins should be safely optimized using evidence-based data, preferably from the

treating institution, and add value to future conformal and possible hypofractionation approaches [18,19].

Treatment uncertainties, and therefore margins, can be significantly reduced using online (and offline) patient positional corrections through in-room image guidance (IG) and adaptive radiotherapy (ART) [2,20–22]. Bony anatomy registration is mostly utilized as a margin reduction technique leaving internal organ motion to be a remaining major contributor towards uncertainty. Organ motion, especially bladder filling, has a significant impact on the CTV geometry and should be thoroughly quantified to define the appropriate internal margin [23,24]. For this reason bladder- and dietary protocols have been proposed to minimize the influence of bladder and rectal filling changes on CTV motion. Pre-treatment variable bladder filling image sets that describe the resulting extent of internal organ motion and subsequent geometry have found favor in determining internal margins. These data sets are also used to predict the probability of the target being in a particular position[24,25]. Most notably bladder protocols requiring a comfortably full bladder succeed in reducing the dose to the small bowel and bladder at the instance of imaging[26–28]. Although these dosimetric benefits have been demonstrated, there is still some controversy regarding the efficacy of bladder protocols[9,28,29]. Further to this, published bladder protocol studies are mainly based on populations in high-income countries (HIC), such as European and North American countries. The stage breakdown for LACC in these countries is approximately 60% Stage II and 40% Stage III and IV[12,25,30–35].

This study performs a thorough investigation of bladder volume variation and its influence on primary and nodal tumor motion using both empty and full bladder protocols during cervix cancer RT in a low-middle-income country (LMIC) population with <30% Stage II and mainly Stage III and IV disease. Challenges in this setting further include limited access to magnetic resonance imaging (MRI), large patient numbers, locally advanced-stage disease, and difficulty in managing bladder and dietary protocols[36].

2.2 Materials and Methods

2.2.1 Patients and treatment

24 patients, 19 treated with an empty - and 5 treated with a full bladder (FB), receiving radical radiotherapy treatment for cervix cancer with daily pre-treatment CBCT imaging for setup correction and positional recording were included in this study. Patients were sequentially selected. EBRT was given as 50 Gy in 25 fractions using a conventional four-field-box technique. Patient and imaging characteristics are provided in Table 1. Bladder volume variations and predictability were investigated by collecting variable bladder filling pre-treatment image sets including a) expected full bladder (bladder volume following a drinking protocol aiming/expecting to achieve a full bladder), b) empty bladder, and c) naturally filling bladder protocols. 76 Pre-treatment image sets were used to test an expected full bladder (FB) against a natural time-filling bladder (19 patients, 4 image sets each), 390 image sets (15 patients, 25 CBCT images, and pre-treatment CT) to test daily reproducibility of an empty bladder, and 130 (5 patients, 25 CBCT images and pre-treatment CT) to test daily reproducibility of a full bladder. The influence of these variations on target motion was then evaluated.

Table 1: Patient and imaging characteristics.

Characteristic	*Median*	*Patients (n)*	*Image sets (n)*
Total eligible patients		*24*	
Age	*56 (29-76)*		
FIGO stage			
IIA		*1*	
IIB		*7*	
IIIB		*17*	
Imaging			
Pre-Treatment CT			
Expected full bladder		*19*	*76*
Full Bladder		*5*	*30*
Treatment CBCT			
Empty bladder		*15*	*390*
Full bladder		*5*	*130*

2.2.2 Bladder filling protocols

19 of the 24 patients were imaged with a bladder protocol similar to that of Bondar *et al.*[25]: The first pre-treatment simulation scan, the expected full bladder scan (CT_{eFB}), was acquired one hour after patients were asked to empty their bladder and drink 500 ml of water. Hereafter, the bladder was voided, and patients drank 300 ml of water. An empty bladder scan (CT_{EB}) and three scans with a natural filling bladder at 20-minute intervals (CT_{20}, CT_{40}, CT_{60}) were acquired. In all 19 image sets, CT_{eFB} could be compared with $CT_{20\text{-}60}$ to verify the accurate prediction of an FB

scan. The image sets of 15 of the 19 patients, treated with EB, were used to investigate EB reproducibility throughout treatment using CT_{EB} and $CBCT_{EB1-25}$.

In addition, 5 patients were included to evaluate FB reproducibility and predictability on 3 consecutive days ($CT_{FB1,3,5}$). Patients received an additional CT scan 20 minutes after the first on each pre-treatment imaging day to study the effect of a 20-minute treatment delay. Upon arrival, patients were required to empty their bladder and consume 500 ml water one hour before the first CT scan (CT_{FB1}) followed by the second scan 20 min thereafter (CT_{FB2}), this was repeated on the following 3 days ($CT_{FB2,4,6}$). $CBCT_{FB1-25\ was}$ acquired in agreement with instructions prior to CT_{FB1} to test the FB reproducibility throughout treatment.

2.2.3 Data acquisition and delineation

A Toshiba Acquilion LB 16 slice CT scanner (Canon Medical Systems) was used to acquire 2mm slice thicknesses. These ranged from the L2 vertebral body to the 10 cm below the ischial tuberosities in the supine position. 25 cm length CBCTs were acquired using the Elekta XVI^{TM} system with protocols yielding optimal image quality and minimal dose, resulting in 5mm slice thicknesses. Target volumes and OARs were manually contoured on all CT and CBCT images by a single observer and verified by multiple experienced Radiation Oncologists using a standardized method of contouring[37]. Contours from our patient sample has been used as input to test and develop an automatic contouring system for cervical cancer which serves as an additional verification of contours[38].

The primary CTV (pCTV) consisted of the utero-cervix and the upper third of the vagina. The nodal CTV (nCTV) consisted of involved nodes and relevant draining nodal groups (common, internal, and external iliac, obturator lymph, and presacral nodes). OARs delineated were the bladder, rectum, sigmoid, and small bowel. Each CT dataset was rigidly registered (utilizing mutual information) to the reference CTs (CT_{EB} and CT_{FB1}) based on bony anatomy matching using Monaco Sim software (Monaco 5, Elekta Oncology Systems).

2.2.4 Internal organ motion

Organ motion was evaluated for both empty- and full bladders. The pCTV was assessed at uterine (U), cervical (C), and vaginal (V) levels (Figure 1a) on nine representative levels (three levels for each structure) on the reference CT [39]. The maximum extent of movement on any of the U, C, or V levels represents the maximum movement of the structure. The center of mass (COM) of each nCTV represents the level at which nodal movement was quantified.

Measurements for each CTV were performed in 4 main directions: anterior 0˚ (A), posterior 180 ˚ (P), left 90˚ (L) and right 270˚ (R) with additional 15˚ increments in-between (Figure 1b). Each level is divided into quadrants: anterior (315˚ to 45˚), left (45˚ to 135˚), posterior (135˚ to 225˚) and right (225˚ to 315˚). Movement in major directions is represented by the maximum extent of movement in each quadrant. Since the superior movement of the cervix and vagina would be accounted for by adjacent structures movement in the superior direction was only evaluated for the uterus. This was done by noting the most superior axial slice on which the uterus was delineated. The same argument applies to the inferior movement of the uterus and cervix. The inferior border of the vagina was based on fixed anatomical landmarks for all image datasets.

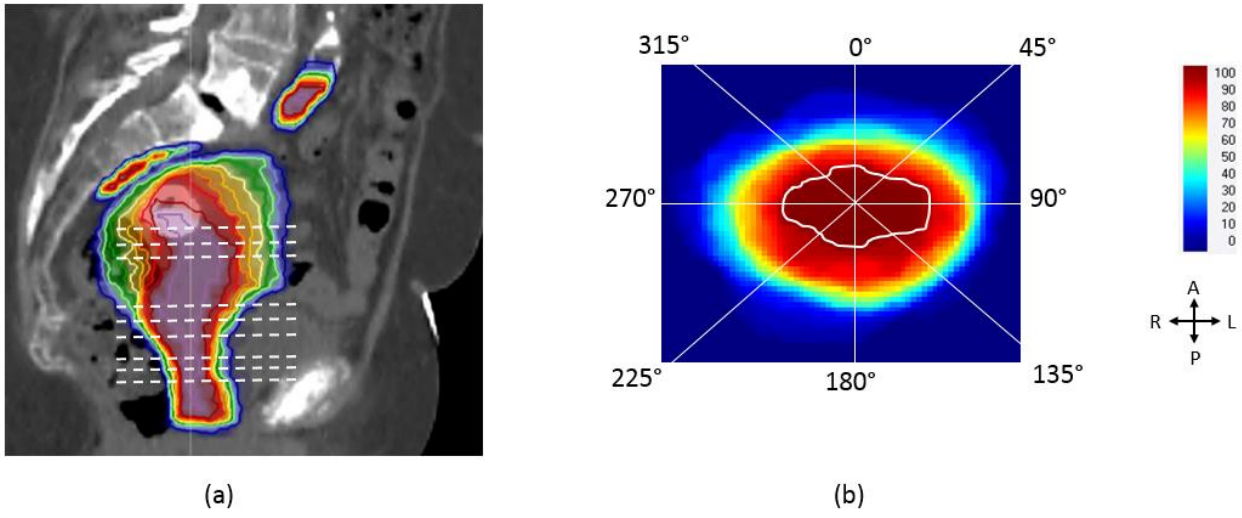

Figure 1: (a) Nine representative levels used for quantification of movement for the uterus, cervix and vaginal canal. (b) Quantification of movement was performed in 4 quadrants (A, P, L and R) for each level. The iso-contours represent different levels of positional occupancy. Dark red= 100% occupancy during 25 treatment fractions, green=50% occupancy and dark blue zero occupancy.

Throughout treatment, the frequency of occupation of a volume of interest (VOI) in the patient coordinate system defines the occupancy probability (OP) for that VOI or point. Considering all CBCTs captured before each treatment fraction, this probability could be calculated [40,41]. OP matrices were established on a 1 x 1 x 1 mm grid for all 9 levels of the pCTV and representative level of nCTV of each patient. From these matrices, OP profiles were generated in 15˚ increments yielding the probability of geometrical deviation of a VOI relative to the reference structure (VOI_{ref}) throughout treatment. An OP of 0.5 corresponds to the maximum extent of movement (mm) of the VOI relative to the VOI_{ref} in 50% of treatment fractions. Similarly, an OP of 0.05 corresponds to 95% of treatment fractions, while an OP of zero relates to the maximum extent of movement during treatment (Figure 2).

2.2.5 Derivation of margins

2.2.5.1 Variable margin (VBM)

Population-based variable margins for each structure (vagina, cervix, and uterus) were derived based on an occupancy probability of each structure as discussed in section 2.2.4. Figure 2 is an example of profiles generated in the four main directions on the cervical level. In this example an occupancy probability of **0.1** corresponds to 18-, 10-, 8- and 7-mm movement in the anterior, posterior, left, and right directions respectively. Margins for the vagina and uterus were derived in the same way. These margins would ensure that the target volume (CTV) would receive 95% of the prescribed dose (planning aim) in **90%** of all treatment fractions. Different occupancy probabilities can be used depending on the dose delivery requirements.

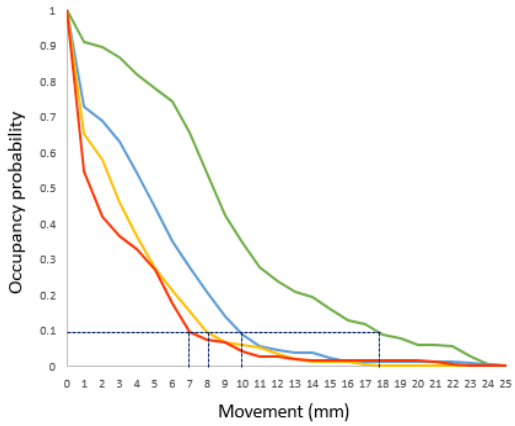

Figure 2: Profiles generated from occupancy probability matrices in the anterior (green), posterior (blue), left (yellow), and right (red) direction. Red dashed lines indicate an occupancy probability of 0.1 corresponding to the maximum extent of movement in 90% of treatment fractions.

2.2.5.2 Internal *target* volume (ITV)

To generate an ITV, a library of pre-treatment CTs is needed generally consisting of variable bladder filling scans ranging from empty to full. The significance, in terms of workload and patient burden, of including various bladder volume scans acquired at different time intervals and days to generate an ITV was investigated. This was done by performing unions of the respective target contours from variable bladder filling pre-treatment scans. Occupancy maps for each of the union structures were generated and used to quantify the geometrical deviation of the target relative to the reference structure (generated ITV) throughout treatment. These deviations were used to determine the range of pCTV movement during treatment. ITVs generated for the empty- (ITV_{EB}) and full bladder (ITV_{FB}) groups are summarized in Table 2 and illustrated in Figure 3.

Table 2: ITVs generated for EB and FB groups.

	Union Structure	Description
ITV_{EB1}	$CT_{EB} \cup CT_{20}$	Empty bladder and natural filling bladder acquired 20 min later.
ITV_{EB2}	$CT_{eFB} \cup CT_{EB} \cup CT_{20}$	Expected full bladder, empty bladder, and natural filling bladder acquired 20 min later.
ITV_{FB1}	$CT_1 \cup CT_2$	Full Bladder and natural filling bladder acquired 20 min later.
ITV_{FB2}	$CT_1 \cup CT_2 \cup CT_3$	Full Bladder, natural filling bladder acquired 20 min later and full bladder acquired on the following day.
ITV_{FB3}	$CT_1 \cup CT_3$	Full bladder was acquired on two consecutive days.
ITV_{FB4}	$CT_1 \cup CT_3 \cup CT_5$	Full bladder scans were acquired on 3 consecutive days.

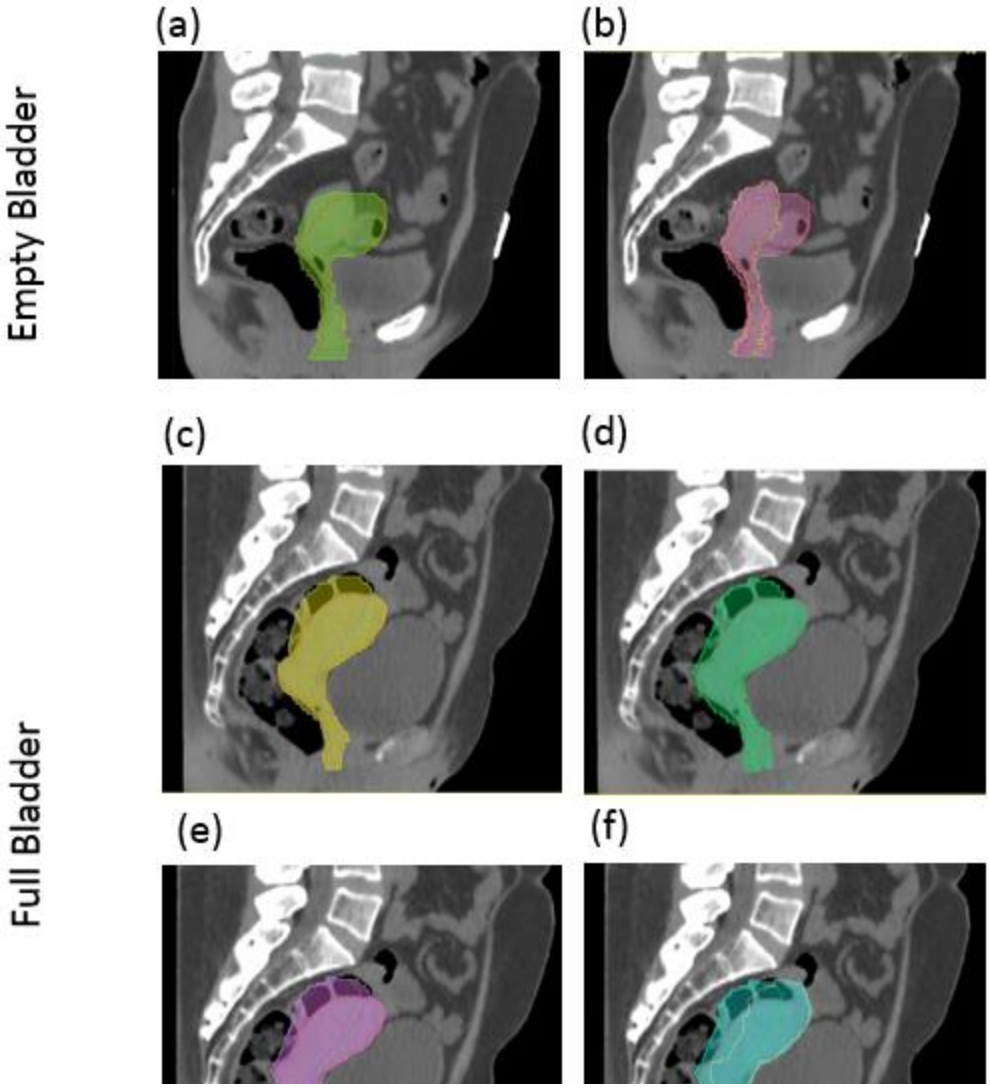

Figure 3: Union structures used for generation of ITVs for patients treated with and empty bladder (a) $CT_{EB} \cup CT_{20}$, (b) $CT_{eFB} \cup CT_{EB} \cup CT_{20}$, and full bladder (c) $CT_1 \cup CT_2$, (d) $CT_1 \cup CT_3$, (e) $CT_1 \cup CT_2 \cup CT_3$, and (f) $CT_1 \cup CT_3 \cup CT_5$.

2.2.6 Statistical analysis

Bladder volume variations were analyzed separately for EB and FB groups. The overall bladder volume variability throughout treatment was calculated as the group-mean (mean of the averages per patient). Intra-patient bladder volume variability was calculated as the standard deviation of daily volumes per patient. The root mean square of all standard deviations calculated over all treatment fractions per patient indicated the group-mean intra-patient variability[17]. Target movement was scored using occupancy probability maps for which a 95th percentile was chosen as a robust estimate of motion.

2.3 Results

A total of 623 image data sets (483 CBCTs and 140 pre-treatment CTs) were acquired and analyzed in this study. On average, patients received 24 ± 1 daily CBCTs. Patients on the EB protocol had little or no complaints and complied well with the protocol instructions. Although there was no difficulty in the execution of the FB protocol (keeping within the specified time intervals and compliance with instructions) some patients complained of discomfort before and during treatment due to full bladders.

2.3.1 Pre-treatment full bladder predictability and reproducibility

When using a FB protocol, it is anticipated that the bladder will be full using the specific drinking instructions (referred to as expected full bladder). When testing the eFB to be predictive of an actual full bladder (obtained after the same period of time as the eFB but with natural filling) with volumes larger than CT_{60}, we found that CT_{eFB} was in fact predictive in only 3/19 patients. The bladder volumes of CT_{20} and CT_{40} were larger than CT_{eFB} in 9/19 and 15/19 patients respectively. The mean volumes are summarized in Table 3.

Evaluating the reproducibility of a full bladder over 3 consecutive days (CT_{FB1}, CT_{FB3}, CT_{FB5}), for patients using a full bladder protocol, the average difference was ± 130 ml on day 2 (CT_{FB1}-CT_{FB3}) and day 3 (CT_{FB1}-CT_{FB5}). Only one patient had a reproducible bladder volume with the largest daily difference being 20 ml in this case. The average increase in bladder volume with a 20 min delay

was 80ml on day one (CT_{FB1}-CT_{FB2}) and two (CT_{FB3}-CT_{FB4}), and 116 ml on day three (CT_{FB5}-CT_{FB6}). The single patient with daily reproducible bladder volumes also displayed large differences in bladder volume on the delayed scans.

Table 3: Bladder filling protocols, imaging and volume variations.

	EB reproducibility (N=15)	**Naturally Filling (N=19)**	**FB reproducibility (N=5)**	**FB + 20 min (N=5)**
Pre-treatment image instances	*15*	*95*	*15*	*15*
Description	CT_{EB}	$CT_{eFB,\ EB,\ 20,\ 40,\ 60}$	$CT_{FB1,3,5}$	$CT_{FB2,4,6}$
Daily CBCTs	*25*		*25*	
Description	$CBCT_{EB1-25}$		$CBCT_{FB1-25}$	
Total no. image sets	*374*	*95*	*139*	*15*
Average bladder volumes ± stdev and range (ml)				
CT_{EB}	*75 ± 34 (44-168)*			
*$CBCT_{EB1-25}$	*81 ± 38 (38-169)*			
CT_{eFB}		*206 ± 123 (53-440)*		
CT_{20}		*189 ± 91 (44-362)*		
CT_{40}		*285 ± 133 (100-510)*		
CT_{60}		*376 ± 155 (151-675)*		
CT_{FB1}			*275 ± 76 (191-372)*	
CT_{FB2}				*354 ±125 (210-516)*
CT_{FB3}			*326 ± 189 (94-551)*	

CT_{FB4}				*407 ± 243 (144-673)*
CT_{FB5}			*292 ± 149 (148-539)*	
CT_{FB6}				*409 ± 166 (258-675)*
$*CBCT_{FB1-25}$			*231 ± 19 (210-254)*	
**Group mean*				

2.3.2 Empty and full bladder reproducibility during treatment

During treatment, the average bladder volume of the EB group was significantly smaller ($p<0.05$) than the FB group with a group-mean of 81 ± 38 ml vs. 231 ± 19 ml (Table 3). The average pre-treatment bladder volume of 75 ± 34 ml for EB patients was closely reproduced during treatment (Figure 4 a). In contrast, a reduction in average bladder volume for FB patients was noted during treatment. Figure 4 b shows a 27% average reduction in bladder volume during the third week of treatment (201 ± 40 ml in the 3rd week vs 275 ± 76 ml at the planning stage) and a reasonably consistent volume for the remainder of the treatment. A smaller group intra-patient variability was seen in EB patients compared to FB patients (33 ml vs. 114 ml).

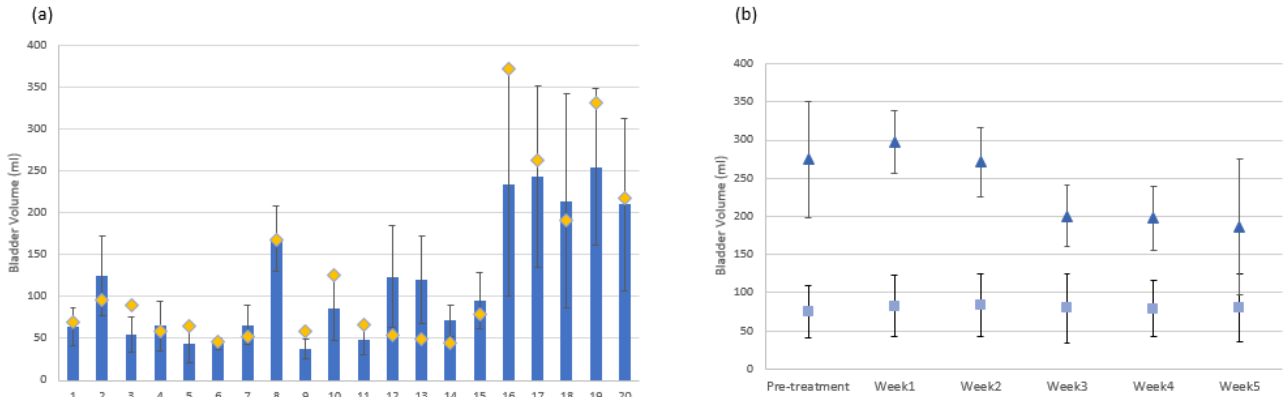

Figure 4: (a) Average treatment bladder volume and standard deviations for all patients. Diamonds indicate pre-treatment bladder volumes. (b) Group mean bladder volumes determined pre-treatment and each week of treatment. EB and FB volumes indicated by squares and triangles respectively.

2.3.3 Primary CTV occupancy probability

The deviations from VOI_{ref} for the pCTV in 15° increments on vaginal, cervical, and uterine levels for the population (empty and full bladders) are shown in the radar plots (Figure 5). The maximum extent of movement for the entire treatment is indicated by the dark blue color illustrating the required expansion (in mm) to an inclusive ITV that would encompass 100% occupancy (OP_{100}) of the pCTV. At the same time, turquoise represents 95% occupancy (OP_{95}) of the moving pCTV and yellow 90% (OP_{90}).

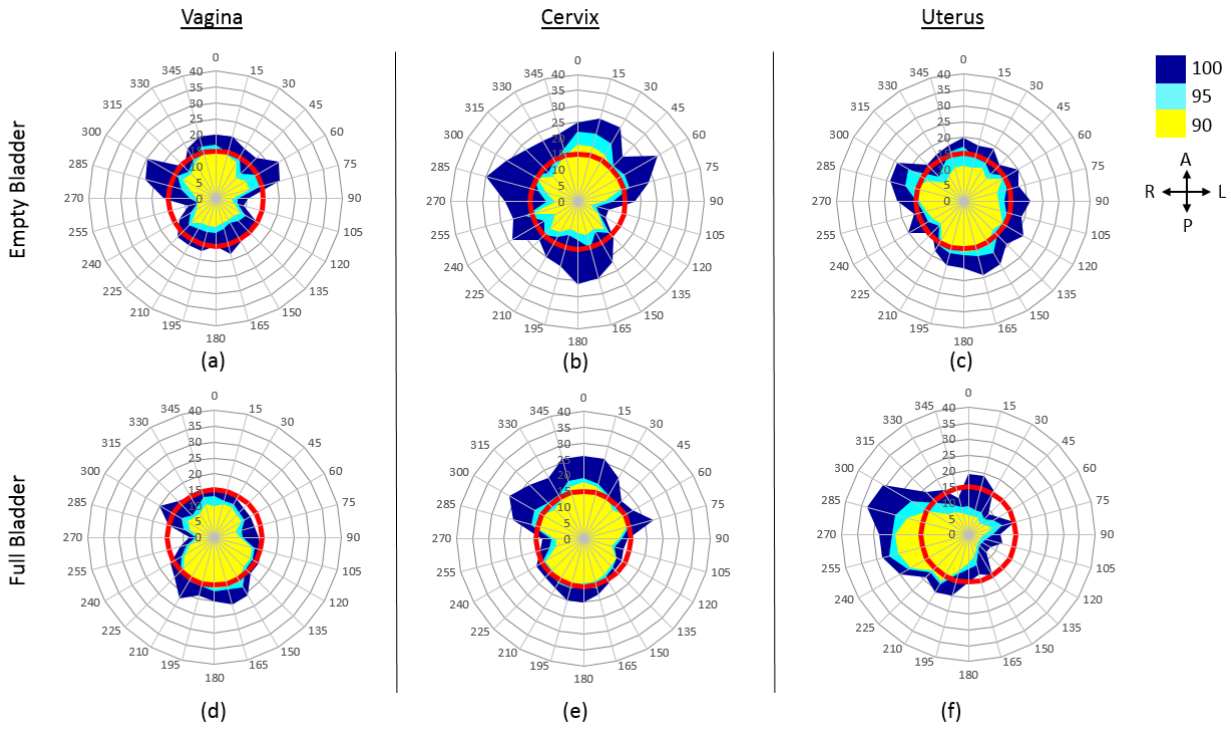

Figure 5: Radar plots of movements in 15˚ increments on the vaginal (a and d), cervical (b and e) and uterine level (c and f) for the empty- and full bladder population. The different colors on each plot indicates the OP of the pCTV throughout treatment (see legend). A 15 mm isotropic margin are shown on all plots.

Although the maximum extent of movement was similar in both groups, there is a visible difference in OPs. A larger probability of lateral movement was seen on vaginal level in the case of EB than FB. Similar probabilities were seen in the anterior and posterior directions. At the level of the cervix, similar probabilities were noted in the anterior direction and significantly larger posterior and lateral movements in the EB group. On uterine level, the EB group showed larger anterior-posterior and left movements while movement to the right was more significant in the FB group. The large movement to the right for FB patients was due to one patient that showed significant anatomical variations (bladder volume reduction and small bowel movement) in two CBCTs. These plots show significant movement associated with bladder filling status, independent of the protocol applied.

2.3.4 Nodal CTV occupancy probability

As in the case of the pCTV, the deviations from VOI_{ref} for all nCTVs in all directions are shown in Figure 6. The maximum extent of movement is represented by the dark blue color. This represents a 100% inclusion of the nCTV. At the same time, turquoise represents 95% occupancy of the moving nCTV and yellow 90%.

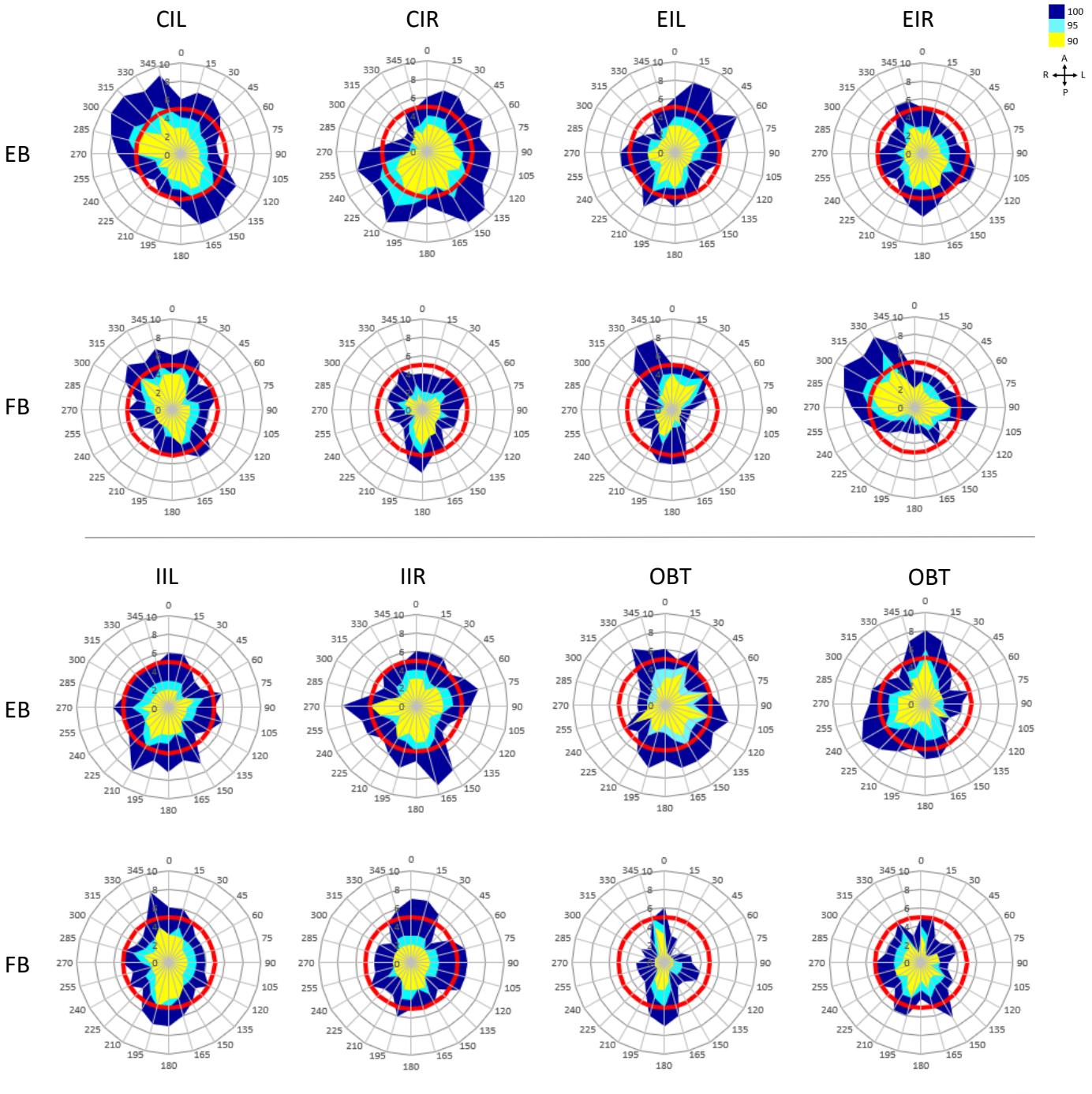

Figure 6: Radar plots of occupancy probabilities in 15˚ increments for all nodal groups (CIL and CIR = common iliac left and right, EIL and EIR = external iliac left and right, IIL and IIR = internal iliac left and right, OBTL and OBTR = obturator left and right) for patients treated with an empty- and full bladder. The different colors on each plot indicates the OP of the nCTV throughout treatment (see legend). A 5 mm isotropic margin is shown on all plots.

The maximum extent of movement (OP_{100}) of each structure for the entire treatment is summarized in Table 4. Also shown are the extent of movement in 95% (OP_{95}) and 90% (OP_{90}) of the fractions. Considerably smaller movements were noted for 95% (OP_{95}) and 90% (OP_{90}) occupancies for all structures. Differences in movement up to 13 and 9 mm between OP_{100} and OP_{95} were measured for the EB and FB groups respectively. OP_{95} movements for the EB and FB groups were comparable except posteriorly on the level of the vagina and laterally on the uterine level. Superior movement of the uterus was slightly, but not significantly, larger in the EB vs. FB group, 22mm vs 18mm. In general, the largest movement was seen on the level of the cervix. The extent of movement averaged over all nodal groups is given in Table 4. Movements for the EB and FB groups are comparable. In general, the maximum extent of movement was 7mm with a 2mm and 3mm reduction in the movement for OP_{95} and OP_{90}. Similar nodal movement between EB and FB patients was noted. Variable margins were based on an occupancy probability of 0.05 for each structure. These margins are indicated in bold (OP_{95}) in Table 4.

Table 4: The required expansion (in mm) for the population that would encompass the pCTV and nCTV for the entire treatment (OP_{100}), 95% (OP_{95}), and 90% (OP_{90}) of the treatment fractions.

	Empty Bladder											
	Vagina			Cervix			Uterus			Nodes		
	OP_{100}	OP_{95}	OP_{90}	OP_{100}	OP_{95}	OP_{90}	OP_{100}	OP_{95}	OP_{90}	OP_{100}	OP_{95}	OP_{90}
A	20	**17**	16	27	**22**	18	20	**17**	12	7	5	4
P	18	**12**	11	26	**15**	12	24	**19**	16	8	5	4
L	23	**15**	11	29	**17**	15	22	**16**	14	7	5	4
R	25	**14**	12	30	**17**	15	24	**17**	14	7	5	4
S							22	**10**	8			
	Full Bladder											
A	16	**13**	11	26	**19**	18	19	**14**	9	7	5	4
P	22	**18**	16	20	**16**	15	21	**18**	17	7	5	4
L	16	**14**	13	23	**16**	15	15	**11**	8	6	4	3
R	20	**15**	14	27	**18**	16	33	**26**	23	6	4	3
S							18	**6**	2			

**A=anterior, P=posterior, L=left, R=right, S=superior*

2.3.5 ITV generation

Figure 7 indicates the deviation of the pCTV on the level of the vagina, cervix, and uterus from different union structures (see Table 2) throughout treatment for the EB and FB groups. Also shown are deviations when only CT_{EB} and CT_{FB1} are used as reference structures (first bar). The results are based on OP_{95}.

For both groups, a gain in terms of capturing movement can be seen when using scans acquired 20 min apart (ITV_{EB1} and ITV_{FB1}) compared to only using the empty (CT_{EB}) or full bladder (CT_{FB1}) scan as reference structure. The largest difference in deviation between ITV_{EB1} and ITV_{EB2} is 3 mm in the anterior direction on vaginal level and left on the level of the cervix. On uterine level a 2 mm difference were noted in the anterior and posterior direction. Compared to ITV_{FB1}, a gain of up to 5 mm was noted when ITV_{FB2} is used. Deviations noted when using $ITVFB_3$ and ITV_{FB4} were in most directions the same. A small gain, if any was noted compared to ITV_{FB2}.

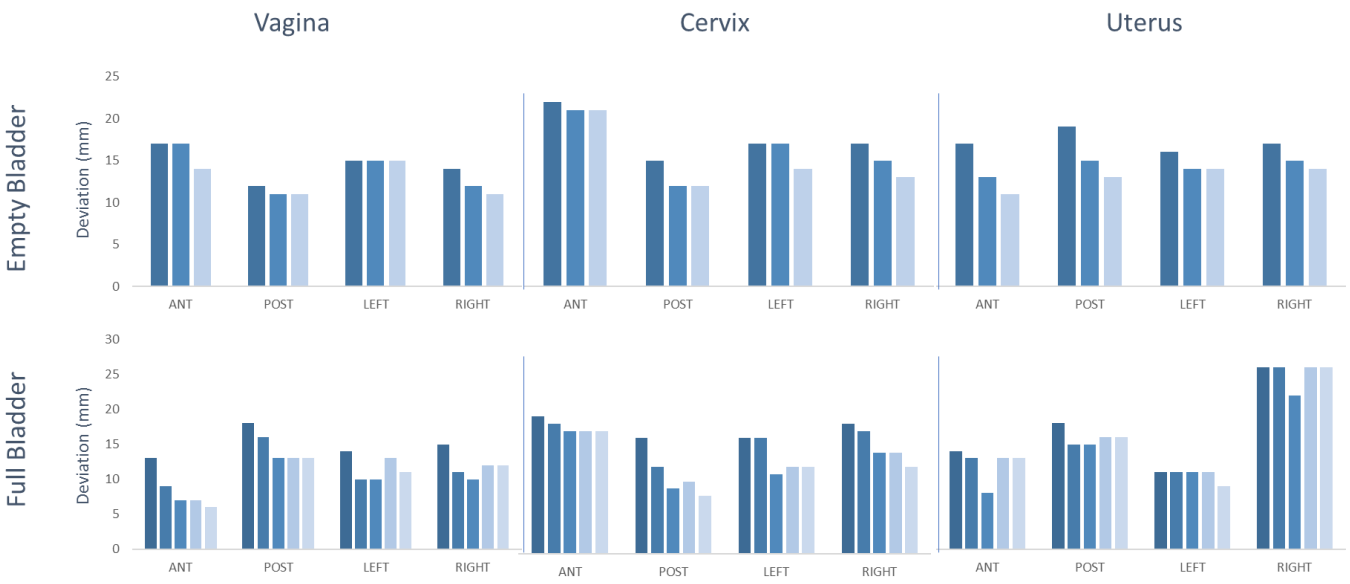

Figure 7: Geometric deviations of the pCTV throughout treatment for the vagina, cervix, and uterus for both empty- (top row) and full bladder (bottom row) groups. Starting at the darkest shade of blue, deviations from CT_{EB}, ITV_{EB1}, and ITV_{EB2} are indicated for the EB patients and deviations from CT_{FB1}, ITV_{FB1}, ITV_{FB2}, ITV_{FB3}, and ITV_{FB4} for the FB patients.

Considering workload and dose burden to the patient due to additional imaging and the gain in terms of capturing movement, ITV_{EB2} and ITV_{FB2} were used as union structures to represent internal movement due to bladder filling. Similar to Bondar et al. [42] ITV_{EB2} and ITV_{FB2} were expanded with an isotropic 10 mm margin and the nCTV with a 5 mm margin to generate a planning target volume.

2.4 Discussion

An extensive dataset of 623 CT and CBCT scans were manually contoured and analyzed to evaluate bladder volume and geometric variations for 24 cervix cancer patients in an LMIC population. The variation of bladder volume, both full- and empty bladder and its influence on target motion have been quantified. From a treatment planning perspective, there is a desire to predict bladder volumes and geometries by utilizing protocols to control volumes during pre-treatment imaging and throughout treatment. FB protocols have been recommended to reduce the dose burden to the bladder itself, displacement of small bowel out of the treatment field, and as a means of limiting dosimetric uncertainty due to bladder filling changes [43,24,44]. As some degree of variation is expected a library of plans, plan of the day, multiple image-based ITV approaches and robust motion planning strategies have been suggested [45–48]. These strategies rely on a chance that a predicted model of plans would deliver the dose to the intended area, requiring investment in multiple treatment plans and quality control from the start. Our data suggest that predictive models have limitations, even more so in treatment centers with large patient numbers, and where simple bladder protocols can be easily followed.

Compared to the natural filling of the bladder, a protocol aimed at achieving a FB after 60 min yielded the largest bladder volume in only 16% of the patients. 47% of the population already had larger bladder volumes 20 mins after water consumption with the natural filling protocol. This indicates that the expected FB may not be achieved as intended by the protocol. The reproducibility of achieving a full bladder was tested on 3 consecutive pre-treatment days. Except for one patient, the bladder volume was not reproducible and variations up to 277 ml were noted for the rest of the patients. For most patients, a simulated treatment delay of 20 min had a notable impact on bladder volume as seen from our results. Intra- and inter-patient volume

differences varied widely ranging from 6 ml up to 185 ml. Ahmad et al observed cervix and uterus displacements of 2 cm/100 ml bladder volume change which indicates that the abovementioned volume changes would have a significant impact on the target volume geometry.[44] These findings were based on pre-treatment image data sets and therefore exclude the effect of radiation on bladder filling. In addition, factors such as hydration levels and physiologic filling rates, which are difficult to predict, will also influence bladder filling and consequently the objective of bladder protocols to achieve reproducible bladder volumes [47,49].

The daily reproducibility of bladder volume during treatment was tested for both the EB and FB populations. We found a smaller intra-patient variability in EB patients compared to FB patients indicating more reproducible bladder volumes throughout treatment. The group intra-patient variability for the treatment volume relative to planning volume in FB is larger compared to the EB group (116.0 vs. 5.5) highlighting the difficulty in achieving the same (full) bladder volume during treatment. This may be due to non-compliance with the prescribed drinking protocol, and the influence of brachytherapy and chemotherapy on the bladder [50]. A comparison of pCTV movement for the FB group in the first two weeks vs the last three weeks of treatment showed an increase in movement which may indicate that margin adaption would be necessary after week 2 of treatment. Although an empty bladder doesn't yield the same dosimetric advantages, bladder volumes seem to be more reproducible during treatment which means a more reproducible geometry with advantages in terms of dose delivery intentions. Bladder and dietary protocols are difficult to manage especially in a resource-limited department with high patient throughput like our institution. Considering the above-mentioned issues and basing our conclusions purely on bladder volume data an EB protocol proves to be the most practical in terms of time efficiency and executability.

Radar plots derived from occupancy matrices are a useful tool for the visual interpretation of geometrical deviations. Profiles were generated at 15˚ intervals to quantify the magnitude of deviations throughout treatment. These graphs indicate the probability of a structure being in a specific position relative to the reference VOI and can aid in decision-making on adequate ITV margin sizes to encompass the CTV in all directions based on the population requirements for tumor dose coverage. On vaginal level movements in the EB group were slightly larger compared

to that of FB patients despite the more reproducible bladder volume during treatment. The largest movements, particularly anteriorly, were observed on the level of the cervix for both groups. These findings support results from the literature indicating the influence of rectal filling on geometrical variations of the cervix and vagina.[51] On the uterine level, movements in all dimensions, except right, were slightly smaller for patients treated with a full bladder. Overall, no significant difference in the movement was found between the EB and FB groups. Treatment preparation can thus purely be based on OAR dose criteria and protocol executability.

We found a notable difference in both the movement of the three structures (vagina, cervix, and uterus) and directions of a specific structure. In agreement with the literature, this confirms the use of anisotropic/variable margins [52]. Based on our population data, the pCTV will be encompassed in all treatment fractions using the following anisotropic ITV margins: For the vagina, 20 and 18 mm in the anterior and posterior directions and 23 and 25 mm in the left and right directions. 27 and 26 mm in the anterior and posterior directions for the cervix and 29 and 30 mm in the left and right directions. On the uterine level, the anterior and posterior margins should be 20 and 24 mm and 22 and 24 mm in the lateral directions. Suggested margins for patients treated with a full bladder are slightly smaller for all structures except in the posterior direction on vaginal and right direction on uterine level. Superiorly the suggested margins are 22 and 18 mm for the empty and full bladder patients respectively. Except for larger lateral margins, our suggested margins agree with proposed anisotropic margins from the literature. Van de Bunt *et al.* used weekly MRI imaging and derived anisotropic margins around the CTV of 24 and 17 mm anterior and posterior, 11 and 8 mm superior and inferior, and 16 and 12 mm left and right [51]. Using daily CBCT image guidance Tyagi *et al.* found uniform CTV-PTV margins of 15 mm would be sufficient to encompass the CTV in only 68% of fractions and margins of 30 mm would be needed to ensure coverage in 95% of fractions. [8]. Consensus guidelines suggest a 7 mm CTV-PTV margin for nodal volumes [53]. Our data underscore the use of this margin. Considering an occupancy probability of 95% margins can be reduced to 5 mm which is in agreement with the EMBRACE II protocol when daily imaging, bony image fusion, and couch corrections are used [3]. Intra-fraction motion should be accounted for in the expansion of the ITV to determine an appropriate PTV. Pre-treatment image data sets acquired 20 mins apart were used to anticipate the magnitude of

intra-fraction motion. The average value was ≤5 mm for EB and FB groups. Considering this and keeping in mind that the dose outside the PTV will not be zero a margin based on an occupancy probability of 95% can be used to significantly reduce margin size and in effect OAR dose while still maintaining clinically acceptable doses in the CTV.

Internal target volumes describe the range of movement which can be expected throughout treatment due to different combinations of organ filling (bladder and bowel). Pre-treatment imaging at different time intervals or days is used to predict these changes. Although patients in this study were treated with specific bladder protocols, large variations in bladder volumes during treatment were seen in both the EB and FB groups for some patients. We, therefore, investigated the use of an ITV approach for this group of patients. Based on our results in terms of capturing movement, workload and additional imaging dose we used two scans acquired 20 mins apart for EB patients and three scans, two acquired 20 mins apart and a third the following day, for FB patients. Considering that these ITVs will be expanded with a 10 mm margin as suggested in literature [42,54] the values obtained will in most cases exceed results obtained for the VBM approach. Acquiring these scans increases the workload which can be counterproductive in a department with high patient throughput and limited staff.

To our knowledge, this is the first such investigative study in a LMIC. Limitations of this study include the relatively small patient cohort used. The current dataset, especially patients treated with a full bladder, needs to be enlarged to draw firm conclusions. Although no MRI data was available studies showed an excellent correlation between cervical volumes delineated on CT and MRI [55].

2.5 Conclusion

A thorough understanding of target movement and the causes thereof is important to optimize treatment strategies (ie. margins, planning, etc.) and delivery. Although a FB protocol has dosimetric benefits, an empty bladder proves to be more reproducible and easier to execute. When a protocol is adopted in a clinic the most practical method should be used. In a resource-limited environment with high patient throughput, an EB protocol proves to be the most efficient in terms of reproducibility, time, and executability. The true motion of the tumor volumes is not

predictable and is a result of a complex integration of multiple organ motion which cannot be assigned to bladder motion only. Occupancy probability matrices are a novel way of quantifying target movement. The knowledge obtained in this study can be used as guidance to derive ITV/PTV margins. This is important for understanding the dosimetric impact of movement which will be investigated in future studies.

2.6 References

1. Chino J, Annunziata CM, Beriwal S, et al. Radiation Therapy for Cervical Cancer: Executive Summary of an ASTRO Clinical Practice Guideline. *Pract Radiat Oncol*. 2020;10(4):220-234. doi:10.1016/j.prro.2020.04.002
2. Tanderup K, Georg D, Pötter R, Kirisits C, Grau C, Lindegaard JC. Adaptive {Management} of {Cervical} {Cancer} {Radiotherapy}. *Semin Radiat Oncol*. 2010;20(2):121-129. doi:10.1016/j.semradonc.2009.11.006
3. Tanderup K, Pötter R, Lindegaard J, et al. Image guided intensity modulated External beam radiochemotherapy and MRI based adaptive brachytherapy in locally advanced cervical cancer EMBRACE-II. *EMBRACE II study Protoc v10*. 2015:0-132. https://www.embracestudy.dk/UserUpload/PublicDocuments/EMBRACE II Protocol.pdf.
4. Haie-Meder C, Pötter R, Van Limbergen E, et al. Recommendations from {Gynaecological} ({GYN}) {GEC}-{ESTRO} {Working} {Group}☆ ({I}): concepts and terms in 3D image based 3D treatment planning in cervix cancer brachytherapy with emphasis on {MRI} assessment of {GTV} and {CTV}. *Radiother Oncol*. 2005;74(3):235-245. doi:10.1016/j.radonc.2004.12.015
5. Dimopoulos JCA, Pötter R, Lang S, et al. Dose-effect relationship for local control of cervical cancer by magnetic resonance image-guided brachytherapy. *Radiother Oncol*. 2009;93(2):311-315. doi:10.1016/j.radonc.2009.07.001
6. Pötter R, Dimopoulos J, Georg P, et al. Clinical impact of MRI assisted dose volume adaptation and dose escalation in brachytherapy of locally advanced cervix cancer. *Radiother Oncol*. 2007;83(2):148-155. doi:10.1016/j.radonc.2007.04.012
7. Tanderup K, Nesvacil N, Kirchheiner K, et al. Evidence-Based Dose Planning Aims and Dose Prescription in Image-Guided Brachytherapy Combined With Radiochemotherapy in Locally Advanced Cervical Cancer. *Semin Radiat Oncol*. 2020;30(4):311-327. doi:10.1016/j.semradonc.2020.05.008
8. Tyagi N, Lewis JH, Yashar CM, et al. Daily {Online} {Cone} {Beam} {Computed} {Tomography} to {Assess} {Interfractional} {Motion} in {Patients} {With} {Intact} {Cervical}

{Cancer}. *Int J Radiat Oncol*. 2011;80(1):273-280. doi:10.1016/j.ijrobp.2010.06.003

9. Eminowicz G, Motlib J, Khan S, Perna C, McCormack M. Pelvic Organ Motion during Radiotherapy for Cervical Cancer: Understanding Patterns and Recommended Patient Preparation. *Clin Oncol*. 2016;28(9):e85-e91. doi:10.1016/j.clon.2016.04.044
10. Corradini S, Alongi F, Andratschke N, et al. MR-guidance in clinical reality: Current treatment challenges and future perspectives. *Radiat Oncol*. 2019;14(1):1-12. doi:10.1186/s13014-019-1308-y
11. Lindegaard JC, Fokdal LU, Nielsen SK, Juul-Christensen J, Tanderup K. MRI-guided adaptive radiotherapy in locally advanced cervical cancer from a Nordic perspective. *Acta Oncol (Madr)*. 2013;52(7):1510-1519. doi:10.3109/0284186X.2013.818253
12. Williamson CW, Green G, Noticewala SS, et al. Prospective Validation of a High Dimensional Shape Model for Organ Motion in Intact Cervical Cancer. *Int J Radiat Oncol Biol Phys*. 2016;96(4):801-807. doi:10.1016/j.ijrobp.2016.08.015
13. Gandhi AK, Sharma DN, Rath GK, et al. Early clinical outcomes and toxicity of intensity modulated versus conventional pelvic radiation therapy for locally advanced cervix carcinoma: A prospective randomized study. *Int J Radiat Oncol Biol Phys*. 2013;87(3):542-548. doi:10.1016/j.ijrobp.2013.06.2059
14. Hasselle MD, Rose BS, Kochanski JD, et al. Clinical {Outcomes} of {Intensity}-{Modulated} {Pelvic} {Radiation} {Therapy} for {Carcinoma} of the {Cervix}. *Int J Radiat Oncol*. 2011;80(5):1436-1445. doi:10.1016/j.ijrobp.2010.04.041
15. Haripotepornkul NH, Nath SK, Scanderbeg D, Saenz C, Yashar CM. Evaluation of intra- and inter-fraction movement of the cervix during intensity modulated radiation therapy. *Radiother Oncol*. 2011;98(3):347-351. doi:10.1016/j.radonc.2010.11.015
16. Chan P, Dinniwell R, Haider MA, et al. Inter- and Intrafractional Tumor and Organ Movement in Patients With Cervical Cancer Undergoing Radiotherapy: A Cinematic-MRI Point-of-Interest Study. *Int J Radiat Oncol Biol Phys*. 2008;70(5):1507-1515. doi:10.1016/j.ijrobp.2007.08.055
17. Van Herk M. Errors and Margins in Radiotherapy. *Semin Radiat Oncol*. 2004;14(1):52-64. doi:10.1053/j.semradonc.2003.10.003

18. Jadon R, Pembroke CA, Hanna CL, et al. A Systematic Review of Organ Motion and Image-guided Strategies in External Beam Radiotherapy for Cervical Cancer. *Clin Oncol*. 2014;26(4):185-196. doi:10.1016/j.clon.2013.11.031
19. Baum C, Birkner M, Alber M, Paulsen F, Nüsslin F. Dosimetric consequences of the application of off-line setup error correction protocols and a hull-volume definition strategy for intensity modulated radiotherapy of prostate cancer. *Radiother Oncol*. 2005;76(1):35.E1--35.E8. doi:10.1016/j.radonc.2005.06.006
20. Stroom JC, de Boer HCJ, Huizenga H, Visser AG. Inclusion of geometrical uncertainties in radiotherapy treatment planning by means of coverage probability. *Int J Radiat Oncol*. 1999;43(4):905-919. doi:10.1016/S0360-3016(98)00468-4
21. Ríos I, Vásquez I, Cuervo E, Garzón Ó, Burbano J. Problems and solutions in IGRT for cervical cancer. *Reports Pract Oncol Radiother*. 2018;23(6):517-527. doi:10.1016/j.rpor.2018.05.002
22. van Herk M. Errors and margins in radiotherapy. *Semin Radiat Oncol*. 2004;14(1):52-64. doi:10.1053/j.semradonc.2003.10.003
23. Jadon R, Pembroke CA, Hanna CL, et al. A {Systematic} {Review} of {Organ} {Motion} and {Image}-guided {Strategies} in {External} {Beam} {Radiotherapy} for {Cervical} {Cancer}. *Clin Oncol*. 2014;26(4):185-196. doi:10.1016/j.clon.2013.11.031
24. Ahmad R, Hoogeman MS, Bondar M, et al. Increasing treatment accuracy for cervical cancer patients using correlations between bladder-filling change and cervix–uterus displacements: {Proof} of principle. *Radiother Oncol*. 2011;98(3):340-346. doi:10.1016/j.radonc.2010.11.010
25. Bondar L, Hoogeman M, Mens JW, et al. Toward an individualized target motion management for {IMRT} of cervical cancer based on model-predicted cervix–uterus shape and position. *Radiother Oncol*. 2011;99(2):240-245. doi:10.1016/j.radonc.2011.03.013
26. Pinkawa M, Gagel B, Demirel C, Schmachtenberg A, Asadpour B, Eble MJ. Dose-volume histogram evaluation of prone and supine patient position in external beam radiotherapy for cervical and endometrial cancer. *Radiother Oncol*. 2003;69(1):99-105. doi:10.1016/S0167-8140(03)00244-5

27. Chen VE, Gillespie EF, Manger RP, et al. The impact of daily bladder filling on small bowel dose for intensity modulated radiation therapy for cervical cancer. *Med Dosim*. 2019;44(2):102-106. doi:10.1016/j.meddos.2018.02.010

28. Ahmad R, Hoogeman MS, Quint S, Mens JW, de Pree I, Heijmen BJM. Inter-fraction bladder filling variations and time trends for cervical cancer patients assessed with a portable 3-dimensional ultrasound bladder scanner. *Radiother Oncol*. 2008;89(2):172-179. doi:10.1016/j.radonc.2008.07.005

29. Ahmad R, Bondar L, Voet P, et al. A margin-of-the-day online adaptive intensity-modulated radiotherapy strategy for cervical cancer provides superior treatment accuracy compared to clinically recommended margins: a dosimetric evaluation. *Acta Oncol*. 2013;52(7):1430-1436. doi:10.3109/0284186X.2013.813640

30. Chan P, Dinniwell R, Haider MA, et al. Inter- and {Intrafractional} {Tumor} and {Organ} {Movement} in {Patients} {With} {Cervical} {Cancer} {Undergoing} {Radiotherapy}: {A} {Cinematic}-{MRI} {Point}-of-{Interest} {Study}. *Int J Radiat Oncol*. 2008;70(5):1507-1515. doi:10.1016/j.ijrobp.2007.08.055

31. Rigaud B, Simon A, Gobeli M, et al. CBCT-guided evolutive library for cervical adaptive IMRT. *Med Phys*. 2018;45(4):1379-1390. doi:10.1002/mp.12818

32. Schippers MGA, Bol GH, De Leeuw AAC, et al. Position shifts and volume changes of pelvic and para-aortic nodes during IMRT for patients with cervical cancer. *Radiother Oncol*. 2014;111(3):442-445. doi:10.1016/j.radonc.2014.05.013

33. Seppenwoolde Y, Stock M, Buschmann M, et al. Impact of organ shape variations on margin concepts for cervix cancer ART. *Radiother Oncol*. 2016;120(3):526-531. doi:10.1016/J.RADONC.2016.08.004

34. Kerkhof EM, van der Put RW, Raaymakers BW, van der Heide UA, Jürgenliemk-Schulz IM, Lagendijk JJW. Intrafraction motion in patients with cervical cancer: {The} benefit of soft tissue registration using {MRI}. *Radiother Oncol*. 2009;93(1):115-121. doi:10.1016/j.radonc.2009.07.010

35. Mayr NA, Taoka T, Yuh WT., et al. Method and timing of tumor volume measurement for outcome prediction in cervical cancer using magnetic resonance imaging. *Int J Radiat*

Oncol. 2002;52(1):14-22. doi:10.1016/S0360-3016(01)01808-9

36. Lavigne AW, Triedman SA, Randall TC, Trimble EL, Viswanathan AN. Cervical cancer in low and middle income countries: Addressing barriers to radiotherapy delivery. 2017. doi:10.1016/j.gore.2017.08.004
37. Toita T, Ohno T, Kaneyasu Y, et al. A Consensus-based guideline defining clinical target volume for primary disease in external beam radiotherapy for intact uterine cervical cancer. *Jpn J Clin Oncol*. 2011;41(9):1119-1126. doi:10.1093/jjco/hyr096
38. Rhee DJ, Jhingran A, Rigaud B, et al. Automatic contouring system for cervical cancer using convolutional neural networks. *Med Phys*. 2020;47(11):5648-5658. doi:10.1002/mp.14467
39. Collen C, Engels B, Duchateau M, et al. Volumetric Imaging by Megavoltage Computed Tomography for Assessment of Internal Organ Motion During Radiotherapy for Cervical Cancer. *Int J Radiat Oncol*. 2010;77(5):1590-1595. doi:10.1016/J.IJROBP.2009.10.021
40. Baum C, Alber M, Birkner M, Nüsslin F. Robust treatment planning for intensity modulated radiotherapy of prostate cancer based on coverage probabilities. *Radiother Oncol*. 2006;78(1):27-35. doi:10.1016/j.radonc.2005.09.005
41. Hysing LB, Söhn M, Muren LP, Alber M. A coverage probability based method to estimate patient-specific small bowel planning volumes for use in radiotherapy. *Radiother Oncol*. 2011;100(3):407-411. doi:10.1016/j.radonc.2011.08.037
42. Bondar L, Hoogeman M, Mens JW, et al. Toward an individualized target motion management for IMRT of cervical cancer based on model-predicted cervix-uterus shape and position. *Radiother Oncol*. 2011;99(2):240-245. doi:10.1016/j.radonc.2011.03.013
43. Chen VE, Gillespie EF, Manger RP, et al. The impact of daily bladder filling on small bowel dose for intensity modulated radiation therapy for cervical cancer. *Med Dosim*. 2019;44(2):102-106. doi:10.1016/J.MEDDOS.2018.02.010
44. Ahmad R, Hoogeman MS, Quint S, Mens JW, Pree I De, Heijmen BJM. Inter-fraction bladder filling variations and time trends for cervical cancer patients assessed with a portable 3-dimensional ultrasound bladder scanner q. *Radiother Oncol*. 2008;89(2):172-179. doi:10.1016/j.radonc.2008.07.005
45. Ahmad R, Bondar L, Voet P, et al. A margin-of-the-day online adaptive intensity-modulated

radiotherapy strategy for cervical cancer provides superior treatment accuracy compared to clinically recommended margins: {A} dosimetric evaluation. *Acta Oncol*. 2013;52(7):1430-1436. doi:10.3109/0284186X.2013.813640

46. Heijkoop ST, Langerak TR, Quint S, et al. Clinical Implementation of an Online Adaptive Plan-of-the-Day Protocol for Nonrigid Motion Management in Locally Advanced Cervical Cancer IMRT. *Radiat Oncol Biol*. 2014;90(3):673-679. doi:10.1016/j.ijrobp.2014.06.046
47. Nováková E, Heijkoop ST, Quint S, et al. What is the optimal number of library plans in ART for locally advanced cervical cancer? *Radiother Oncol*. 2017;125(3):470-477. doi:10.1016/j.radonc.2017.08.033
48. Buschmann M, Majercakova K, Sturdza A, et al. Image guided adaptive external beam radiation therapy for cervix cancer: Evaluation of a clinically implemented plan-of-the-day technique. *Z Med Phys*. 2018;28(3):184-195. doi:10.1016/j.zemedi.2017.09.004
49. Jensen NBK, Assenholt MS, Fokdal LU, et al. Cone beam computed tomography-based monitoring and management of target and organ motion during external beam radiotherapy in cervical cancer. *Phys Imaging Radiat Oncol*. 2018;9(December 2018):14-20. doi:10.1016/j.phro.2018.12.002
50. Bandanatham S, Gururajachar JM, Somashekar MK. Compliance with bladder protocol during concurrent chemoradiation for cancer of the cervix and its impact on enteritis: A prospective observational study. *Reports Pract Oncol Radiother*. 2018;23(2):69-74. doi:10.1016/j.rpor.2017.12.005
51. van de Bunt L, Jürgenliemk-Schulz IM, de Kort GAP, Roesink JM, Tersteeg RJHA, van der Heide UA. Motion and deformation of the target volumes during IMRT for cervical cancer: What margins do we need? *Radiother Oncol*. 2008;88(2):233-240. doi:10.1016/j.radonc.2007.12.017
52. Jadon R, Pembroke CA, Hanna CL, et al. A {Systematic} {Review} of {Organ} {Motion} and {Image}-guided {Strategies} in {External} {Beam} {Radiotherapy} for {Cervical} {Cancer}. *Clin Oncol*. 2014;26(4):185-196. doi:10.1016/j.clon.2013.11.031
53. Sun R, Mazeron R, Chargari C, Barillot I. Du CTV au PTV dans les cancers du col utérin : vers une radiothérapie adaptative. *Cancer/Radiotherapie*. 2016;20(6-7):622-628.

doi:10.1016/j.canrad.2016.07.088

54. Pötter R, Tanderup K, Kirisits C, et al. The EMBRACE II study: The outcome and prospect of two decades of evolution within the GEC-ESTRO GYN working group and the EMBRACE studies. *Clin Transl Radiat Oncol*. 2018;9:48-60. doi:10.1016/j.ctro.2018.01.001

55. Beadle BM, Jhingran A, Salehpour M, Sam M, Iyer RB, Eifel PJ. Cervix Regression and Motion During the Course of External Beam Chemoradiation for Cervical Cancer. *Int J Radiat Oncol Biol Phys*. 2009;73(1):235-241. doi:10.1016/j.ijrobp.2008.03.064

Chapter 3: IGART strategies for cervix cancer

This chapter includes work published by the author – Appendix I (O'Reilly FHJ, Shaw W, Phys. Med. (2016), http://dx.doi.org/10.1016/j.ejmp.2016.06.003)

3.1 Introduction

Treatment of locally advanced cervix cancer is generally a combined modality approach of radiotherapy and chemotherapy [1]. This combination yields an increase of 6% overall and disease-free survival at 10 years post-treatment compared to radiotherapy alone and in addition, reduces the rate of distant metastases occurrence [2,3]. A local control rate, even in advanced disease, of >90–95% is achievable when external beam radiotherapy (EBRT) and chemotherapy is combined with image-guided adaptive brachytherapy (IGABT) [4]. While these excellent local control rates can be achieved, the predominant mode of failure for these patients is distant metastases [2,5]. Generally the whole pelvis four-field box technique is used to ensure adequate coverage of the lymphatic drainage system (common-, internal and external iliac nodes) and the primary tumour, consisting of the uterus, cervix, and vagina [6,7]. However, the dose that can be delivered in this approach is limited by the incidence and severity of late toxicity of the surrounding organs at risk (OARs) including the bowel, rectum, bladder, and vagina of which a considerable volume is included in the treatment fields [8]. Gastrointestinal (GU), genitourinary (GI), and bone marrow toxicities are commonly associated with this technique and are the primary drivers for implementation of more conformal and high precision EBRT such as intensity-modulated radiotherapy (IMRT) for OAR sparing [9,10]. Compared to conventional techniques, IMRT offers significant OAR dose sparing with similar or improved tumour control and survival [4]. The improved OAR sparing of IMRT also offers the possibility for the safe and effective use of concomitant boost to the para-aortic lymph node region [5]. These promising results are however inhibited by the potential for underdosing the target due

to substantial inter-and intrafraction motion in the female pelvis [11]. In addition, tumour regression may be in the order of 60–80% of the pre-therapeutic tumour volume allowing the OARs to frequently move into the high dose area [12]. To address this complex and patient-specific anatomical motion, large planning margins, frequent imaging, or plan adaptation would likely be required to ensure adequate EBRT tumour coverage.

Several image-guided adaptive radiotherapy (IGART) methods for the treatment of cervical cancer have been proposed [13,14]. Such methods are effective as treatment techniques to address geometrical variations in a large population of patients as they cater for the individual, whereas non-adaptive techniques run the risk of sub-optimal treatment for some patients. In this retrospective planning study, we perform a dosimetric evaluation of two IGART strategies utilizing the equivalent uniform dose (EUD) metric for targets and generalized EUD (gEUD) metric for OARs [15,16]. The first strategy utilizes a lower workload off-line 'wait-and-see' concept and adapts the treatment based on what has been delivered in the past, while the second strategy is a higher workload online margin of the day (MOD) approach and relies on the current geometrical configuration for selection of an acceptable treatment plan. A fixed margin approach was used as a benchmark to evaluate the effectiveness of these strategies.

3.2 Materials and Methods

3.2.1 Treatment and patient data

Two patient groups receiving radical radiotherapy treatment for cervix cancer were included in this retrospective planning study. IGART strategies were simulated for both groups, the first group (study 1) consisted of 10 patients with a limited number of computed tomography (CT) images per patient. The second group (study 2) included 20 patients, 15 imaged and treated with an empty bladder (EB) and 5 with a full bladder (FB) protocol. Patients in study 2 had a planning CT as well as daily pre-treatment cone-beam CT (CBCT) imaging for setup correction. A detailed summary of patient characteristics and imaging for this group is given in Chapter 2, Table 1. Study 1 was used to validate the IGART strategies while study 2 was used to test these strategies.

This study received ethical approval from the local ethics committee (ECUFS 28/2014A). Both these groups received EBRT in the form of a four-field box technique and treatment plans were generated using planning CT-based image datasets. The prescribed dose was 50.0 Gy in 25 fractions of 2.0 Gy to the ICRU reference point and the distribution of International Federation of Gynecology and Obstetrics (FIGO) stage classification for local tumor stage was IIB = 3 and IIIB = 7 for study 1, and IIB = 4 and IIIB = 16 for study 2. Concomitant weekly Cisplatin-based chemotherapy (5–6 x 25 mg/m^2 body surface area) was also administered during this time. Patients received an additional 5 fractions brachytherapy boost of at least 15.0 Gy to point A in the third week of EBRT. Overall treatment time was less than 44 days.

3.2.2 Imaging and delineation

3.2.2.1 Study *1*

During treatment, an additional set of 9 CT scans were acquired of each patient. A Toshiba Acquilion LB 16 slice CT scanner (Canon Medical Systems) was used to acquire 2mm slice thicknesses. These ranged from the L2 vertebral body to the 10 cm below the ischial tuberosities in the supine position. These datasets consisted of 4 pre-treatment CTs and one consecutive weekly CT during the five weeks of EBRT. The 4 pre-treatment set of images represent random movement of the tumour and OARs during the stage of treatment planning when tumour regression has not begun and conventional planned dose distributions are governed by a single snapshot in time of the tumour and OAR positions. No bladder or bowel protocol was followed in this study and the additional 9 CT image datasets played no part in the actual treatment of the patients.

The target volume and organs at risk were manually contoured on all CT scans. Delineation was performed by an experienced Radiation Oncologist using a standardized method of contouring[17]. The primary clinical target volume (pCTV) consisted of the utero-cervix and the upper third of the vagina (depending on the tumour extent). The organs at risk included the bladder-, sigmoid- and rectal wall, as well as the small bowel plus peritoneal cavity.

The nodal CTV (nCTV) included involved nodes and relevant draining node groups (common, internal, and external iliac and obturator and pre-sacral lymph nodes). Dosimetric assessments were done for the nCTV and not each nodal group individually.

3.2.2.2 Study 2

The scanning protocol from study 1 was used to acquire a planning CT. In addition, daily CBCTs (25 cm length) were acquired using the Elekta XVI^{TM} system. CBCT protocols were optimized to achieve optimal image quality and minimal dose, resulting in 5mm slice thicknesses. Target volumes and OARs, similar to study 1, were manually contoured on all CT and CBCT images by a single observer and verified by multiple experienced Radiation Oncologists using a standardized method of contouring [17,18]. As opposed to study 1, the entire OAR was delineated and not the wall of the rectum, bladder and sigmoid. For simplicity OARs of both studies will be referred to as rectum, bladder and sigmoid. For the small bowel a reference volume of 200 cm^3 was used for calculations due to the fact that less than the whole bowel volume was contoured [19]. Dosimetric assessments were done for each nodal group individually in this study.

For both studies each CT dataset was rigidly registered (utilizing mutual information) with the original planning CT based on bony anatomy matching using Monaco Sim software (Monaco® 5, Elekta Oncology Systems). Registration was performed automatically and adjusted manually when required. The above-mentioned structures were contoured on each of the CBCT datasets and copied to the original planning CT for further dose assessments. The relative electron densities of all low-density structures and cavities on the first CT dataset were overridden with the density of water to eliminate low-density dose artefacts.

3.2.3 Treatment planning

The Hyperion (University of Tübingen, Germany) treatment planning system (TPS) was used to generate treatment plans. Hyperion utilizes a method of biological optimization employing the equivalent uniform dose (EUD)[20]. The TPS uses Monte Carlo (MC) dose calculations to compute IMRT segments that are modified and weighed during dose optimization[21]. Planning objectives

and constraints were derived from the Quantitative Analysis of Normal Tissue Effect in the Clinic (QUANTEC), EMBRACE-II protocol, and published EUD data[22–25]. Table 1 provides a summary of the most important objectives and constraints employed for plan optimization. For simplicity, we refer to both the EUD and gEUD as EUD only. The total volume of the PTV, as well as OAR planning volumes, were included in the calculation of the cost function values.

3.2.3.1 Study 1

For EUD calculations, $\alpha = 0.4$ was used in the case of the Poisson Cell Kill and the volume effect parameters for the gEUD calculations were a = 12 for the rectum, sigmoid and small bowel, and a = 8 for the bladder. A library of IMRT treatment plans with uniform incrementally increasing pCTV-to-primary planning target volume (pCTV) margins (5, 7, 10, 15, 20 and 25 mm) based on the delineated structures on the first CT scan was constructed. A fixed 7 mm nCTV margin was used for the nodal CTV. 6 MV IMRT plans using nine equi-distant beam angles were created to deliver a prescribed dose of 50.0 Gy to the primary and nodal PTVs.

3.2.3.2 Study 2

10 MV VMAT plans were created to deliver a prescribed dose of 45.0 Gy in 25 fractions to the primary and nodal PTVs. For this study the treatment regime as suggested by EMBRACE II were followed [26]. A library consisting of 4 plans with a 7-, 10-, 15-, and 20 mm fixed CTV-to-PTV margin was generated based delineated structures from the planning CT. From our experience an $\alpha = 0.8$ resulted in better pCTV coverage and was therefore used in calculations. Volume parameters used in this study was a = 12 for the rectum and sigmoid, a = 8 for the bladder and a = 4 for the small bowel. These values were based on more recent published data [19,27,28].

Table 1: Summary of the most relevant EUD planning objectives and constraints used for the generation of plans.

	Objectives (Gy)		Constraints (Gy)	
	Study 1	Study 2	Study 1	Study 2
pCTV	≥49.8	≥44.9		
nCTV	≥49.8	≥44.9		
Rectum			≤ 48.0	≤ 42
Bladder			≤ 47.0	≤ 42
Sigmoid			≤ 48.0	≤ 43
Small Bowel			≤ 47.0	≤ 32

3.2.4 Treatment simulation

Treatment simulation will be explained for study 1. The same procedure was used in study 2. Important differences will be emphasized.

3.2.4.1 Fixed margin

A fixed margin (FM) approach was used as a dosimetric benchmark to test the effectiveness of the adaptive treatment strategies. Fixed primary PTV margins were applied to the first fraction (i = 1) and CT delineated pCTV (pCTV$_1$) and the rest of the treatment was simulated by scoring the dose to all delineated volumes of the successive delineated CTs as the structures were copied from their respective CTs to the first one. This was repeated for the margin sizes in the libraries. For the sequential delineated structures, the average EUDs could be computed via

$$EUD_{ave} = \frac{1}{n}\sum_{i=1}^{n} EUD_i \quad (1)$$

Here, i is the simulated treatment fraction and n the total CT datasets (and thus treatment fractions) included in the calculation of EUD_{ave} (maximum value of n = 9 and n = 25 for study 1 and 2 respectively). Dose scoring was done without any intervention or adaptation to the original optimized IMRT plan. Regardless of the strategy employed, the nodal CTV (nCTV) was contained inside a fixed 7- and 5 mm nPTV margin for study 1 and 2 respectively.

3.2.4.2 Offline adaptation

An individual offline plan adaptation strategy was simulated with full dosimetric analysis performed *between* treatment fractions *i* and j, i being the last fraction that was treated and j the fraction to be treated. $pCTV_i$ was contoured offline, disregarding all other contours, and $EUD_{(i,x)}$ calculated for each margin plan in the existing library where $x = marginsize\ (x \in$ 5, … 25 mm) and X the margin used for treatment. The first treatment fraction was delivered using a 15 mm pCTV margin plan ($X = 15$ mm). Thus, the actual delivered dose recorded for fraction 1 was $EUD_{(1,15\ mm)}$. The smallest margin size selection with adequate tumour coverage and to obtain OAR dose sparing for the rest of the simulated treatment fractions (j = 2,…n), was performed using the following procedure: If j is the fraction to be treated and a margin size (x needs to be determined for j, we determine x such that after j fractions,

$$EUD_{ave} = \frac{1}{j-1}\sum_{i=1}^{j-1} EUD_{i,X} \tag{2}$$

$$\frac{EUD_{(i,x)} + EUD_{(ave)}}{2} \geq C \tag{3}$$

And **C** = 49.8 Gy and 44.9 Gy EUD for studies 1 and 2 respectively. In Eq. (3), $EUD_{(i,x)}$, serves as an estimate of what dose will be delivered in fraction j if the geometry in j is similar to the geometry in the past fraction, i. This method is optimistic in the sense that the most recent pCTV geometry will persist in fraction j.

However, as a safety feature to prevent tumour under-dosage a minimum margin size for treatment fractions $j \geq 3$ was calculated using a moving average approach,

$$x_{min} = \frac{1}{j-2}\sum_{i=2}^{j-1} x_i \quad (4)$$

From our experience, a 0.2 Gy drop from 50 Gy prescribed EUD is mostly comparable to an approximately 5% dose reduction from 50 Gy prescribed dose in the pCTV as recommended by the ICRU in terms of dose-volume histogram (DVH) parameters [29]. When Eq. (3) resulted in an under-dosage the margin with the maximum EUD_i was chosen.

3.2.4.3 Online adaptation

Lastly, we investigated an individualized online adaptive strategy where the adaptation in the treatment is based on the daily $pCTV_j$ position and geometry that will be treated. Thus, $pCTV_j$ was contoured with the patient in the treatment position and the most appropriate margin-of-the-day (MOD) was selected online from the library of plans with the criterion that the $pCTV_j$ will receive a EUD of at least 49.8 Gy (study 1) and 44.9 Gy (study 2), regardless of the OAR dose. In contrast to the off-line strategy, contouring and subsequent plan selection should be performed before treatment. As per the off-line strategy the pCTV always has priority when selecting a margin size plan.

3.2.5 Dose accumulation and data analysis

One method of dose calculation in four dimensions (4D) is to accumulate the dose in a reference geometry through deformation fields, obtained from deformable image registration (DIR). However, this is a largely unsolved problem in the pelvic region. Alternatively, Sobotta et. al. [30] exploited the mathematical properties of concave and convex score functions, like the EUD for tumours and OARs, to calculate a reliable worst-case estimate of the accumulated dose in multiple geometry instances. In effect, the accumulated

instance EUDs will never be lower than this estimate for a tumor, and never be higher than the estimate for an OAR. These estimates are computed without the need for DIR and are a quick scoring method of a treatment plan at only a fraction of the computational cost of a full dosimetric analysis.

In this study, we promulgate the use of EUD dose metrics for IGART for two reasons: (a) The EUD is a quick, reliable, and repeatable cumulative dose scoring method underpinned by the Jensen Inequality, and (b) it is safe to use in the absence of proper deformation fields and computes upper and lower bounds that err on the safe side [30–32]. The EUD was used as a dose metric in this study to investigate the effectiveness of these planning strategies while DVH parameters were scored in addition. Tumor EUD_{ave} values were required to be at least at a level of 49.8 Gy (study 1) and 44.9 Gy (study 2) for the treatment to be regarded as dosimetrically acceptable. On the other hand, successful OAR sparing required that EUD_{ave} be equal to or lower than the optimization result of the first (planning) CT. In addition to the EUD results, common DVH parameters used in EBRT plan assessment were calculated to describe the fluctuations in dose distributions related to tumor and OAR motion and geometrical changes to be comparable to other published results. They included D_{98} for the tumor, while D_{50}, and D_{30} were calculated for the OARs. For study 2, V_{30} and V_{40} were scored for the bladder, rectum and sigmoid and V_{15} and V_{45} for the small bowel.

3.2.6 Statistical analysis

The Wilcoxon signed ranked test and paired t-test were used to test statistical differences in CTV and OAR doses for the different strategies. Statistical significance was defined as $p < 0.05$.

3.3 Results

3.3.1 Timeline and tumour shrinkage

The median tumour volume on the planning CT was 211 cm^3 and ranged from 175 – 336 cm^3 and 218 cm^3 and ranged from 93 – 489 cm^3 in studies 1 and 2 respectively. In study 1 no significant changes in these volumes during the first 4 CT scans before treatment and similarly no changes in the first two weeks of treatment were noted. However, significant average pCTV volume reductions from the third week of treatment (9% reduction) to the final week (18% reduction, range 5% - 54%) were seen. In study 2 the largest reduction in pCTV volume was also seen from the third week of treatment (22% reduction, range 7 % - 44%) to a 32% reduction in the final week (range 10 % – 57 %).

3.3.2 Fixed margin strategy

3.3.2.1 Study 1

When utilizing a fixed pCTV-pPTV planning margin, the EUD_{ave} for the population of patients ranged from 46.9 ± 10.5 Gy to the pCTV and 52.3 ± 1.7 Gy to the nCTV for a 5 mm margin, to 51.1 ± 2.3 Gy to the pCTV and 52.5 ± 2.1 Gy to the nCTV for a 25 mm margin from the 9 treatment simulations. The OAR EUDs ranged from 46.4 ± 3.2 Gy, 46.9 ± 3.9 Gy, 48.9 ± 3.6 Gy,44.7 ± 3.2 Gy to the rectum, bladder, sigmoid and small bowel respectively in the case of a 5 mm margin, to 50.1 ± 0.9 Gy, 49.7 ± 1.7 Gy, 50.7 ± 2.1 Gy, 45.9 ± 3.0 Gy for the same structures with a 25 mm margin. Results are summarized in Appendix, Table A1.

3.3.2.2 Study 2

The pCTV EUD_{ave} for the EB group ranged from 43.92 ± 1.64 Gy for a 7 mm margin to 45.45 ± 0.30 Gy for a 20 mm margin and 44.43 ± 0.96 Gy to 45.33 ± 0.14 Gy for the FB group. The EUD_{ave} for all nodal groups were ≥ 44.9 Gy for all margins in the library (Table 2) and both groups. The average EUDs for OARs in the EB patient group ranged from 41.48 ± 1.20 Gy, 40.45 ± 1.26 Gy, 42.43 ± 1.23 Gy and 28.83 ± 3.22 for the rectum, bladder, sigmoid and small bowel for a 7 mm

margin to 44.04 ± 0.46 Gy, 43.27 Gy ± 0.75, 44.10 ± 0.73 Gy and 29.75 ± 3.71 Gy for a 20 mm margin. The average rectum and sigmoid EUDs for the full bladder patients were comparable to that of the EB group. However, for all margin sizes increased bladder and small bowel sparing were noted for FB patients (Table A1). For both studies, the pCTV EUD_{ave} were statistically greater for each incremental increase in margin size with $p < 0.05$ in all cases. The nCTV showed no difference.

Table 2: Study 2 - Average EUDs (Gy) ± stdev to the nodal groups using a fixed margin approach.

	7	10	15	20
Empty bladder				
CIR	46.1 ± 0.8	46.2 ± 1.0	46.0 ± 0.9	46.0 ± 0.9
CIL	46.0 ± 1.0	46.2 ± 0.9	45.9 ± 0.9	46.0 ± 0.9
EIR	45.8 ± 0.4	46.1 ± 0.3	45.8 ± 0.3	45.7 ± 0.4
EIL	45.7 ± 0.5	45.9 ± 0.6	45.6 ± 0.5	45.5 ± 0.5
IIR	46.1 ± 0.3	46.2 ± 0.3	45.9 ± 0.3	45.7 ± 0.5
IIL	46.2 ± 0.2	46.4 ± 0.2	46.0 ± 0.3	45.4 ± 0.6
OBTL	45.7 ± 0.9	46.0 ± 0.9	45.6 ± 0.8	45.4 ± 0.8
OBTR	45.9 ± 0.5	46.1 ± 0.4	45.4 ± 1.2	45.2 ± 0.7
PreSac	45.5 ± 0.7	45.7 ± 0.6	45.5 ± 0.6	45.4 ± 0.4
Full bladder				
CIR	46.5 ± 0.2	46.8 ± 0.3	46.3 ± 0.5	46.4 ± 0.5
CIL	46.4 ± 0.3	46.6 ± 0.3	46.3 ± 0.2	46.3 ± 0.2
EIR	45.8 ± 0.2	46.2 ± 0.3	45.8 ± 0.3	45.8 ± 0.2
EIL	45.8 ± 0.3	46.0 ± 0.4	45.7 ± 0.3	45.5 ± 0.4
IIR	46.3 ± 0.1	46.5 ± 0.2	45.9 ± 0.4	45.8 ± 0.3
IIL	46.0 ± 0.3	46.3 ± 0.4	45.7 ± 0.3	45.7 ± 0.3
OBTL	45.9 ± 0.1	46.2 ± 0.2	45.7 ± 0.4	45.5 ± 0.3
OBTR	45.9 ± 2.0	46.3 ± 0.3	45.6 ± 0.3	45.5 ± 0.3
PreSac	45.0 ± 1.9	45.2 ± 2.6	45.0 ± 1.7	45.1 ± 1.0

**CIR and CIL = common iliac right and left, EIR and EIL = external iliac right and left, IIR and IIL = internal iliac right and left, OBTR and OBTL = obturator right and left, PreSac = Presacral*

Figure 1 and Figure 2 provides a graphical presentation of box-whisker plots of the distribution of the EUD_{ave} and DVH parameter metrics for the fixed margin approach. Adequate CTV coverage, 49.8 Gy and 44.9 Gy, were seen for margins ≥ 15 mm in both studies. Therefore, the 15 mm margin will be used as a benchmark to test other strategies. Significant under-dosages (<49.8 Gy and 44.9 Gy) were seen for margins ≤ 10 mm. These results are supported by both the EUD and DVH parameter metrics, while other authors found similar results [33,34].

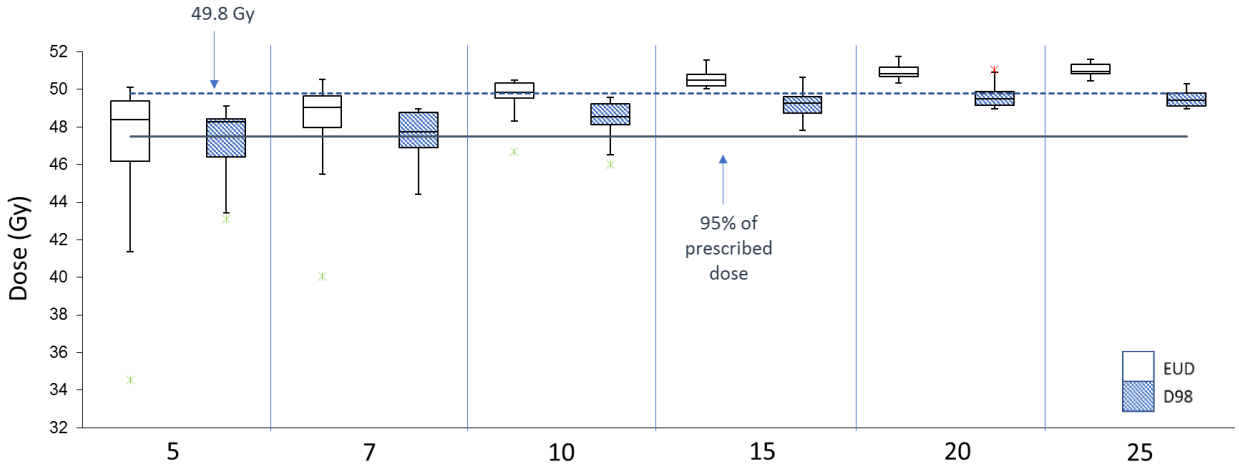

Figure 1: Study 1 - Box-whisker plots of EUD_{ave} (open) and the dose to 98% volume (D_{98}) (striped) for the pCTV for increasing CTV-PTV margin sizes using a fixed margin approach. The deviation of parameters for the whole population around the median is shown.

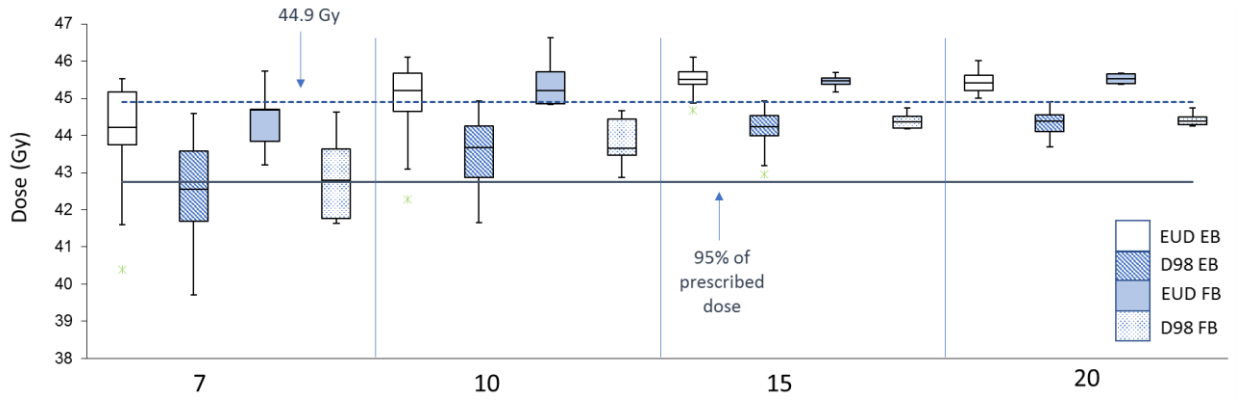

Figure 2: Study 2 - Box-whisker plots of EUD_{ave} and the dose to 98% volume (D_{98}) for the pCTV for increasing CTV-PTV margin sizes using a fixed margin approach. The deviation of parameters for the whole population around the median is shown for the empty and full bladder patients.

When smaller margins are applied, the OAR doses are on average much smaller than planning with larger margins due to the larger overlap of PTV and OAR in the case where large margins are used (OAR EUD and DVH parameter box-whisker plots for study 1 are provided in the Appendix, Figure A1 and DVH parameters of study 2 in Figure A2). OAR EUDs for the empty- and full bladder patients from study 2 are shown in Figure 3. Smaller margins thus lead to significant OAR sparing but, too small margins lead to sub-optimal tumour doses due to geometric miss.

When comparing the resultant OAR doses to those used for initial optimization in Table 1, acceptable OAR doses were observed for small margins. Larger volumes of the OAR overlap with the pPTV as the margin increases and at some stage, there is no room for OAR sparing anymore as the overlap region is just too big. In such cases, there is virtually no difference in terms of OAR dose compared to conventional four-field box techniques, although non-specified normal tissue dose can still be reduced to some extent with IMRT. In both studies, similar trends of dose increases are observed for the rectum, bladder, and sigmoid. These increases were statistically significant for the rectum and bladder. The increase in sigmoid doses was statistically significant for small margins but remained relatively constant for margins ≥15 mm. The small bowel on the other hand exhibited smaller variations in dose as the margins increased. These results are supported by the DVH parameters (see Appendix Fig. A1 and A2). It is expected that full bladders

will move healthy tissue, such as the small bowel and part of the bladder away from the treatment field [35]. This is indeed the case as illustrated in Figure 3 where notably higher EUDs to the bladder and small bowel are seen in the EB group compared to the FB group.

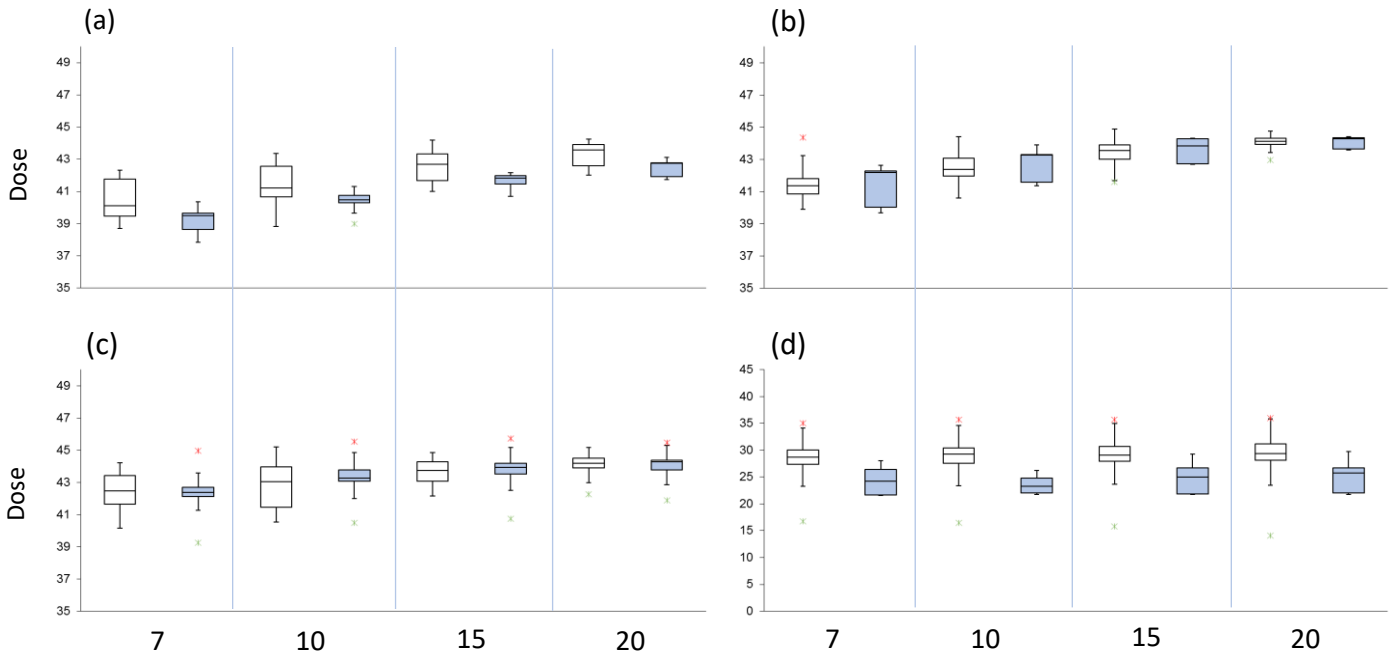

Figure 3: Box-whisker plots of of EUD_{ave} of the a) bladder, b) rectum, c) sigmoid, and d) small bowel with increasing CTV-PTV margin sizes using a fixed margin approach. Results shown are for study 2, empty bladder (open) and full bladder (solid).

3.3.3 Offline and online strategy

3.3.3.1 Study 1

The EUD_{ave} for the population of patients using the off-line strategy were 50.0 ± 5.0 Gy for the pCTV and 52.1 ± 1.8 Gy for the nCTV. The OAR EUDs were 48.1 ± 3.6 Gy, 48.1 ± 5.3 Gy, 49.8 ± 3.9 Gy, and 45.2 ± 3.6 Gy for the rectum, bladder, sigmoid and small bowel respectively (Table 4). As illustrated in Figure 4a, sufficient CTV coverage was achieved for all patients with only a slight total EUD under-dosage in one patient (49.7 Gy). Under-dosages were found in some fractions, but the adaptation was able to recover the total required dose for all patients except this one.

Using the most appropriate MOD based on the daily $pCTV_i$ position and geometry yield an EUD_{ave} for the population of 50.4 ± 2.0 Gy for the pCTV and 52.0 ± 1.5 Gy for the nCTV. The OAR EUDs was 48.2 ± 4.5 Gy, 48.0 ± 5.2 Gy, 49.8 ± 4.2 Gy, and 45.1 ± 3.4 Gy for the rectum, bladder, sigmoid and small bowel respectively (Table 3). In this strategy, none of the patients received a pCTV dose lower than 49.9 Gy which is above the tumour objective (Figure 4a). The D_{98} parameter supports the EUD results with no under-dosage. Results demonstrated that whenever a fractional under-dosage occurred, it was small in magnitude and the delivered dose in fractions preceding these under-dosages were large enough in magnitude to offset such small under-dosages.

Table 3: Summary of the average EUDs (Gy) to the pCTV, nCTV and OARs for the population of patients using the offline and online approach.

	pCTV	nCTV	Rectum	Bladder	Sigmoid	Small bowel
Study 1						
Offline	50.0 ± 5.0	52.1 ± 1.8	48.1 ± 3.6	48.1 ± 5.3	49.8 ± 3.9	45.2 ± 3.6
Online	50.4 ± 2.0	52.0 ± 1.5	48.2 ± 4.5	48.0 ± 5.2	49.8 ± 4.2	45.1 ± 3.4
Study 2 – empty bladder						
Offline	45.3 ± 0.5		42.2 ± 1.4	41.4 ± 1.3	43.0 ± 1.2	29.7 ± 2.0
Online	45.4 ± 0.3		41.3 ± 2.3	40.6 ± 1.6	42.4 ± 1.2	29.6 ± 2.0
Study 2 – full bladder						
Offline	45.4 ± 0.3		42.4 ± 1.1	40.0 ± 1.4	41.8 ± 2.1	24.7 ± 3.4
Online	45.5 ± 0.2		41.6 ± 1.1	39.2 ± 1.6	41.3 ± 2.1	24.2 ± 3.4

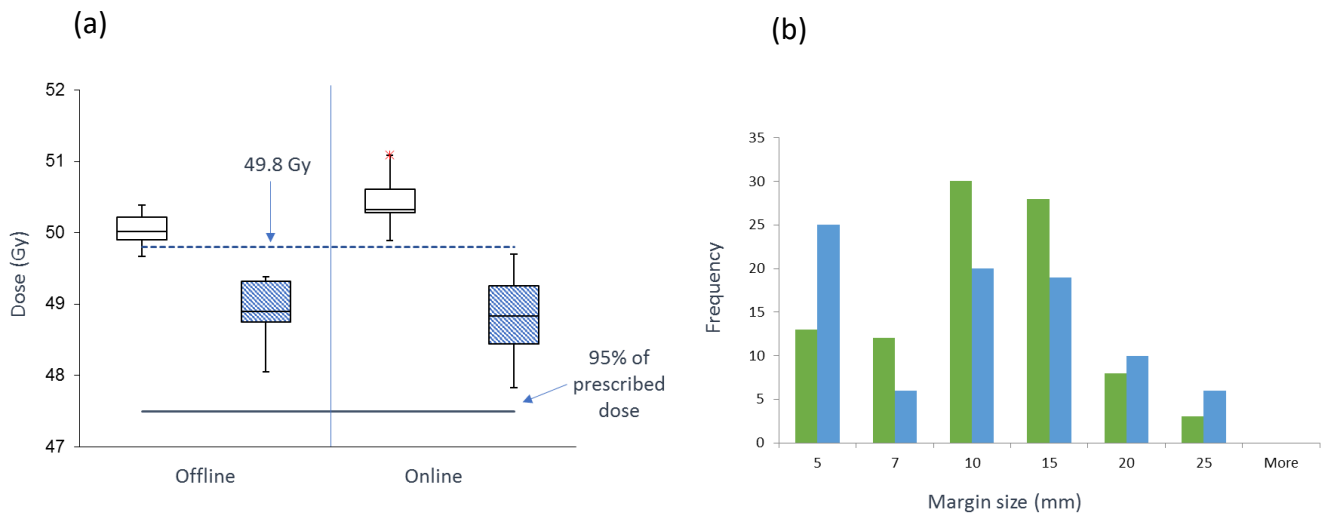

Figure 4: Study 1 - (a) Box-whisker plots of EUD_{ave} (open) and dose to 98% volume (D_{98}, patterned) for the pCTV when using an off- and online approach. The deviation of parameters for the whole population around the median is displayed. (b) Frequency distribution of margin sizes used for treatment for the entire patient population in the offline (green) and online (blue) adaptation strategies.

3.3.3.2 Study 2

The EUD_{ave} for the pCTV using the off-line strategy were 45.29 ± 0.49 Gy and 45.43 ± 0.28 Gy for the empty- and full bladder patients respectively (Table 4). The EUD_{ave} for all relevant nodal groups was≥ 45.0 Gy (Table 5). Although the median EUD for the EB patients was≥44.9 Gy, under dosages were seen in 3 patients (Figure 5a). No under dosages were seen in the FB group (Figure 5c). For both groups, the D_{98} parameter showed sufficient coverage with no under dosages.
The online adaptive strategy resulted in average EUD values of 45.40 ± 0.27 Gy and 45.47 ± 0.20 Gy to the pCTV of the EB and FB patients respectively (Table 3). As seen in the offline strategy all nodal groups received doses larger than 45.0 Gy (Table 4). No under dosages were seen in either of the groups (Figure 5a and c). The D_{98} parameter showed sufficient coverage (≥42.75 Gy) for both groups.

In general, the OARs EUDs for the off- and online strategies were comparable. With the offline strategy EUD_{ave} for the EB patients were 41.36 ± 1.27 Gy, 42.24 ± 1.38 Gy, 42.95 ± 1.21 Gy, and 29.74 ± 2.00 Gy for the bladder, rectum, sigmoid and small bowel respectively and with the online

strategy 40.63 ± 1.63, 41.31 ± 2.29 Gy, 42.42 ± 1.22 Gy and 29.56 ± 1.98 Gy. From figure 6 it can be seen that the rectal and sigmoid EUDs obtained for the EB and FB group were similar (Table 3) with bladder and small bowel EUDs being notably lower. The increased sparing for the bladder and small bowel in the FB group were seen for both strategies. These results are supported by DVH parameters (Appendix, Figure A3 and A4). These results agree with data from the FM strategies.

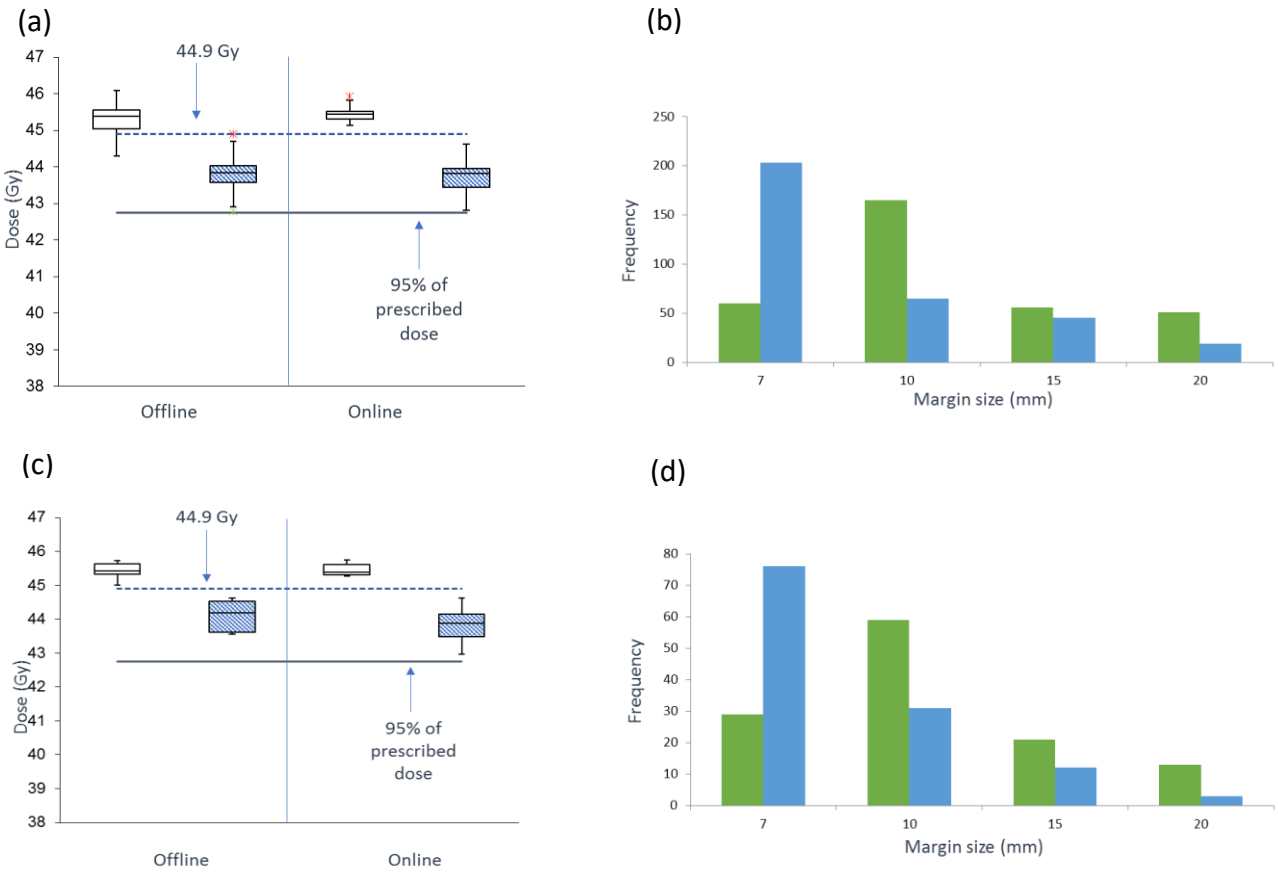

Figure 5: Study 2 - Box-whisker plots of EUD_{ave} (open) and dose to 98% volume ($D_{98,}$ patterned) for the pCTV when using an off- and online approach for (a) empty bladder and (c) full bladder patients. The deviation of parameters for the whole population around the median is displayed. Frequency distribution of margin sizes used for treatment for the entire patient population in the offline (green) and online (blue) adaptation strategies for (b) empty bladder and (d) full bladder

Table 4: Study 2 – Average EUDs (Gy) ± stdev to the nodal groups using an off- and online adaptive strategy.

	Offline	Online
Empty bladder		
CIR	46.1 ± 0.9	46.1 ± 0.9
CIL	46.1 ± 0.9	46.1 ± 1.0
EIR	45.8 ± 0.5	45.6 ± 0.7
EIL	45.7 ± 0.5	45.6 ± 0.7
IIR	46.1 ± 0.4	46.1 ± 0.3
IIL	46.0 ± 0.6	46.1 ± 0.5
OBTL	45.8 ± 0.9	45.8 ± 0.9
OBTR	45.8 ± 0.6	45.6 ± 0.7
PreSac	45.6 ± 0.6	45.6 ± 0.6
Full bladder		
CIR	46.6 ± 0.4	46.6 ± 0.2
CIL	46.4 ± 0.3	46.4 ± 0.3
EIR	46.0 ± 0.3	45.9 ± 0.2
EIL	46.0 ± 0.4	45.9 ± 0.4
IIR	46.2 ± 0.3	46.3 ± 0.1
IIL	46.0 ± 0.4	46.0 ± 0.2
OBTL	46.0 ± 0.3	45.9 ± 0.1
OBTR	46.0 ± 0.4	46.0 ± 0.1
PreSac	45.4 ± 1.6	45.1 ± 1.9

**CIR and CIL = common iliac right and left, EIR and EIL = external iliac right and left, IIR and IIL = internal iliac right and left, OBTR and OBTL = obturator right and left, PreSac = Presacral*

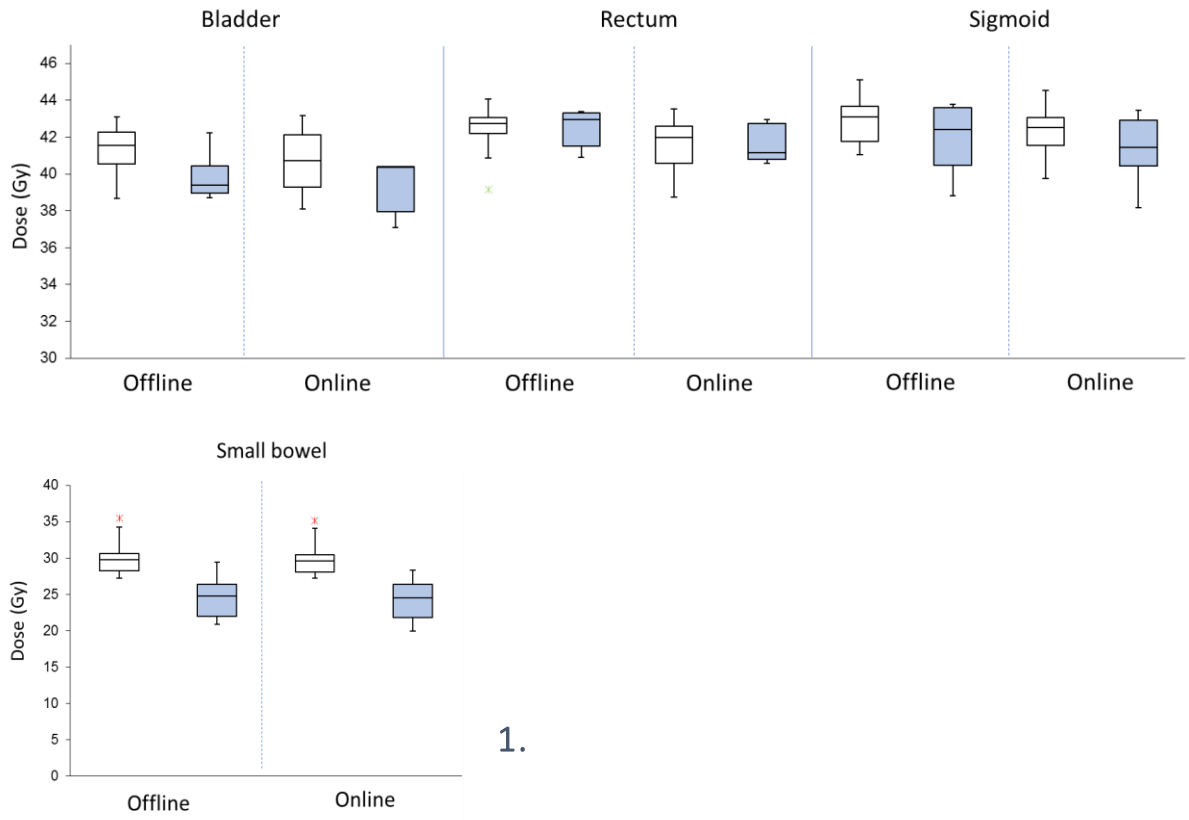

1.

Figure 6: Box-whisker plots of EUD_{ave} of the bladder, rectum, sigmoid, and small bowel for the off- and online adaptive strategies. Results shown are for study 2, empty bladder (open) and full bladder (solid).

3.3.4 Comparison

The offline and online strategy resulted in the frequent use of smaller margins (Figure 4b and Figure 4b and d). Similar trends were seen in studies 1 and 2. It is expected that the use of smaller margins in this way would result in reduced OAR doses compared to FM. This was indeed the case (Figure 7 and Figure 8) as statistically lower OAR doses were found in this technique for all OARs, supported by EUD and DVH dose metrics. When the off-line strategy is compared to a 15 mm FM strategy, the off-line strategy resulted in a distribution of pCTV EUD_{ave} that was lower than the FM strategy. However, sufficient coverage was still evident when applying the off-line strategy. There were insignificant differences in the distribution of EUD_{ave} to the pCTV when the online strategy was compared to FM. Ultimately, for the same pCTV dose as in the FM strategy, significant OAR sparing for the bladder, rectum, sigmoid were found (Figure 7 and Figure 8). OAR sparing for the small bowel was more pronounced in the FB group. In general, the median

EUD_{ave} was lower for the online strategy demonstrating the advantage of this technique for individuals in a population. The FM strategy does not allow this advantage for individuals. To summarize the results both adaptive strategies and the 15 mm FM resulted in adequate pCTV coverage. The advantage of the two adaptive strategies is that the MOD resulted in a very high tumour dose while some OARs could be spared. The off-line strategy did not achieve the same tumour dose distribution, but the doses still conformed to the prescription while all OAR were spared.

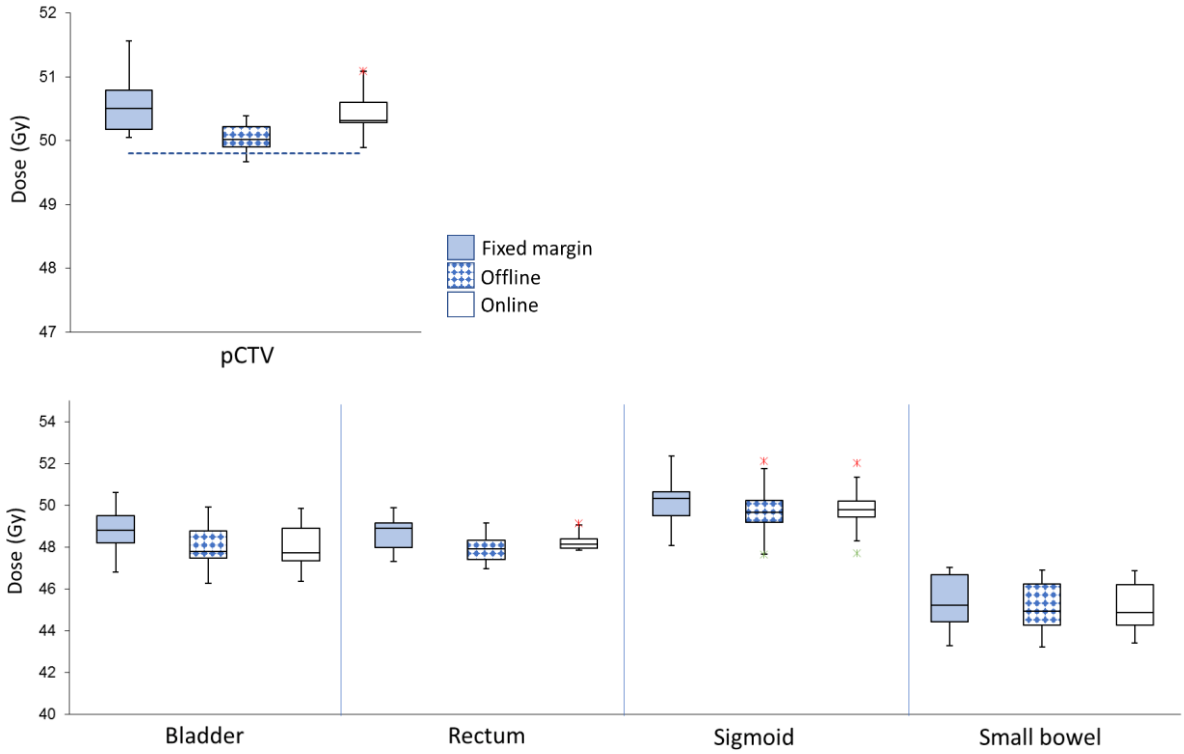

Figure 7: Study 1 - Box-whisker plots of EUD_{ave} for the pCTV and OARs using a fixed margin, off-line, and on-line approach. The deviation of parameters for the whole population around the median is shown.

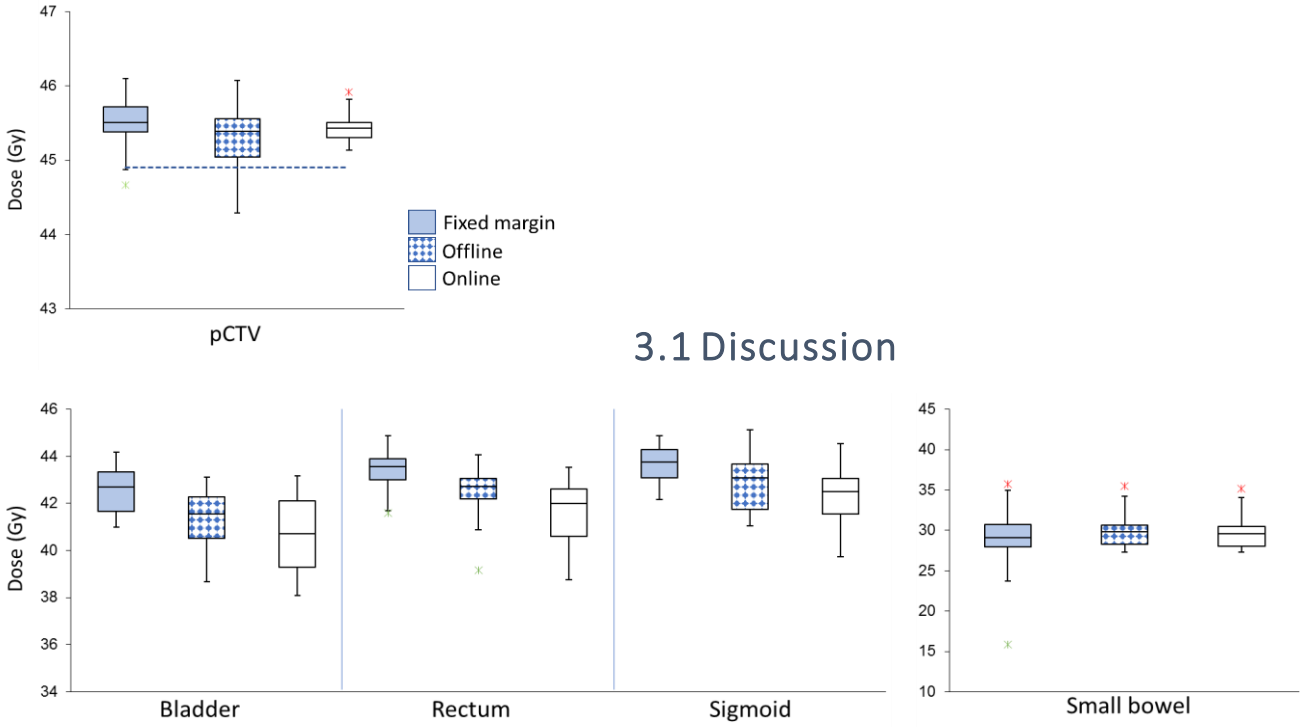

Figure 8: Study 2 - Box-whisker plots of EUD_{ave} for the pCTV and OARs using a fixed margin, off-line, and on-line approach. The deviation of parameters for the whole population around the median is shown.

Applying the fixed margin strategy, three findings across the patient population were found: (I) The planning intent could only be satisfied for margins ≥15 mm, (II) Small margins (5 and 7 mm) yield adequate CTV coverage for patients with very stable organ and tumour geometries, and (III) using margins ≤10 mm will always lead to under-dosage in a large number of patients. Even with a 10 mm margin, under-dosages can be frequent. The advantage of IMRT treatment plans utilizing smaller CTV-PTV margins is very attractive since OARs can effectively be spared, but this must be offset with adequate tumour coverage. From the results found here, adequate tumour coverage was not achievable with fixed margins smaller than 15 mm, concurrent with previous studies [17,34]. The D_{98} evaluation supports the EUD results that 10 mm margins would lead to tumour under dosage for some patients and would be classified as risky.

Considering the population, a 15 mm FM would yield adequate results as reported by Yilmaz et al. [34]. However, using adaptive strategies treatment can be individualized yielding adequate pCTV

coverage with additional OAR dose sparing. This is particularly valuable considering the high brachytherapy doses (80-85 Gy biologically equivalent dose in 2 Gy (EQD2)) necessary to achieve local control rates in the range of 80-90% [36]. Overall, adequate tumour coverage was obtained when the off-line strategy was applied. Yet, a large under dosage in one fraction critically influences the rest of the treatment as it is difficult to restore the EUD_{ave} to what was intended. Such large under-dosages can be prevented by using past geometries to determine a minimum margin size to be used for the remainder of the treatment. Although the 15 mm margin was used often in the off-line method, smaller margins were also used offering better OAR sparing compared to the 15 mm FM.

The under-dosages seen in patients when the off-line strategy is used are mostly related to significant changes in the bladder volumes from day to day and in some cases to sudden sigmoid movements. This eludes to the fact that the off-line strategy is, (i) based on an optimistic approach using geometries from the previous fraction and (ii) can only correct for slow-changing geometries or systematic deviations as opposed to the online strategy that corrects for random deviations as well. Therefore, the off-line pCTV doses in the population will always be slightly lower than those of online. However, the selection of a minimum margin size in the off-line approach proved to act, to a reasonable extent, as a safeguard to prevent future under-dosages.

Application of an online strategy prevents geometric misses as it utilizes images of the most recent organ geometries and a MOD that ensures adequate pCTV coverage. This is supported by the results found here, as no patient received a pCTV dose lower than 49.9 Gy and 45.0 Gy EUD when this strategy was applied. Although comparable to the OAR doses of a 15 mm FM, the online strategy offers the advantage of significant OAR sparing for some individuals in a population. The nCTV dose was constant and similar for all strategies applied. This emphasizes the fact that there is virtually no inter-fraction change in nodal geometries even when a 5 mm nPTV margin, the margin sized used in study 2, is used. This supports EMBRACE II study stating

that a 5 mm nPTV margin is adequate when daily imaging, bony fusion, and couch corrections are done [26].

IGART attempts to prevent tumour under-dosage on a per fraction basis. Our results revealed that off-line strategy violations are usually a result of random anatomical changes like bladder and rectal filling which can occur in a shorter period. The optimistic approach based on previous geometries can cause heavy under dosages due to these changes which makes it difficult to recover the required dose. In contrast, the online strategy used the most recent geometries. Therefore, violations were very small and were a direct result of major geometrical changes that require additional larger margin plans in the library. Nevertheless, for this population of patients, the online strategy never resulted in any total under- dosage.

The novel use of EUD as a dose metric avoids the use of deformation fields and the associated calculation effort for dose accumulation in both off-line and online adaptation strategies. Our results demonstrate that when the target and OAR EUDs are effectively controlled, all DVH parameters are controlled at the same time, as was found in other studies [37,38]. The use of DIR for dose accumulation requires considerable extension in the already lengthy replan-time [39], while studies that did not employ DIR could make very few assumptions about the accumulated dose [33]. Thus, the EUD method is an excellent way to bypass these limitations.

It is also evident that the EUD is sensitive to pronounced under-dosage in small volumes. This is because the EUD considers the entire DVH of the tumour and not just a single point on the DVH. Importantly, we considered the dose to the primary CTV and not PTVs. The under-dosages in the EUD results that at the same time received an adequate D_{98} support this. Thus, the EUD is an even more sensitive metric to evaluate dose distributions and tumour under dosage compared to DVH parameters as small volumes of the CTV may still receive significantly low doses. Shaw et al. [37] found similar results for OAR overdosages when performing DVH-metric-only analyses in

brachytherapy. They specifically considered high doses to small volumes in the OARs that demonstrated the sensitivity of the EUD to high doses in small volumes.

Dose analyses for the off-line strategy was done between fractions with no influence on machine time, offering a lower workload compared to the MOD strategy where plan adaptation was done directly before each fraction considering the most recent organ geometries. Thus, the benefit gained by a somewhat higher CTV dose is defied by a higher workload necessary for an online strategy. Based on results found here an offline strategy offers all the benefits of an online strategy and further requires a lower workload and less machine time. Therefore, the offline strategy proves to be clinically more practical and feasible. Other studies had similar conclusions, while hybrid adaptive methods also exist[39]. To further impact the workload associated with adaptive methods, auto-contouring and planning, and bladder-filling models have been suggested [39,40]. Any of these methods could benefit from the use of EUD metrics.

In study 1 we have used only the 9 CT datasets in addition to the planning CT dataset to represent the full course of treatment. Like other similar studies [33,39], this is a limitation of our study. However, the random nature of organ movement and its influence on the absorbed dose could well be reflected in this limited image dataset: The first 4 CT scans were acquired daily during the week before treatment commenced. From our results, it was evident that there was very little change in CTV volume from CT1 to CT7. Significant differences in CTV volume were only noted from the 8th CT, which in our study represents week 3 of treatment when concomitant brachytherapy starts. The use of the first 4 CTs was an approximation made because dose deviations due to geometric variations in the first three weeks of treatment were expected to be larger than tumour shrinkage. The assumption made about slow initial tumour regression in this study was proved valid by evaluating daily tumour volumes for patients in study 2. The largest reduction in volumes were noted in the third week of treatment.

Study 2 included daily CBCTs of patients receiving treatment. Therefore, the results obtained in study 2 are a validation of the strategies proposed in study 1 as similar results in terms of the metrics scored were seen in both studies. On the contrary, the larger group of patients and image sets used emphasized the OAR sparing for both the offline and online strategies as seen in study 1. In addition, the increased OAR sparing of the bladder and small bowel when using a full bladder protocol was confirmed [35].

The results from both studies stress the importance of accounting for tissue movement and geometry variations in the female pelvis. The selection of patients may also be regarded as a limitation to this study as they are representative of a population found in one treatment center. The results found here may be different from other centers in their magnitude. However, we expect that the principles identified in this study are universal and applicable in similar ways.

3.4 Conclusion

The dosimetric evaluation of a fixed margin IMRT treatment planning approach was performed in this study and two adaptive treatment strategies were evaluated against this approach. It was found that the use of a fixed primary CTV margin ≤10 mm for the treatment of cervix cancer would lead to primary tumour under-dosages in some patients. Tumour regression and random organ movement in the female pelvis have an undesirable effect on target coverage and OAR sparing that warrants the implementation of individualized adaptive treatment strategies. On-line and off-line strategies utilizing EUD dose metrics is a fast and safe method through which CTV coverage can be restored at acceptable OAR dose levels. Considering workload and time on the treatment machine, the off-line strategy proves to be sufficient and more practical with the current infrastructure.

3.5 References

1. Portelance L, Chao KS, Grigsby PW, Bennet H, Low D. Intensity-modulated radiation therapy ({IMRT}) reduces small bowel, rectum, and bladder doses in patients with cervical cancer receiving pelvic and para-aortic irradiation. *Int J Radiat Oncol Biol Phys*. 2001;51(1):261-266.
2. Schmid MP, Franckena M, Kirchheiner K, et al. Distant metastasis in patients with cervical cancer after primary radiotherapy with or without chemotherapy and image guided adaptive brachytherapy. *Gynecol Oncol*. 2014;133(2):256-262. doi:10.1016/j.ygyno.2014.02.004
3. Kirwan JM, Symonds P, Green JA, Tierney J, Collingwood M, Williams CJ. A systematic review of acute and late toxicity of concomitant chemoradiation for cervical cancer. *Radiother Oncol*. 2003;68(3):217-226. doi:10.1016/S0167-8140(03)00197-X
4. Tanderup K, Georg D, Pötter R, Kirisits C, Grau C, Lindegaard JC. Adaptive {Management} of {Cervical} {Cancer} {Radiotherapy}. *Semin Radiat Oncol*. 2010;20(2):121-129. doi:10.1016/j.semradonc.2009.11.006
5. Vargo JA, Kim H, Choi S, et al. Extended {Field} {Intensity} {Modulated} {Radiation} {Therapy} {With} {Concomitant} {Boost} for {Lymph} {Node}–{Positive} {Cervical} {Cancer}: {Analysis} of {Regional} {Control} and {Recurrence} {Patterns} in the {Positron} {Emission} {Tomography}/{Comput. *Int J Radiat Oncol*. 2014;90(5):1091-1098. doi:10.1016/j.ijrobp.2014.08.013
6. Zunino S, Rosato O, Lucino S, Jauregui E, Rossi L, Venencia D. Anatomic study of the pelvis in carcinoma of the uterine cervix as related to the box technique. *Int J Radiat Oncol Biol Phys*. 1999;44(1):53-59. doi:10.1016/S0360-3016(98)00538-0
7. van de Bunt L, van der Heide UA, Ketelaars M, de Kort GAP, Jürgenliemk-Schulz IM. Conventional, conformal, and intensity-modulated radiation therapy treatment planning of external beam radiotherapy for cervical cancer: The impact of tumor regression. *Int J Radiat Oncol Biol Phys*. 2006;64(1):189-196. doi:10.1016/j.ijrobp.2005.04.025
8. Roszak A, Wareńczak-Florczak zaneta, Bratos K, Milecki P. Incidence of radiation toxicity in cervical cancer and endometrial cancer patients treated with radiotherapy alone versus

adjuvant radiotherapy. *Reports Pract Oncol Radiother*. 2012;17(6):332. doi:10.1016/J.RPOR.2012.07.005

9. Hasselle MD, Rose BS, Kochanski JD, et al. Clinical outcomes of intensity-modulated pelvic radiation therapy for carcinoma of the cervix. *Int J Radiat Oncol Biol Phys*. 2011;80(5):1436-1445. doi:10.1016/j.ijrobp.2010.04.041
10. Mundt AJ, Lujan AE, Rotmensch J, et al. Intensity-modulated whole pelvic radiotherapy in women with gynecologic malignancies. *Int J Radiat Oncol Biol Phys*. 2002;52(5):1330-1337. doi:10.1016/S0360-3016(01)02785-7
11. Chan P, Dinniwell R, Haider MA, et al. Inter- and Intrafractional Tumor and Organ Movement in Patients With Cervical Cancer Undergoing Radiotherapy: A Cinematic-MRI Point-of-Interest Study. *Int J Radiat Oncol Biol Phys*. 2008;70(5):1507-1515. doi:10.1016/j.ijrobp.2007.08.055
12. van de Bunt L, Jürgenliemk-Schulz IM, de Kort GAP, Roesink JM, Tersteeg RJHA, van der Heide UA. Motion and deformation of the target volumes during {IMRT} for cervical cancer: {What} margins do we need? *Radiother Oncol*. 2008;88(2):233-240. doi:10.1016/j.radonc.2007.12.017
13. Oh S, Stewart J, Moseley J, et al. Hybrid adaptive radiotherapy with on-line {MRI} in cervix cancer {IMRT}. *Radiother Oncol*. 2014;110(2):323-328. doi:10.1016/j.radonc.2013.11.006
14. Ahmad R, Bondar L, Voet P, et al. A margin-of-the-day online adaptive intensity-modulated radiotherapy strategy for cervical cancer provides superior treatment accuracy compared to clinically recommended margins: a dosimetric evaluation. *Acta Oncol*. 2013;52(7):1430-1436. doi:10.3109/0284186X.2013.813640
15. Niemierko A. Reporting and analyzing dose distributions: {A} concept of equivalent uniform dose. *Med Phys*. 1997;24(1):103-110. doi:10.1118/1.598063
16. Niemierko A. A generalized concept of equivalent uniform dose ({EUD}) [abstract]. *Med Phys*. 1999;26:1100.
17. Lim K, Small Jr. W, Portelance L, et al. Consensus {Guidelines} for {Delineation} of {Clinical} {Target} {Volume} for {Intensity}-{Modulated} {Pelvic} {Radiotherapy} for the {Definitive} {Treatment} of {Cervix} {Cancer}. *Int J Radiat Oncol*. 2011;79(2):348-355.

doi:10.1016/j.ijrobp.2009.10.075

18. Toita T, Ohno T, Kaneyasu Y, et al. A Consensus-based guideline defining clinical target volume for primary disease in external beam radiotherapy for intact uterine cervical cancer. *Jpn J Clin Oncol*. 2011;41(9):1119-1126. doi:10.1093/jjco/hyr096
19. Hysing LB, Skorpen TN, Alber M, Fjellsbø LB, Helle SI, Muren LP. Influence of Organ Motion on Conformal vs. Intensity-Modulated Pelvic Radiotherapy for Prostate Cancer. *Int J Radiat Oncol Biol Phys*. 2008;71(5):1496-1503. doi:10.1016/j.ijrobp.2008.04.011
20. Alber M, Nüsslin F. An objective function for radiation treatment optimization based on local biological measures. *Phys Med Biol*. 1999;44(2):479-493.
21. Laub W, Alber M, Birkner M, Nüsslin F. Monte Carlo dose computation for IMRT optimization. *Phys Med Biol*. 2000;45(7):1741-1754. doi:10.1088/0031-9155/45/7/303
22. Söhn M, Yan D, Liang J, Meldolesi E, Vargas C, Alber M. Incidence of late rectal bleeding in high-dose conformal radiotherapy of prostate cancer using equivalent uniform dose–based and dose–volume–based normal tissue complication probability models. *Int J Radiat Oncol * Biol * Phys*. 2007;67(4):1066-1073. doi:10.1016/j.ijrobp.2006.10.014
23. Michalski JM, Gay H, Jackson A, Tucker SL, Deasy JO. Radiation {Dose}–{Volume} {Effects} in {Radiation}-{Induced} {Rectal} {Injury}. *Int J Radiat Oncol*. 2010;76(3, Supplement):S123--S129. doi:10.1016/j.ijrobp.2009.03.078
24. Viswanathan AN, Yorke ED, Marks LB, Eifel PJ, Shipley WU. Radiation {Dose}–{Volume} {Effects} of the {Urinary} {Bladder}. *Int J Radiat Oncol*. 2010;76(3, Supplement):S116--S122. doi:10.1016/j.ijrobp.2009.02.090
25. Kavanagh BD, Pan CC, Dawson LA, et al. Radiation dose-volume effects in the stomach and small bowel. *Int J Radiat Oncol Biol Phys*. 2010;76(3 Suppl):S101--107. doi:10.1016/j.ijrobp.2009.05.071
26. Pötter R, Tanderup K, Kirisits C, et al. The EMBRACE II study: The outcome and prospect of two decades of evolution within the GEC-ESTRO GYN working group and the EMBRACE studies. *Clin Transl Radiat Oncol*. 2018;9:48-60. doi:10.1016/j.ctro.2018.01.001
27. Söhn M, Yan D, Liang J, Meldolesi E, Vargas C, Alber M. Incidence of late rectal bleeding in high-dose conformal radiotherapy of prostate cancer using equivalent uniform dose-based

and dose-volume-based normal tissue complication probability models. *Int J Radiat Oncol Biol Phys*. 2007;67(4):1066-1073. doi:10.1016/j.ijrobp.2006.10.014

28. Roeske JC, Bonta D, Mell LK, Lujan AE, Mundt AJ. A dosimetric analysis of acute gastrointestinal toxicity in women receiving intensity-modulated whole-pelvic radiation therapy. *Radiother Oncol*. 2003;69(2):201-207.
29. on Radiation Units IIC, Measurements. *Prescribing, Recording and Reporting Photon Beam Intensity-Modulated Therapy ({IMRT})*.; 2010.
30. Sobotta B, Söhn M, Shaw W, Alber M. On expedient properties of common biological score functions for multi-modality, adaptive and 4D dose optimization. *Phys Med Biol*. 2011;56(10):N123--129. doi:10.1088/0031-9155/56/10/N01
31. Niyazi M, Karin I, Söhn M, et al. Analysis of equivalent uniform dose (EUD) and conventional radiation treatment parameters after primary and re-irradiation of malignant glioma. Published online 2013:1-7.
32. Moyennes LESV. '(a + b),. Published online 1995:175-193.
33. Ahmad R, Bondar L, Voet P, et al. A margin-of-the-day online adaptive intensity-modulated radiotherapy strategy for cervical cancer provides superior treatment accuracy compared to clinically recommended margins: {A} dosimetric evaluation. *Acta Oncol*. 2013;52(7):1430-1436. doi:10.3109/0284186X.2013.813640
34. Yilmaz C, Gultekin M, Eren G, Yuce D, Yildiz F. Determination of optimal planning target volume margins in patients with gynecological cancer. *Phys Medica*. 2015;31(7):708-713. doi:10.1016/j.ejmp.2015.05.003
35. Dees-Ribbers HM, Betgen A, Pos FJ, Witteveen T, Remeijer P, van Herk M. Inter- and intra-fractional bladder motion during radiotherapy for bladder cancer: A comparison of full and empty bladders. *Radiother Oncol*. 2014;113(2):254-259. doi:10.1016/J.RADONC.2014.08.019
36. Tanderup K, Georg D, Pötter R, Kirisits C, Grau C, Lindegaard JC. Adaptive {Management} of {Cervical} {Cancer} {Radiotherapy}. *Semin Radiat Oncol*. 2010;20(2):121-129. doi:10.1016/j.semradonc.2009.11.006
37. Shaw W, Rae WID, Alber ML. Equivalence of {Gyn} {GEC}-{ESTRO} guidelines for image

guided cervical brachytherapy with {EUD}-based dose prescription. *Radiat Oncol*. 2013;8(1):266. doi:10.1186/1748-717X-8-266

38. Wu Q, Mohan R, Niemierko A, Schmidt-Ullrich R. Optimization of Intensity-Modulated Radiotherapy plans based on the Equivalent Uniform Dose. *Int J Radiat Oncol * Biol * Phys*. 2002;53(1):224-235.
39. Oh S, Stewart J, Moseley J, et al. Hybrid adaptive radiotherapy with on-line {MRI} in cervix cancer {IMRT}. *Radiother Oncol*. 2014;110(2):323-328. doi:10.1016/j.radonc.2013.11.006
40. Bondar L, Hoogeman M, Mens JW, et al. Toward an individualized target motion management for IMRT of cervical cancer based on model-predicted cervix-uterus shape and position. *Radiother Oncol*. 2011;99(2):240-245. doi:10.1016/j.radonc.2011.03.013

Appendix: Chapter 3

Table A1: Average EUDs (Gy) ± stdev to the pCTV, nCTV and OARs using a fixed margin approach.

Study 1						
Margin Size (mm)	pCTV	nCTV	Rectum	Bladder	Sigmoid	Small Bowel
5	46.9 ± 10.5	52.3 ± 1.7	46.4 ± 3.2	46.9 ± 3.9	48.9 ± 3.6	44.7 ± 3.2
7	47.9 ± 9.2	52.3 ± 1.5	46.8 ± 2.9	47.1 ± 3.6	49.3 ± 3.3	44.9 ± 3.6
10	49.5 ± 6.3	52.4 ± 1.8	47.6 ± 2.2	47.7 ± 3.1	49.7 ± 3.0	45.0 ± 3.3
15	50.6 ± 3.2	52.4 ± 2.0	48.7 ± 1.5	48.8 ± 2.5	50.2 ± 2.7	45.4 ± 3.3
20	51.0 ± 2.5	52.5 ± 2.0	49.6 ± 1.4	49.4 ± 2.4	50.5 ± 2.3	45.5 ± 3.2
25	51.1 ± 2.3	52.5 ± 2.1	50.1 ± 0.9	49.7 ± 1.7	50.7 ± 2.1	45.9 ± 3.0
Study 2 – Empty Bladder						
7	43.92 ± 1.64		41.48 ± 1.20	40.45 ± 1.26	42.43 ± 1.23	28.83 ± 3.22
10	44.90 ± 1.21		42.43 ± 1.10	41.36 ± 1.31	42.84 ± 1.45	29.16 ± 3.21
15	45.54 ± 0.37		43.44 ± 0.77	42.58 ± 0.99	43.69 ± 0.80	29.47 ± 3.42
20	45.45 ± 0.30		44.04 ± 0.46	43.27 ± 0.75	44.10 ± 0.73	29.75 ± 3.71
Study 2 – Full Bladder						
7	44.43 ± 0.96		41.35 ± 1.38	39.25 ± 0.95	42.28 ± 2.03	24.39 ± 2.82
10	45.45 ± 0.75		42.66 ± 1.13	40.42 ± 0.81	43.22 ± 1.80	23.62 ± 1.90
15	45.45 ± 0.20		43.55 ± 0.80	41.66 ± 0.57	43.61 ± 1.80	24.94 ± 3.17
20	45.53 ± 0.14		44.05 ± 0.40	42.48 ± 0.59	43.95 ± 1.30	25.20 ± 3.38

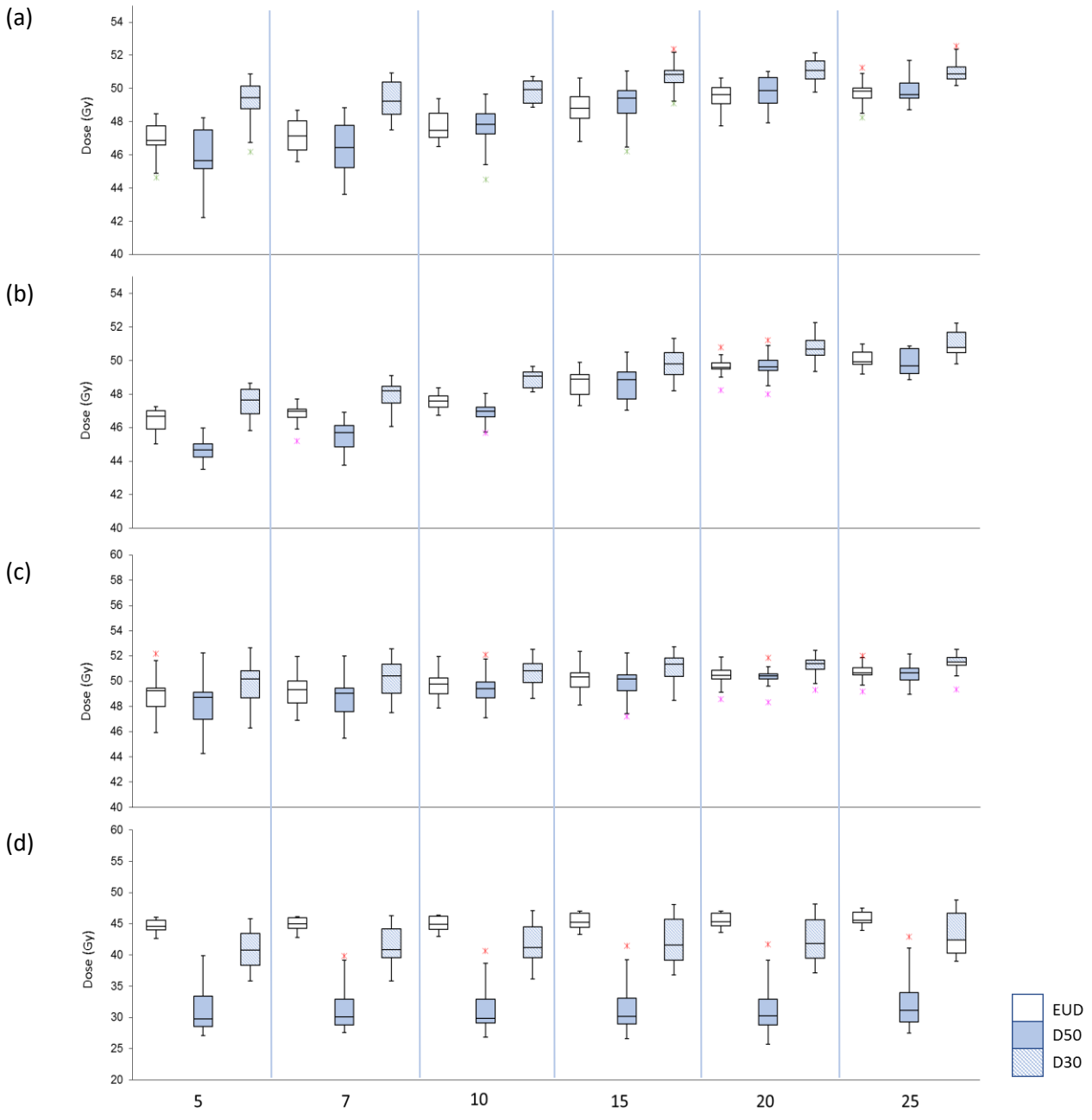

Figure A1: Study 1 - Box-whisker plots of EUD_{ave} and dose to 50% and 30% (D_{50} and D_{30}) of the a) rectal, b) bladder, c) sigmoid, and d) small bowel with increasing CTV-PTV margin sizes using a fixed margin approach.

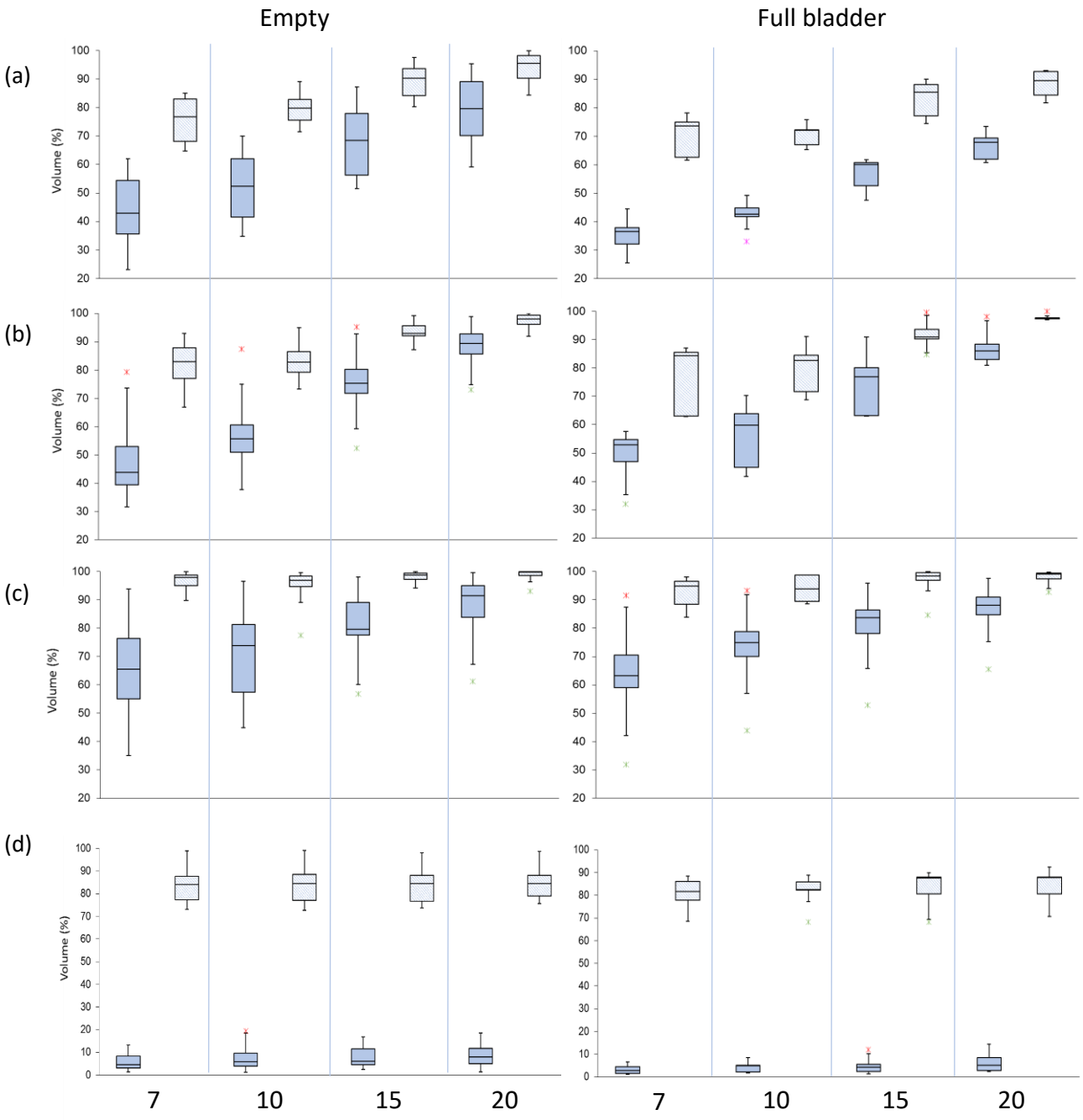

Figure A2: Box-whisker plots of the volumes receiving 40 Gy (V_{40},solid) and 30 Gy (V30, patterned) for the a) bladder, b) rectum, and c) sigmoid, and 45 Gy (V_{45} ,solid) and 15 Gy (V_{15} , patterned) for the d) small bowel with increasing CTV-PTV margin sizes using a fixed margin approach for study 2. Empty bladder patients are shown in the left- and full bladder patients in the right panel.

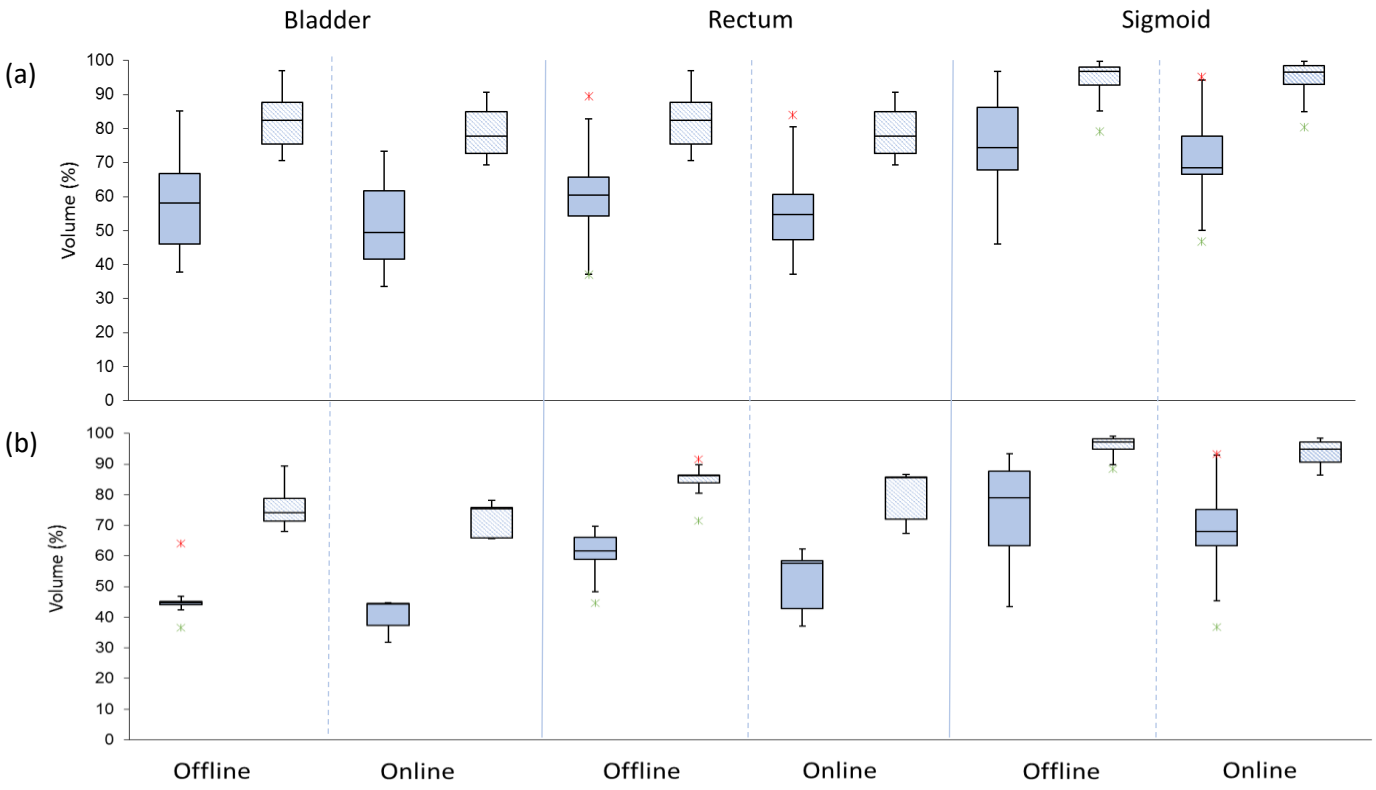

Figure A3: Study 2 - Box-whisker plots of the bladder, rectum, and sigmoid volumes receiving 40 Gy (V_{40},solid) and 30 Gy (V30, patterned) with the offline and online adaptive strategies. Empty bladder patients are shown in (a) and full bladder patients in (b).

Chapter 4: Comparison of treatment strategies

4.1 Introduction

Locally advanced cervical cancer (LACC) is generally treated with a combination of external beam radiotherapy (EBRT), chemotherapy and brachytherapy (BT). Intensity modulated radiotherapy (IMRT) offers the potential to escalate target dose while decreasing the volume of irradiated normal tissue during EBRT [1–5]. Anatomical variations during the course of treatment reduces the clinical benefit of using highly conformal techniques risking overdosage of OARs and tumor underdosage [6–10]. Traditionally, large population-based planning target volume (PTV) margins are used to accommodate these variations [11].

Different treatment strategies, aiming at reducing these margins while delivering radiotherapy precisely and accurately in the presence of anatomical changes have been proposed. The impact of changes in the filling status of the rectum and the bladder on target geometry have been reported by numerous groups [7,12–15]. A common approach is to use variable bladder filling (VBF) pre-treatment scans to create a library of plans for various target positions based on measured bladder volumes [3,13]. VBF pre-treatment scans are also used to generate an internal target volume (ITV) to account for internal organ movements [6,16,17]. Yan et al. [18] proposed customizing treatment for an individual patient through adaptive radiotherapy (ART). Different offline and online strategies exist including a margin-of the-day technique, mid treatment re-planning and weekly re-planning based on soft tissue imaging and deformable dose accumulation [19–22]. Although these strategies appear promising especially in the pelvic area where large and random movement are significant, the workload associated in terms of creating a deliverable plan, segmentation and quality assurance (QA) may make this approach clinically infeasible [23]. The

dosimetric improvements achieved by advanced planning strategies should be balanced by the increased clinical effort.

The aim of this study is to perform dosimetric analyses and compare different planning strategies considering outcome in terms of target coverage, normal tissue toxicities and workload associated with the strategy. Strategies were compared using dose volume parameters and the equivalent uniform dose (EUD) metric.

4.2 Materials and Methods

4.2.1 Patient data, imaging and delineation

20 patients treated for cervical cancer were included in this retrospective planning study. 15 were imaged and treated with and empty- and 5 with a full bladder protocol. Image guidance was performed by using daily pre-treatment CBCTs of the patient in the treatment position. A detailed description of patient characteristics, imaging parameters and bladder filling protocols is given in Chapter 2. Target volumes and OARs were manually contoured on all CT and CBCT images as described in Chapter 2 and 3. We virtually eliminate all translational and rotational setup errors using daily imaging, bony fusion and couch corrections for all patients We regard this level of IGRT as a minimum requirement in the delivery IMRT.

4.2.2 Treatment planning

Five treatment strategies were dosimetrically simulated for each patient:

(I) Fixed Margin strategy (FM) based on empty- (CT_{EB}) and full bladder (CT_{FB1}) planning CTs. Four VMAT plans with a 7, 10, 15 and 20-mm isotropic CTV-to-PTV margin was constructed. A fixed 5 mm nodal PTV (nPTV) margin were used for all plans.

(II) Individualized Internal target volume (ITV) approach. An ITV was created by combining the delineated CTV from two pre-treatment scans (ITV_{EB1}, $CT_{EB} \cup CT_{20}$) for empty bladder patients and three scans (ITV_{FB2}, $CT_1 \cup CT_2 \cup CT_3$) for full bladder patients (See Chapter 2 for details). ITVs were expanded by a 10 mm PTV margin and nodal CTVs by a 5 mm PTV margin. Margins are based on study by Bondar et al. which confirmed the

appropriateness of these margins to also account for intrafraction motion by analyzing post fraction CBCT scans. [16,26]

(III) A population-based variable margin (VBM) strategy based on target movement derived from occupancy probability matrices. An occupancy probability of 95% were used (OP_{95}) to derive these margins (details in Chapter 2).

(IV) Offline IGART and,

(V) Online IGART strategy utilizing the equivalent uniform dose (EUD) metric.

A comprehensive description of treatment simulation for the FM and adaptive strategies are given in Chapter 3. All strategies were simulated in the same way using the same planning objectives and constraints.

Volumetric Modulated Arc Therapy (VMAT) optimization was performed by utilizing biological optimization employing the EUD in the Hyperion® (University of Tübingen, Germany) treatment planning system (TPS) [27]. Monte Carlo (MC) dose calculations are used to compute IMRT segments that are weighed and modified during dose optimization [28]. For simplicity we refer to both the EUD and gEUD as EUD only. In the case of the Poisson cell kill EUD a $\alpha = 0.8$ were used. The volume effect parameters used for gEUD calculations were a = 4, 8 and 12 for the small bowel, bladder and rectum respectively.

Patients were treated in the supine position. 10 MV photons were used to deliver a total dose of 45 Gy in 25 daily fractions, with at least 95% of the PTV covered by 95% of the prescribed dose. The average EUD of the pCTV should be ≥44.9 Gy for a plan to be regarded as acceptable. Planning objectives and constraints are summarized in Table 1 and were derived from EMBRACE II protocol, RTOG 0418 guidelines and published EUD data [29–34]. OAR constraints were used as optimization constraints and violation of these parameters did not render a plan unacceptable. PTV coverage had the highest priority. OAR constraints were therefore relaxed until target coverage was met.

Table 1: Dose volume constraints and objectives for targets and OARs

	DVH		EUD (Gy)	
	Objectives	**Constraints**	**Objectives**	**Constraints**
pPTV	$V_{95\%}$ > 95%		≥ 44.9	
	D_{max} < 107%			
nPTV	V_{95} > 95%		≥ 44.9	
	D_{max} < 107%			
Small bowel	D_{max} < 105%	V40 < 30%[b]		≤ 32
Bladder	D_{max} < 105%	V40 < 75%[a]		≤42
		V30 < 85%[a]		
		V45 < 35%[b]		
Rectum	D_{max} < 105%	V40 < 85%[a]		≤ 42
		V30 < 95%[a]		
Sigmoid	D_{max} < 105%	V40 < 85%[a]		≤43
		V30 < 95%[a]		

[a] *EMBRACE II*

[b] *RTOG 0418*

4.2.3 Dosimetric evaluation of strategies

To illustrate the dosimetric impact of the strategies each strategy was simulated for all patients and dosimetric analysis of dose distributions were performed using dose volume parameters and the EUD metric.

4.2.3.1 Dose volume histogram (DVH) evaluation

All data was based on DVHs obtained from Hyperion® with a resolution of 0.05 Gy. The dose to a certain volume (V), D_V, were the average value for all patients. In the same way, V_D, were the average volume for a fixed dose (D) [35]. Population mean DVHs were calculated for each volume

to illustrate the average values for each strategy and volume of interest. The following dosimetric indices were calculated to compare strategies: the CTV (in %) receiving at least 95% and 98% of the prescribed dose ($V_{42.75}$ and $V_{44.1}$). The dose delivered to 95% and 98% of the CTV volume (D_{95} and D_{98}); V_{40} and V_{30} for the bladder, rectum and sigmoid and V_{15} and V_{45} for the small bowel.

4.2.3.2 *Equivalent* uniform dose (EUD)

In addition, the EUD for targets and OARs as suggested by Niemierko were used to evaluate and compare plans [36,37]. The generalized EUD (gEUD) is calculated by:

$$gEUD = \left(\frac{1}{N}\sum_{i=1}^{N} D_i^a\right)^{\frac{1}{a}} \quad (1)$$

Where N is the number of voxels in the volume of interest, D_i is the dose in the *i*th voxel and a is a tissue specific parameter that describes the dose-volume effect for target or normal tissues. Due to the fact that less than the whole bowel volume was contoured on the planning CTs and CBCTs are acquire with a smaller field of view we calculated the gEUD of the small bowel relative to an absolute reference volume (V_{ref}) as proposed by Hysing et al.[38]:

$$gEUD = \left(\frac{1}{V_{ref}}\sum_i v_i D_i^a\right)^{\frac{1}{a}} \quad (2)$$

Where (vi, Di) represents the ith bin of the differential DVH, and a is associated with the volume effect of the organ considered. Roeske *et al*. found *a* = 3.2 ± 1.1 to provide the best fit between the incidence of Grade 2 acute diarrhea and V_{45} for the small bowel. Based on these results we chose a= 4 and V_{ref} = 200cm^3 for the bowel [38,39]. The volume effect for the rectum is well known (*a* = 12) [29]. A a value of 8 was used for the bladder as derived from clinical experience of EUD-based optimization om IMRT at the University Clinic in Tübingen (Germany) [38].

4.2.3.3 Score functions

An objective function based on EUD as described by Wu et al. [40] was used to score and compare planning strategies. The objective function is given by:

$$F = \prod_j f_j \tag{3}$$

Where the sub score for targets were calculated using

$$f_T = \frac{1}{1 + \left(\frac{EUD_0}{EUD}\right)^n} \tag{4}$$

And for normal tissues,

$$f_{OAR} = \frac{1}{1 + \left(\frac{EUD}{EUD_0}\right)^n} \tag{5}$$

EUD_0 is the desired dose parameter for targets and the maximal tolerable dose for normal tissues, and *n* is a weight or penalty indicating the importance of the structure specific endpoint. Higher penalties (*n*) yield steeper gradients of the sigmoidal shape of the function *f* causing a more pronounced drop or rise in the sub score when EUD deviates from EUD_0. A penalty of *n*=20 was used to ensure high sensitivity to tumor underdosage or OAR overdose. For simplicity the same functions were used for comparison of strategies based on dose-volume parameters.

The planning objectives reported in Table 1 were used to calculate the sub scores for all structures. For example, the sub score for targets using the EUD planning objectives, pPTV ≥ 44.9 Gy, was calculated by:

$$f_{T_{EUD}} = \frac{1}{1 + \left(\frac{44.9}{EUD}\right)^n} \tag{6}$$

and for dose-volume planning objectives, $V_{95\%}$ > 95%,

$$f_{T_{DVH}} = \frac{1}{1 + \left(\frac{95}{V_{95}}\right)^n} \tag{7}$$

Sub scores for OARs based on EUDs were calculated using single EUD constraint values as given inTable 1. OAR sub scores based on dose volume parameters were calculated using different

check points. For example, bladder has three check points, V_{30}, V_{40} and V_{45} (Table 1). $f_{OAR_{DVH}}$ was calculated for each check point. The average of all check points was taken as the sub score for the specific organ. The final OAR sub score was determined by using the average of all OARs as it treats every organ and check point equally, therefore, no single dose check point can dominate the outcome. The denominator (allowable percentage volume of the OAR) serves as an intrinsic weighting. The user may define this according to specific outcomes that need to be monitored. For example, the sub score for the three bladder check points were calculated as:

$$f_{bladder_{DVH}} = \frac{1}{3}\left(f_{bladder_{DVH1}} + f_{bladder_{DVH2}} + f_{bladder_{DVH3}}\right) \tag{8}$$

where,

$$f_{bladder_{DVH1}} = \frac{1}{1+\left(\frac{V_{30}}{85}\right)^n} \quad ; \quad f_{bladder_{DVH2}} = \frac{1}{1+\left(\frac{V_{40}}{75}\right)^n} \quad ; \quad f_{bladder_{DVH3}} = \frac{1}{1+\left(\frac{V_{45}}{35}\right)^n}$$

The OAR sub score, for both DVH and EUD based parameters, was then calculated by:

$$f_{OAR} = \frac{1}{4}\left(f_{bladder} + f_{rectum} + f_{sigmoid} + f_{smallbowel}\right) \tag{9}$$

The final score F (equation 1) of a strategy was determined by the product of all the target and OAR sub score. Scores were calculated for each fraction of each patient separately. The average of all patients was used to calculate the population mean. The values for the sub scores range from 0 to 1 with small values indicating dose values below the specified EUD_0 for targets and doses exceeding tolerance limits for OARs. Eight planning strategies, 4 fixed isotropic CTV-PTV margins (7, 10, 15 and 20 mm), variable margin (VBM), ITV approach and offline and online adaptive strategies were compared. Strategies were ranked from one to eight with one being the strategy with the highest F score yielding the best outcome based on target coverage and OAR sparing.

4.3 Results

4.3.1 DVH evaluation

The median D_{95} values for all strategies and both groups (EB and FB) were above the minimum requirement of 42.75 Gy (95% of the prescribed dose) as illustrated in Figure 1a. Only one EB patient didn't meet the minimum requirement when a 7 mm margin was used. Approximately half of the patients had D_{98} values below 42.75 Gy for both groups when a 7 mm FM was used and 25% of EB patients had D_{98} values below the tolerance with a 10 mm margin. A notable larger spread of values is seen for 7- and 10 mm margins. The range and median for all other strategies are comparable with D_{98} being slightly lower for the off- and online strategies. Mean values ± standard deviations for dosimetric indices are shown in the Appendix, Table A1.

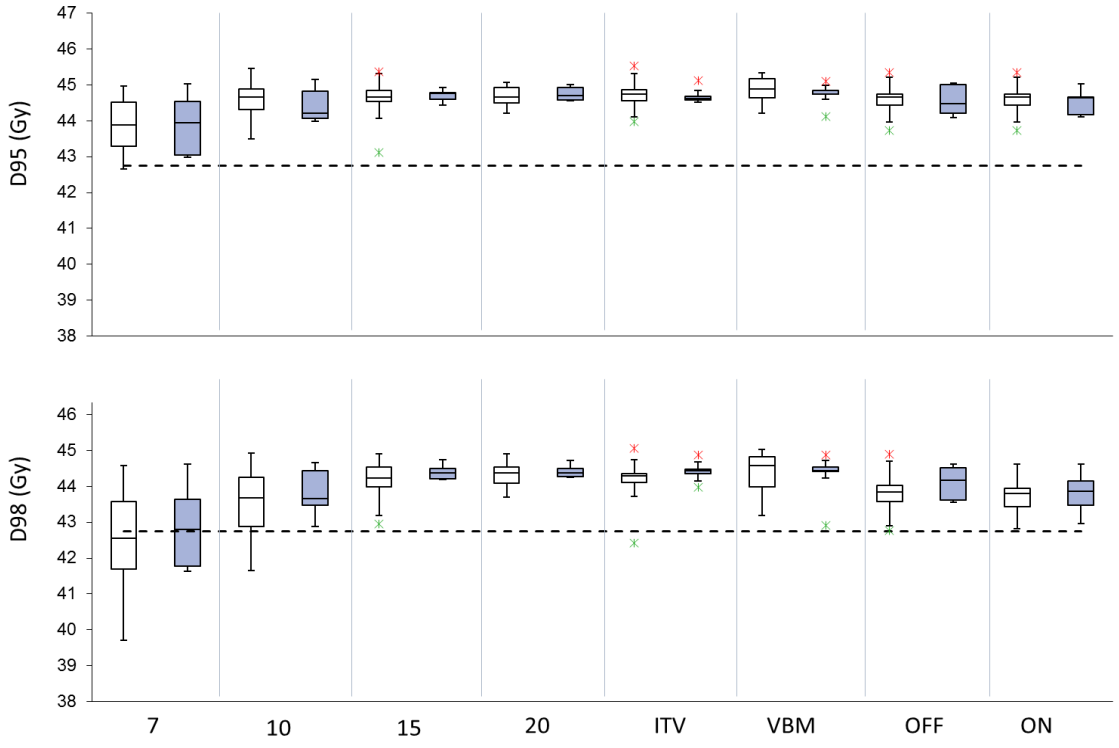

Figure 1: Box-whisker plots of the dose to (a) 95% (D_{95}) and (b) 98% (D_{98}) volume for pCTV for different strategies. The deviation of D_{95} for empty bladder (open) and full bladder (solid) patients around the median is shown. The planning objective is indicated by the dashed line, 95% (42.75 Gy) of the prescribed dose.

Figure 2 shows the volume receiving 40 Gy for the bladder, rectum and sigmoid. Due to the enlarged overlap of larger PTV margins with OARs, the largest V_{40} values were noted for a 20 mm margin and smallest for the 7 mm margin for both groups. For EB patients median V_{40} values of the rectum and bladder using a 15 mm margin were comparable to the VBM strategy and the 10 mm margin to the online strategy with the online strategy performing slightly better. The ITV approach resulted in better rectum and bladder sparing than a 15 mm FM. For the sigmoid, on- and off-line strategies lead to lower median V_{40} values compared to a 15 mm FM while both the ITV and VBM approaches resulted in higher values. Results for the FB group were similar except that the VBM strategy caused more OAR sparing with values slightly lower than a 15 mm FM. In general, lower V_{40} values were noted for online vs offline. The volume of the bladder receiving 40 Gy for patient in the FB group were visibly lower compared to the EB group. The same trends were observed for V_{30}. Mean values ± standard deviations for all OARs and dosimetric indices are shown in the Appendix, Table A2.

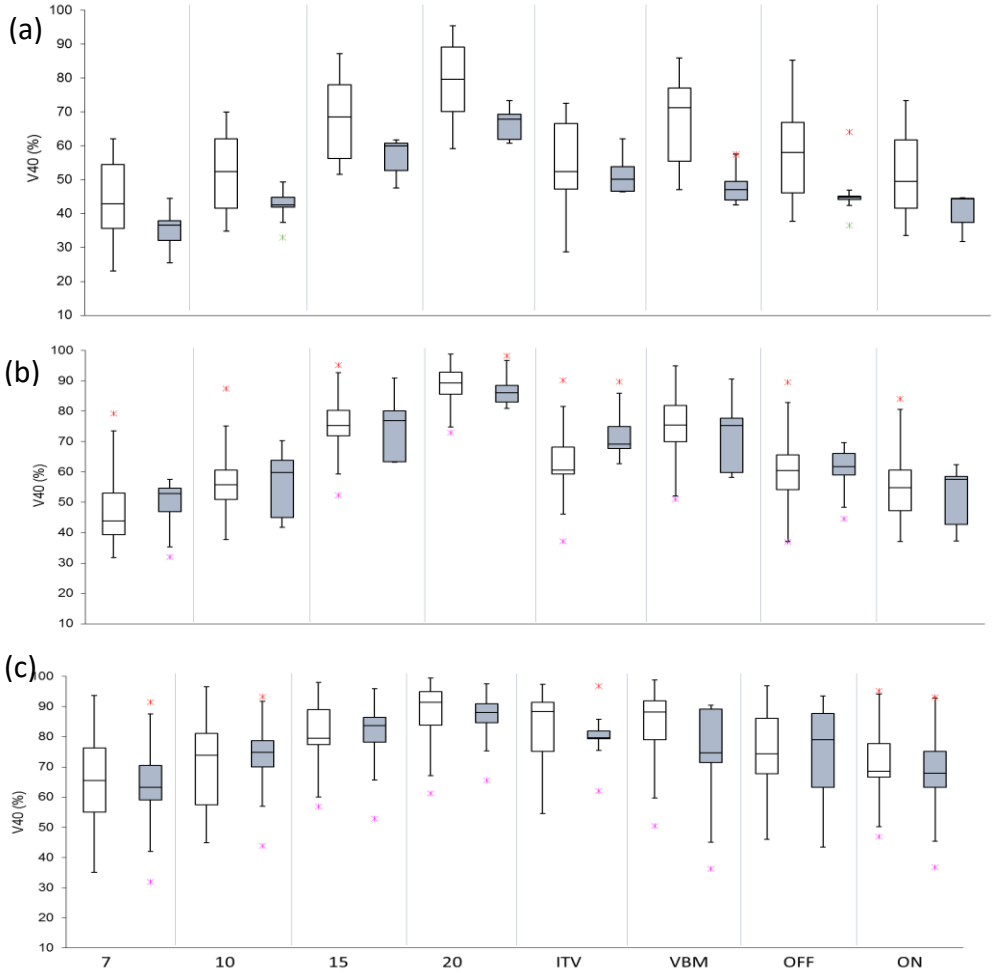

Figure 2: Box-whisker plots of the volume(%) receiving 40 Gy for the (a) bladder, (b) rectum, and (c) sigmoid volume for different strategies. The deviation of V_{40} for empty- (open) and full bladder (solid) patients around the median is shown.

The volume of the small bowel receiving 15 and 45 Gy are shown in Figure 3. The median V_{15} values for all strategies and both groups are comparable. The lowest V_{15} values for the EB group were noted in the off- and on-line strategies and in the VBM and 7 mm strategy for the FB group. A notable difference can be seen in the median V_{45} values between the EB and FB groups with overall lower values in the latter.

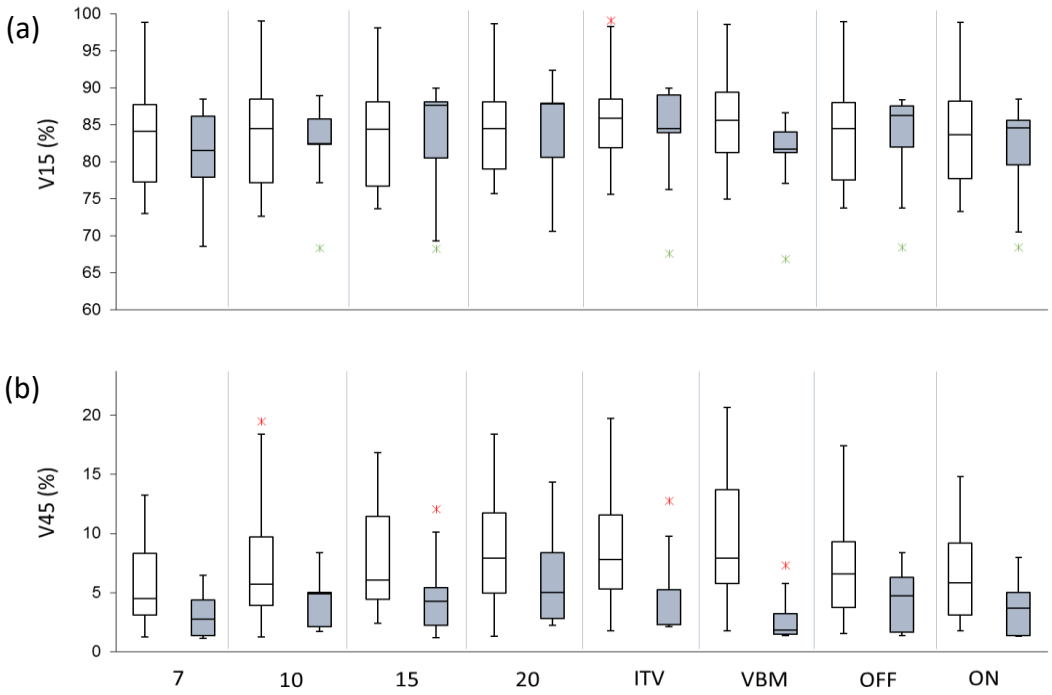

Figure 3: Box-whisker plots of the volume (%) of small bowel receiving (a) 15 Gy and (b) 45 Gy for different strategies. The deviation of V_{15} and V_{45} for empty- (open) and full bladder (solid) patients around the median is shown.

To obtain a sense of typical curves and their variability, DVH curves for the pCTV and all OARS for an empty- and full bladder patient showing all treatment fractions and strategies are shown in figure 4 and figure 6 respectively. Population-mean dose volume histograms (DVHs) of the pCTV for all strategies for the empty- and full bladder patients are shown in Figure 5 and Figure 7 respectively. The high dose region is expanded to demonstrate the differences between strategies. The range of values for the two strategies with the smallest and largest dose gradients are represented by the light and dark grey bands.

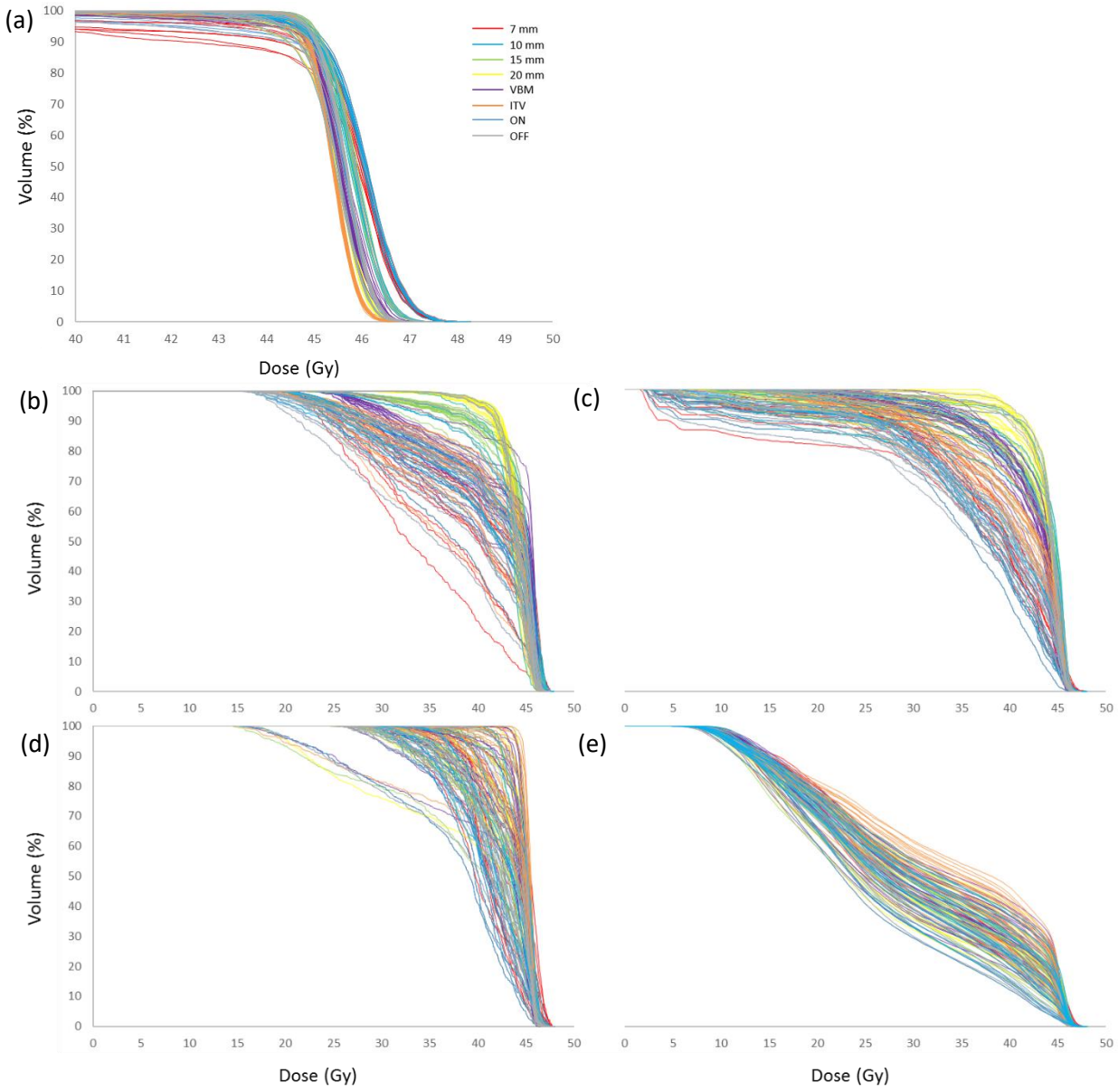

Figure 4: DVH curves of all treatment fractions and all treatment strategies for a single EB patient for the (a) pCTV, (b) Bladder, (c) Rectum, (d) Sigmoid, and (e) Small Bowel.

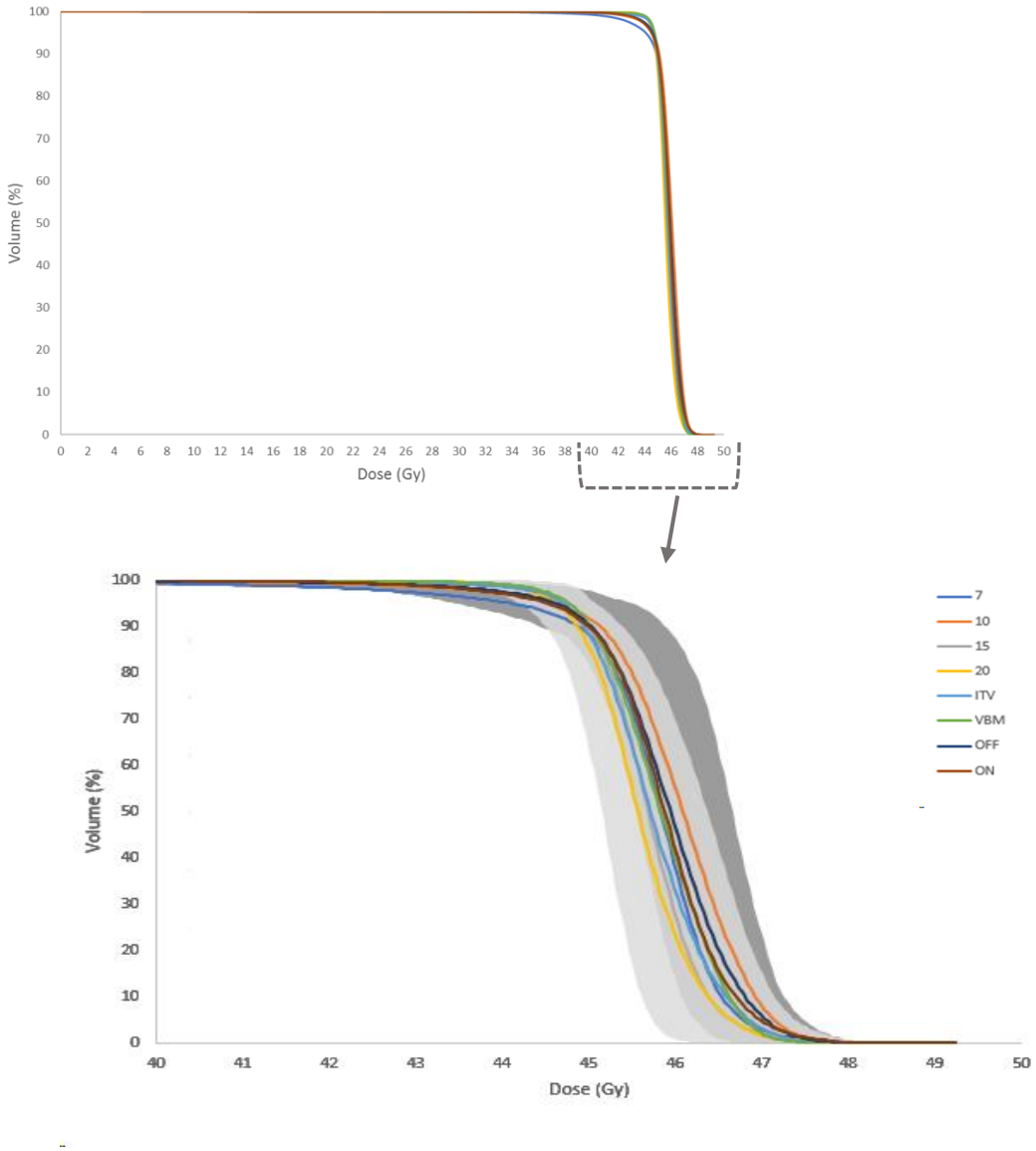

Figure 5: Population-mean dose volume histograms of the pCTV for empty bladder patients comparing different treatment strategies.

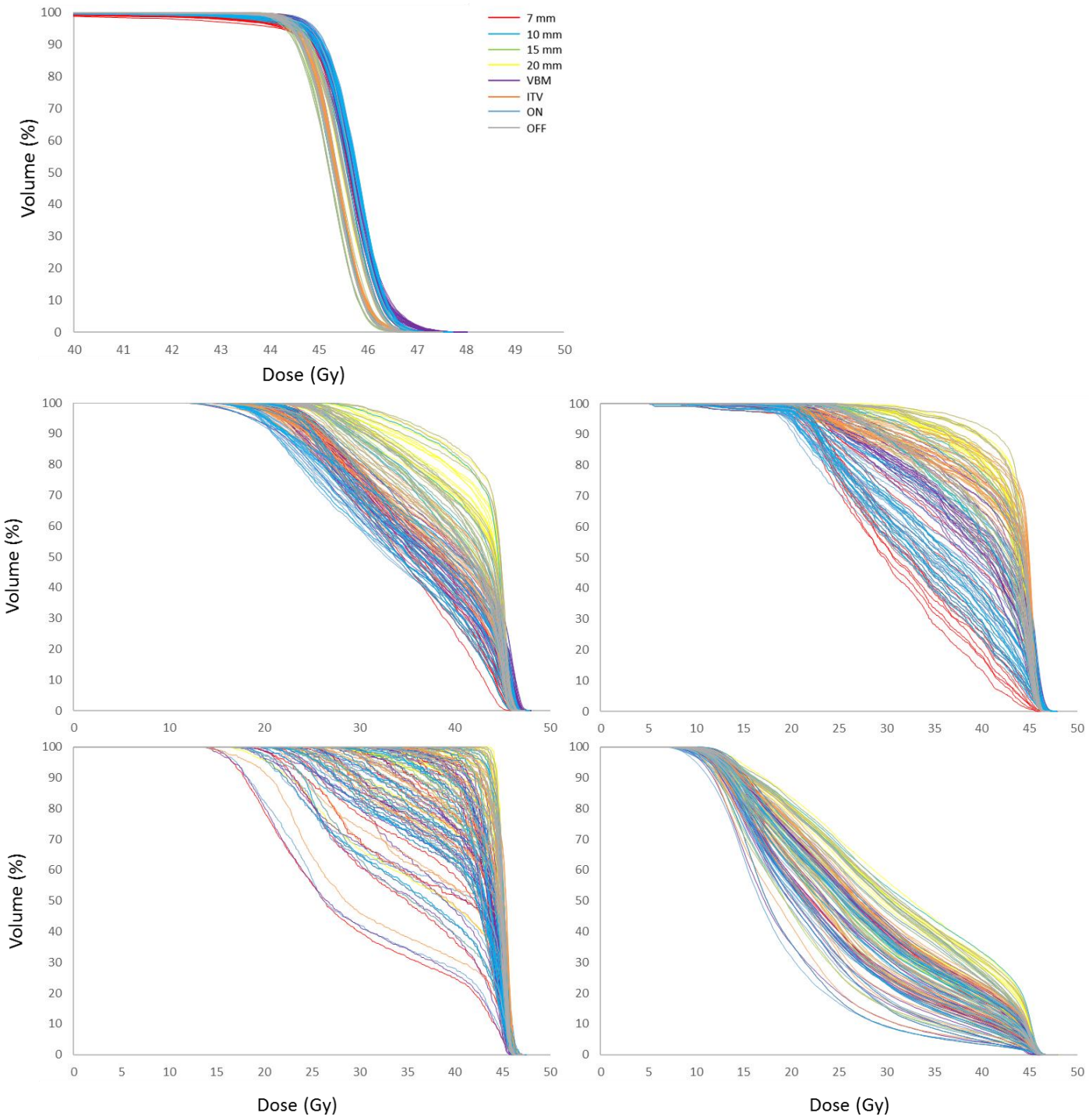

Figure 6: DVH curves of all treatment fractions and all treatment strategies for a single full bladder patient for the (a) pCTV, (b) Bladder, (c) Rectum, (d) Sigmoid, and (e) Small Bowel.

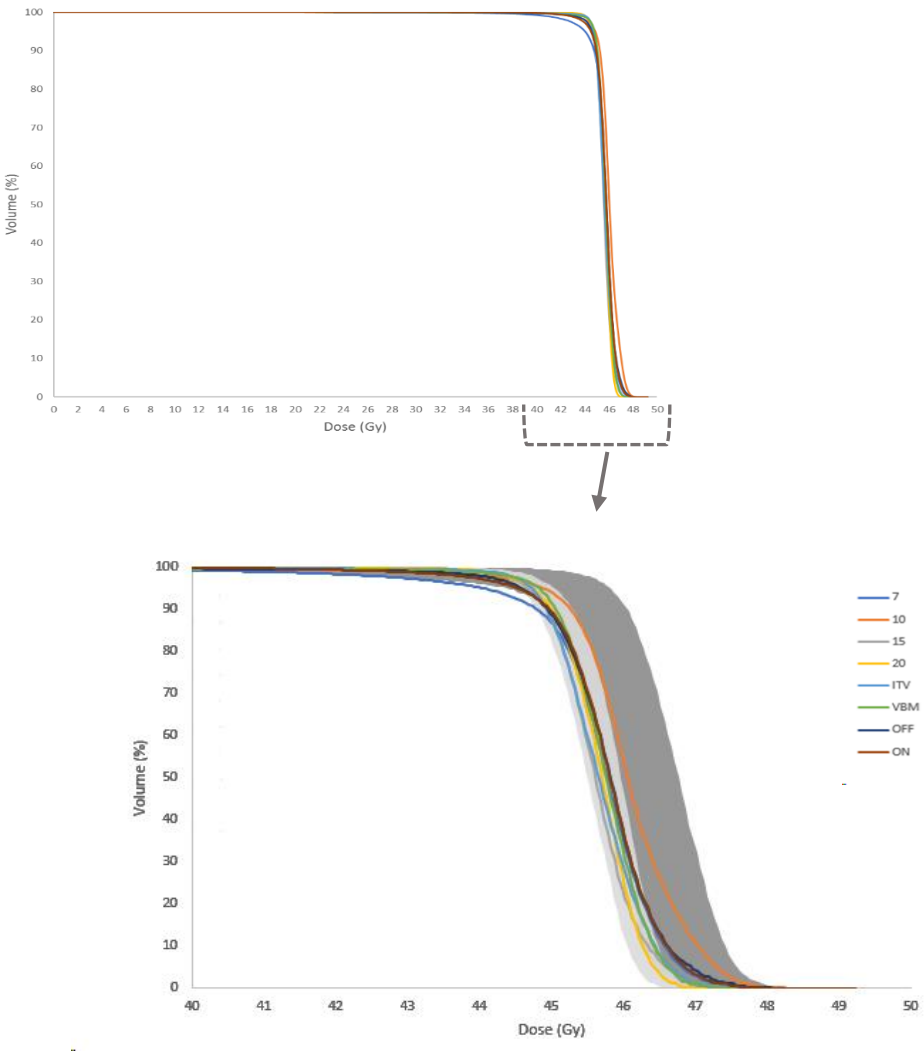

Figure 7: Population-mean dose volume histograms of the pCTV for full bladder patients comparing different treatment strategies.

The DVHs of smaller margins in particular clearly demonstrate what is seen in Figure 1 as well. The D_{95} parameter may be sufficient and meet planning aims but a decrease in percentage volume receiving doses > 40 Gy cause cold spots in terms of the D_{98} parameter.

Population-mean dose volume histograms for all OARs are shown in Figure 8 and Figure 9. Steepest dose gradient is seen when a 7 mm margin is used whereas a 20 mm margin yields the largest gradients in all OARs. The ranges for these strategies are indicated by the light and dark grey bands respectively. Figure 6a illustrates the increased bladder sparing for FB patients compared to EB patients as seen from V_{40} and V_{30} parameters. The range of values for the rectum and sigmoid is more comparable between EB and FB (Figure 8b and c).

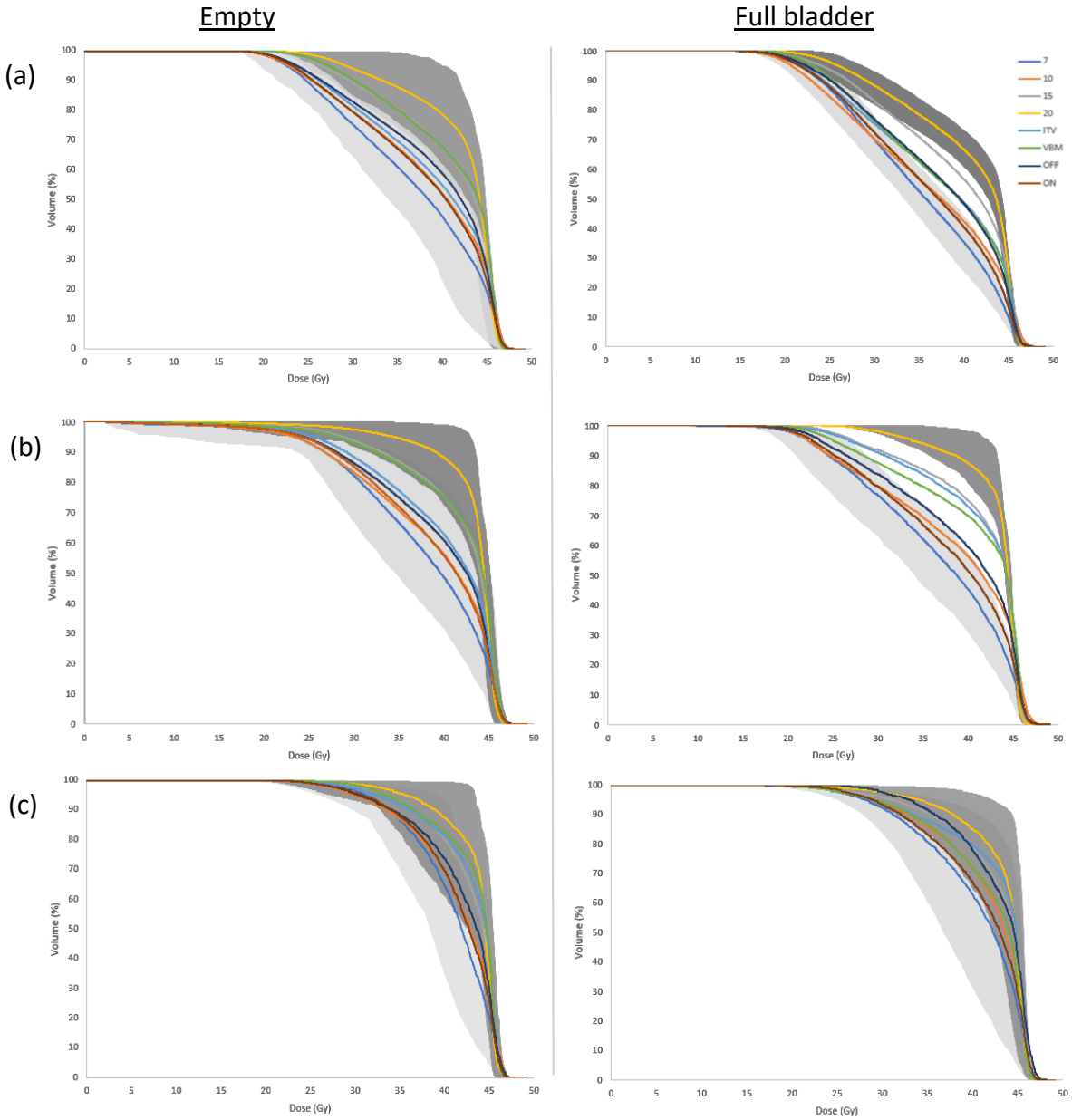

Figure 8: Population-mean dose volume histograms for empty- (left) and full (right) bladder patients comparing different treatment strategies for (a) bladder, (b) rectum, and (c) sigmoid.

Figure 9 illustrates the increased sparing of the small bowel for patients treated with a full bladder. This is also seen when comparing the DVH curves for the individual patients (figure 4 & 6). The average D_{50} values is ± 30 Gy for the EB group and ± 25 Gy for the FB group.

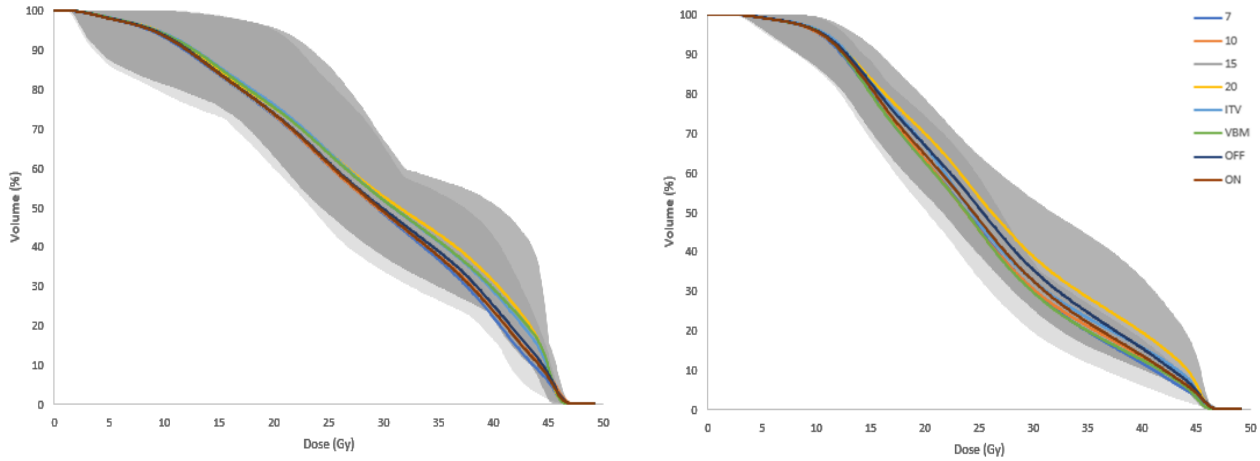

Figure 9: Population-mean dose volume histograms for empty- (left) and full (right) bladder patients comparing different treatment strategies for the small bowel.

4.3.2 Equivalent uniform dose (EUD)

The average EUD (EUD_{ave}) for the majority of patients didn't meet the planning objective when a 7 mm margin was used. Although the median values for the 10mm, ITV, VBM and offline strategies were > 44.9 Gy some patients, especially in the EB group, were underdosed. Based on the average EUD, adequate pCTV coverage was obtained for all patients utilizing a 20 mm FM and online strategy (Figure 8). In the EB group, one patient was slightly underdosed (44.7 Gy) when a 15 mm FM was used. Except for the 7 mm, 10 mm and VBM approach no underdosages were seen in the FB group. EUD values and standard deviations are shown in Table 2.

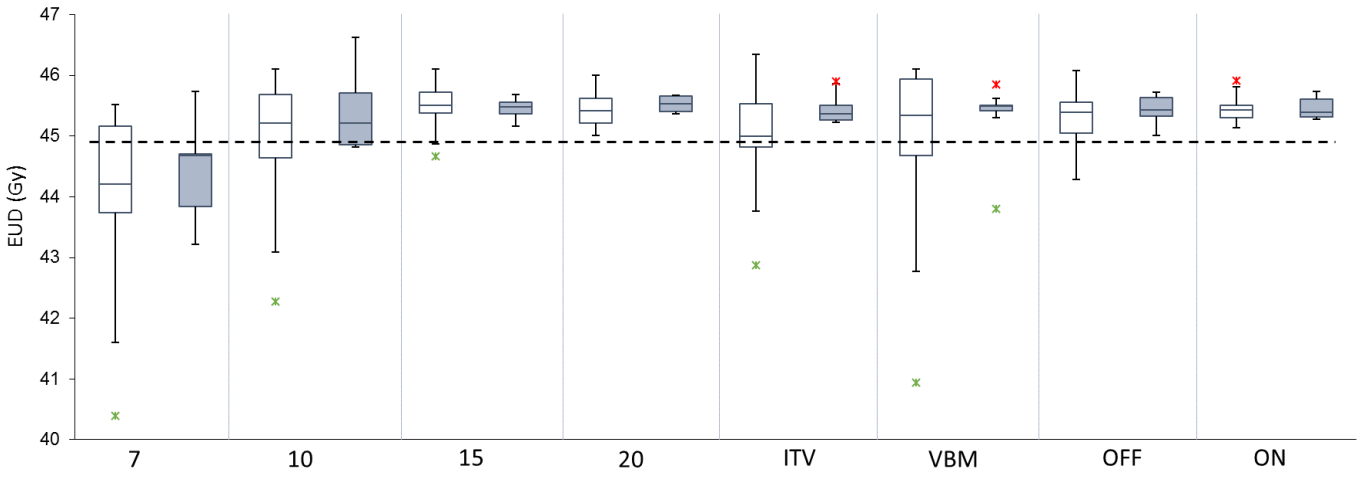

Figure 10: Box-whisker plots of the EUD_{ave} for the pCTV using different strategies. The deviation for the whole population of empty- (open) and full bladder (solid) patients around the median is shown. The planning objective (44.9 Gy) is indicated by the dashed line.

Table 2: Average EUD ± standard deviation for the pCTV using different planning strategies.

EUD_{avg} (Gy)		
	EB	FB
7	43.9 ± 1.6	44.4 ± 1.0
10	44.9 ± 1.2	45.5 ± 0.8
15	45.5 ± 0.4	45.5 ± 0.2
20	45.5 ± 0.3	45.5 ± 0.1
ITV	45.0 ± 0.8	45.5 ± 0.3
VBM	45.1 ± 1.3	45.2 ± 0.8
OFF	45.3 ± 0.5	45.4 ± 0.3
ON	45.4 ± 0.3	45.5 ± 0.2

The average EUD values for all OARs and different strategies are shown in Figure 9 and Figure 10. Average bladder EUDs are slightly higher for EB patients compared to FB patients. Similar results were obtained for the rectum and sigmoid in both groups. EUD_{ave} for the rectum was slightly lower for EB patients when the ITV strategy was used. Lower EUD values were seen in the FB patients when using VBM, offline and online strategies. Although the median values for the small bowel is comparable for all strategies it is evident from Figure 10 that lower EUD values were obtained in the FB group. The same results were obtained when DVH parameters were evaluated. For the sake of comparison between EB and FB average EUD values and standard deviations for each strategy are shown in Appendix, Table A3.

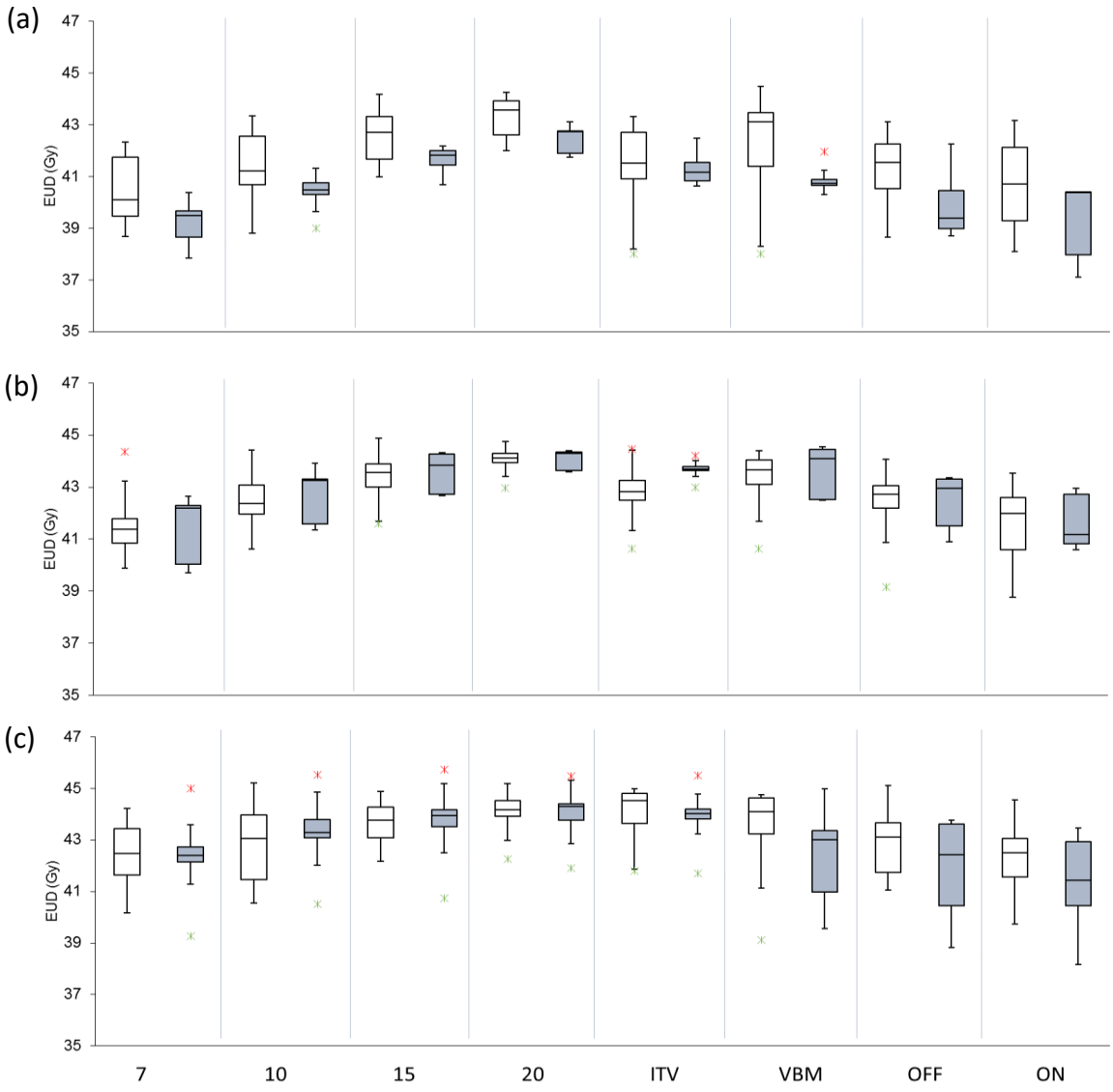

Figure 11: Box-whisker plots of the EUD_{ave} for the (a) bladder, (b) rectum, and (c) sigmoid using different strategies. The deviation for the whole population of empty- (open) and full bladder (solid) patients around the median is shown.

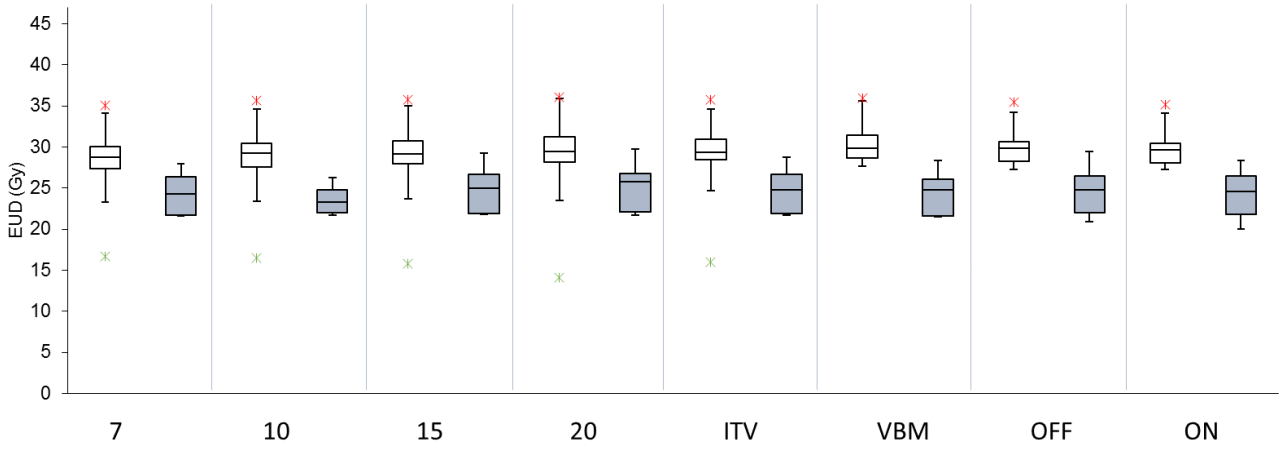

Figure 12: Box-whisker plots of the EUD_{ave} for the small bowel using different strategies. The deviation for the whole population of empty- (open) and full bladder (solid) patients around the median is shown.

The average EUDs for all relevant nodal groups when a 7 mm FM, 20 mm FM and on-line adaptive strategy was used are shown in Figure 11.For all treatment strategies the median EUD_{ave} for all nodal groups was above 44.9 Gy. Average EUD values ± standard devitions for the fixed margins and adaptive strategies are given in Chapter 3. Values for the ITV and VBM approaches is given in the appendix, table A3. Except for the pre-sacral nodes no underdosages were seen in the any nodal groups for the FB patients. Underdosages seen were for various patients randomly distributed trhoughout the group. Due to the fact that the average EUDs for nodal groups of the various planning strategies were approximately the same, these results were not included in the determination of F scores for strategies.

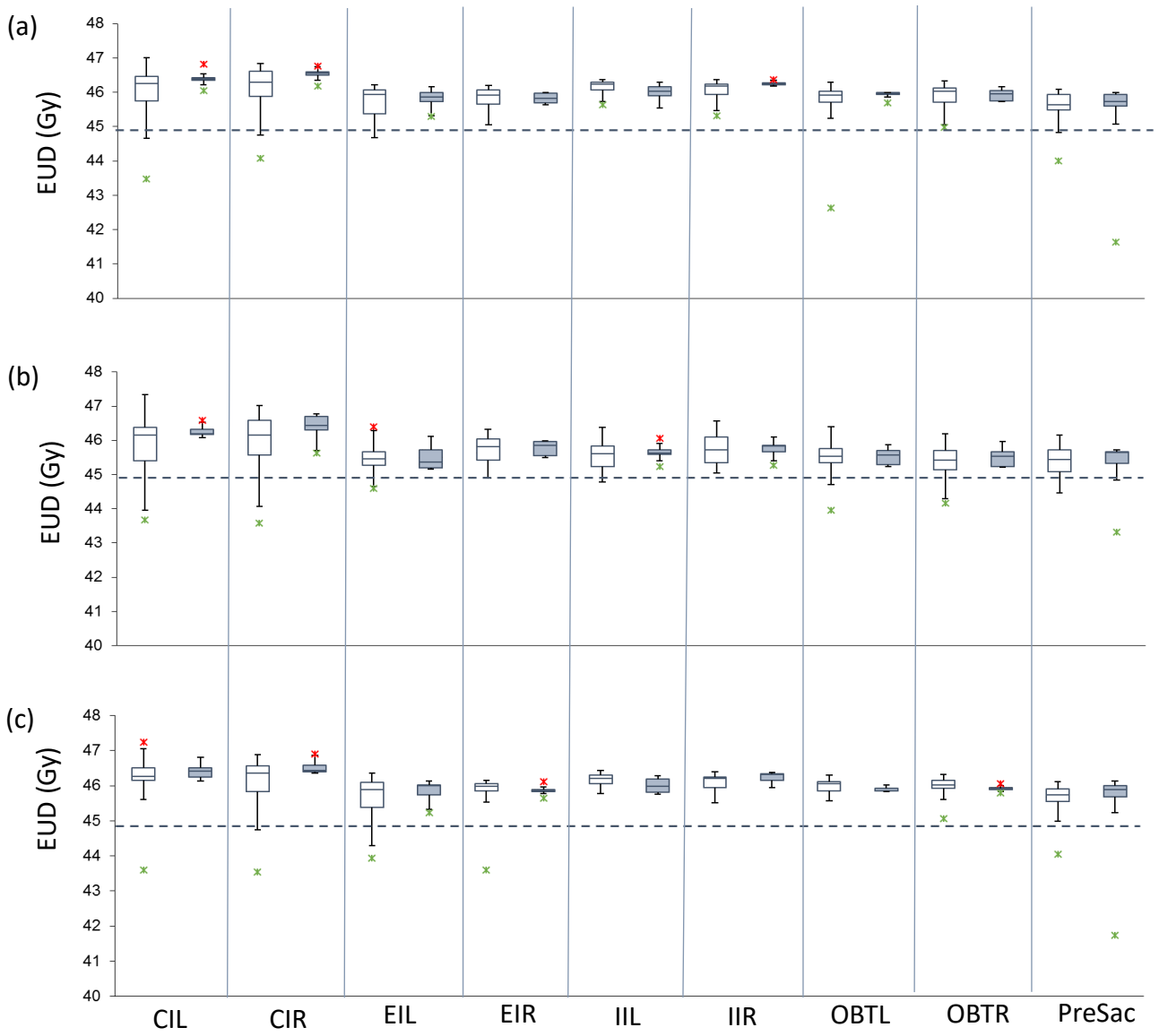

Figure 13: Box-whisker plots of the EUD_{ave} for all relevant nodal groups for a (a) 7 mm FM, (b) 20 mm FM, and (c) on-line planning strategy. The deviation for the whole population of empty- (open) and full bladder (solid) patients around the median is shown. CIR and CIL = common iliac right and left, EIR and EIL = external iliac right and left, IIR and IIL = internal iliac right and left, OBTR and OBTL = obturator right and left, PreSac = Presacral

4.3.3 Comparison of strategies

Target and OAR sub scores based on DVH parameters is summarized in Table 3. Sub scores of each OAR separately is given in the appendix (table A4 and A5). Red indicates the strategy with the highest score and green the lowest. For both groups the highest and lowest target sub score were noted for a 20- and 7 mm margin respectively. Best OAR sparing was achieved with a 7 mm margin and the worst with a 20 mm margin. The online adaptive strategy had the highest *F* score for both groups, with a 10 mm fixed margin second. A 20 mm fixed margin scored the lowest for both EB and FB patients. Ranking of strategies based on the *F* scores is shown in Table 6 and Figure 12.

Table 3: Sub score for targets and OARs using DVH metrics for the EB and FB groups. Strategies are ranked based on the final score, F.

	$f_{T_{DVH}}$		$f_{OAR_{DVH}}$		F_{DVH}	
	EB	FB	EB	FB	EB	FB
7	0.627	0.637	0.853	0.916	0.534	0.585
10	0.683	0.696	0.805	0.901	0.548	0.630
15	0.678	0.725	0.621	0.763	0.410	0.554
20	0.733	0.731	0.410	0.574	0.301	0.421
ITV	0.713	0.720	0.666	0.804	0.475	0.580
VBM	0.676	0.713	0.533	0.833	0.357	0.595
OFF	0.695	0.699	0.765	0.857	0.530	0.599
ON	0.696	0.695	0.830	0.906	0.577	0.631

low
high

From Figure 12 the increase in f_T values (blue bars) moving from a 7 mm to a 20 mm margin can clearly be seen. This indicates better target coverage for an increase in margin size. The opposite is seen for OAR sparing indicated by the decrease in f_{OAR} values (green bars). Although the target sub score for a 10- and 15 mm FM is in the same range the superior OARs sparing of a 10 mm FM warrants a higher *F* score. The same result is seen when comparing the ITV, VBM, offline, and

online strategies. The VBM strategy performed significantly better in the FB compared to the EB group.

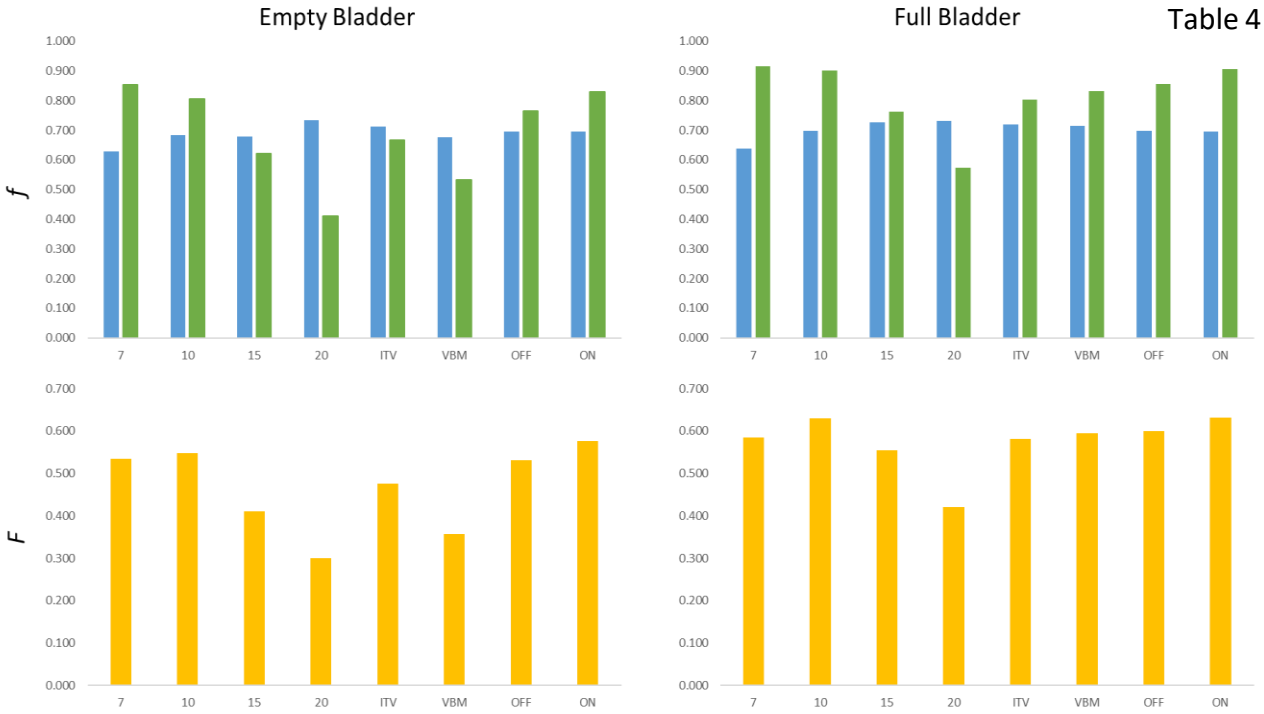

Table 4

Figure 14: Sub scores, based on DVH parameters, for the targets (blue) and OARs (green) are illustrated in the top panel. The lower panel shows the final score, F, obtained for each strategy.

reports the sub scores for targets and OARs based on the EUD. A 15 mm fixed margin yield the best target coverage for the EB group while a 20 mm margin had the highest target sub score in the FB group. A 7 mm margin had the lowest target sub score in both groups. Although the best OAR sparing was achieved using a 7 mm fixed margin the online strategy scored comparable results. The worst OAR sparing was noted for a 20 mm margin in agreement with results obtained when DVH metrics were used. The online strategy had the highest *F* score with the offline strategy second. The 7 mm fixed margin had the lowest *F* score for both groups (Table 5 and Figure 13).

Table 4: Sub score for targets and OARs using the EUD metric for the EB and FB groups. Strategies are ranked based on the final score, F.

	$f_{T_{EUD}}$		$f_{OAR_{EUD}}$		F_{EUD}	
	EB	FB	EB	FB	EB	FB
7	0.406	0.449	0.811	0.831	0.329	0.373
10	0.502	0.558	0.758	0.765	0.381	0.427
15	0.569	0.561	0.682	0.706	0.388	0.396
20	0.560	0.569	0.632	0.663	0.353	0.377
ITV	0.510	0.560	0.711	0.705	0.363	0.395
VBM	0.520	0.534	0.677	0.750	0.352	0.401
OFF	0.543	0.558	0.760	0.805	0.413	0.449
ON	0.555	0.562	0.800	0.846	0.444	0.475

Similar trends with regards to target coverage, OAR sparing, and margin size observed with DVH metrics is seen when the EUD metric is used (Figure 13). However, a more distinct difference in target sub scores are seen especially when smaller margins are used. A 15 mm FM performed better than a 10 FM in the EB group whereas the opposite is seen for FB patients. In agreement with DVH metrics, the VBM strategy achieved a better result in the FB group compared to EB group.

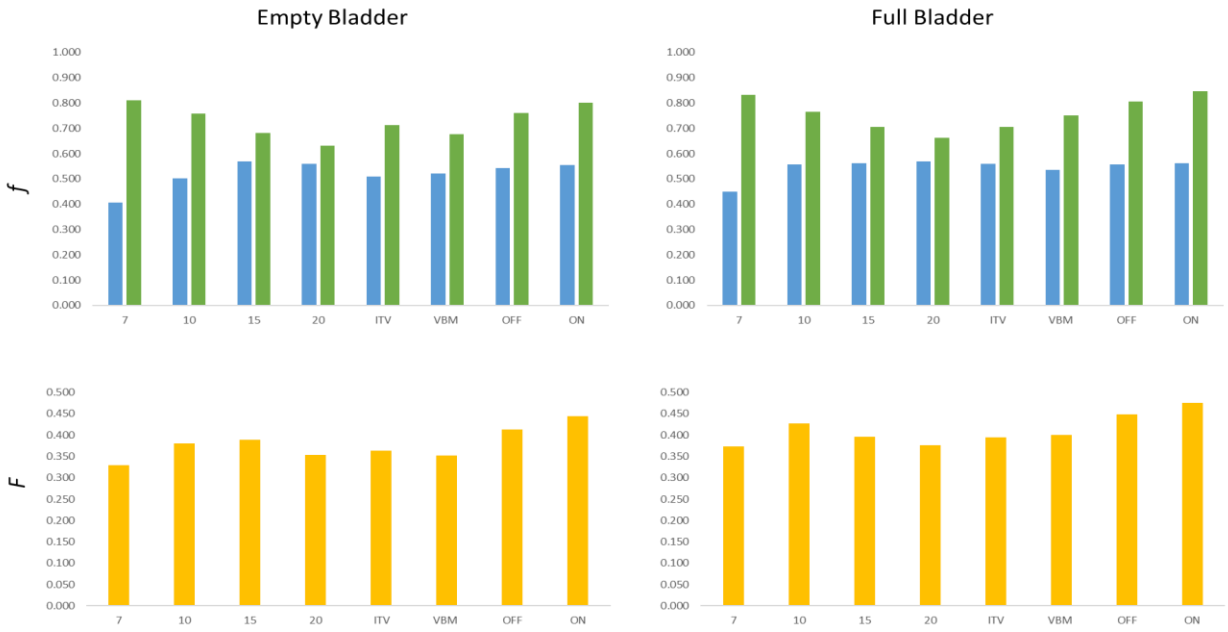

Figure 15: Sub scores, based on EUD, for the targets (blue) and OARs (green) are illustrated in the top panel. The lower panel shows the final score, F, obtained for each strategy.

Ranking of strategies based on their *F* scores are given in Table 5 with 1 being the strategy with the highest and 8 the lowest *F* score. The online adaptive strategy ranked number 1 in both patient groups for both metrics. Based on DVH metrics a 20 mm FM ranks last (8) while a 7 mm FM takes the 8th place when the EUD is used. When dosimetric analysis are based on DVH metrics a 10 mm FM is the second strategy of choice and a 7 mm FM preferred to a 15 mm FM. With the EUD as dose metric the offline strategy comes in second place with 15 mm FM and 10 mm third for EB and FB patients respectively. The rankings of the ITV and VBM strategies are the same irrespective of dose metric used.

Table 5: Ranking of strategies from best (1) to worst (8) based on dose volume parameters and EUDs considering target coverage and normal tissue sparing.

	DVH		**EUD**	
	EB	FB	EB	FB
1	ON	ON	ON	ON
2	10	10	OFF	OFF
3	7	OFF	15	10
4	OFF	VBM	10	VBM
5	ITV	7	ITV	15
6	15	ITV	20	ITV
7	VBM	15	VBM	20
8	20	20	7	7

4.4 Discussion

Various planning strategies including fixed margins, an internal target volume approach, variable margins, and offline and online adaptations have been evaluated and compared for twenty cervical cancer patients. This group of patients included patients imaged and treated with an empty (n=15) and full bladder (n=5) protocol. Treatment strategies were compared based on an objective function from Wu et al.[40] evaluating target coverage and normal tissue sparing. Metrics were calculated using both the traditional dose volume constraints as well as the EUD dose metric. Strategies were ranked from the best (no.1) to the worst (no.8) based on these metrics. Enabling differentiation of strategies with regards to target coverage and normal tissue sparing. Workload (creating plans, imaging, segmentation and quality control) associated with each strategy is a determining factor with regards the clinical feasibility of a strategy.

The target sub scores for all strategies yield adequate coverage ($F \geq 0.5$) when DVH metrics were used. However, when using the EUD metric a 7 mm FM had inadequate coverage ($F < 0.5$) in both groups. Although D_{95} was above the minimum requirement ($D_{95} \geq 42.75$ Gy) in all but one patient, the D_{98} indicated underdosage in more than half the patients when using a 7 mm FM for both groups (Figure 1). The same was seen in the EB group when a FM of 10 mm was used. D_{98} for all strategies except the aforementioned cases were above the minimum requirement indicating adequate target coverage according to the planning protocol. The EUD metric presented a different outcome indicating underdosages ($EUD_{avg} < 44.9$ Gy) in all strategies except the 20 mm FM and on-line strategy. This highlights one of the important properties of using EUD in optimization which is, even if only a small part of the tumor is significantly underdosed it will have a drastic effect on the EUD [40,41]. As expected, the 7 mm FM strategy had the highest OAR sub scores indicating superior normal tissue sparing, but inadequate target coverage significantly reduces the ranking of this strategy. Using the EUD metric the 7 mm FM strategy ranked last demonstrating the sensitivity of the EUD with regards to cold spots. Although, according to DVH metrics a 10 mm FM ranked second overall and first considering only fixed margins, the D_{98} underdosages especially in the EB patients would justify rather using a 15 mm FM which is confirmed by EUD rankings.

A review of by Jadon et al. summarizing internal organ motion from nine studies proposed isotropic margins from 15 to 21 mm around the CTV. Anisotropic margins of 12 to 32 mm in the anterior-posterior, 8 to 20 mm superior-inferior and 7 to 17 mm lateral directions [17,42]. Site-specific non-uniform margins of up to 40 mm around the uterine fundus and 13 mm around the cervix were proposed by Chan et al [43]. Gordon et al [44] suggested tapered margins of 24 mm around the fundus narrowing to 10 mm around the cervix. The variable margin (VBM) approach used in this study utilized population-based margins derived from movement quantification based on occupancy probabilities of 95% (see Chapter 2 for details). Margins were comparable to those stated above with 9 to 22 mm in the AP and 11 to 17 mm in the lateral directions. The VBM strategy ranked 4th for the FB group and 7th for the EB group regardless of the metric being used. The OAR sub score is meaningfully higher in the FB group hence the higher ranking compared to EB patients. Using smaller margins would be beneficial with regards to OAR sparing, resulting in a better ranking for this strategy. Deriving margins based on 90% occupancy probabilities instead would reduce margins with up to 5 mm on uterine level and 4 mm on both cervix and vaginal level. The magnitude of margins would then be comparable to a 15 mm FM strategy (see Chapter 2, table 4) and based on our results we anticipate that target coverage will still be adequate, but OAR sparing will be improved.

Defining an internal target volume (ITV) is a simple solution to overcome the risk of CTV underdosage due to organ motion often times with a disadvantage in terms of OAR sparing. Generally variable bladder filling pre-treatment scans are used to individualize ITV margins [19,45,46]. A detailed explanation of ITV generation for this study can be found in Chapter 2. The target sub score for the ITV strategy is comparable to a 10 mm FM for the EB patients and 15 mm FM and online strategy for FB patients. OAR sub scores ranked 5th for the EB group and 7th for the FB group indicating reduced OAR sparing. ITVs for the EB group were generated using naturally filling bladder scans acquired 20 mins apart. For the FB group 3 scans were used, 2 acquired on the same day 20 mins apart plus one FB scan acquired the following day. The scans selected to generate the ITV was based on the fact that the typical duration of a treatment fraction is ± 20 min [43]. Thus, the union structures used would capture movement expected during a treatment

fraction but not the full range of movement (empty to full bladder) due to bladder filling changes. Since patients were scanned and treated with specific bladder protocols a certain bladder volume (and target geometry) was anticipated which we expected to be in the range covered by the ITV. Similarly, to Bondar et al. Individualized ITVs were expanded with a 10 mm PTV margin which was proven to account for intra fraction motion as well [26]. The underdosage of patients in the EB group indicates the influence of organs such as rectum and small bowel on the geometry of the target [8,47]. Bowel preparation protocols can be used to minimize the influence of filling changes of these organs [48]. The inclusion of a third scan might be beneficial in terms of capturing a larger range of movement, however this would increase workload in terms of imaging. CBCT monitoring can also be used to assess motion patterns and decide if re-planning is necessary [45].

Individualization of treatment is a technique proposed by Yan et al. [18]. The concept of ART was to use an imaging feedback loop to quantify anatomical changes and modify the treatment plan accordingly [49,50]. Adaptation can be performed between (offline) or during (online) treatment fractions. In this study a margin of the day (MoD) strategy was simulated for both the offline and online approach. A library of plans with incremental CTV-PTV margins were used to determine the best plan of the day based on daily CBCTs. A detailed explanation can be found in Chapter 3. The on-line ART strategy ranked the highest for both groups (EB and FB) irrespective of the metric being used. Based on EUDs the off-line strategy ranked second while DVH metrics resulted in a 4th and 3rd ranking for the EB and FB groups respectively. Median EUD values for the target as well as the OARs for the two strategies are comparable. Although D_{95} and D_{98} median values are as comparable a notable difference in the OAR dose volume parameters are seen with higher OAR values for the offline strategy. Hence the lower rankings for the off-line strategy based on DVH metrics. Based on DVH metrics no underdosages were noted. However, in the EB group the EUD showed underdosages in four patients using the offline strategy and none using the online strategy. This demonstrate the sensitivity of the EUD metric to underdosages as previously mentioned. The target coverage for adaptive strategies were better than 10 mm FM and comparable to a 15 mm FM. OAR sparing were as good as 7- and 10 mm FM strategies for EB patients and even better sparing were noted for the online strategy in the FB group. Online

adaptive strategies account for both systematic and random anatomical changes making this the most effective strategy to correct organ motion and time trends [49,51]. Results from our study dosimetrically confirms the abovementioned statement.

Using the EUD metric to compare and rank plans is reliable in the sense that a worst case scenario is given where a lower boundary for targets and upper boundary for OARs are computed [52]. From the EUD based rankings it is evident that adaptive strategies are most efficient in terms of target coverage and OAR sparing. When target sub scores are capped at a value of 0.5 meaning strategies would not be credited for target coverage larger than the minimum requirement (44.9 Gy EUD) a change in rankings were observed. Adaptive strategies still remained in the same spot while a 10 mm FM and the ITV approach moved to third and fourth place indicating superior OAR sparing compared to the 15 mm FM which moved down to fifth place. The VBM strategy moved up on place to number six while the 20 mm FM ranked last due to high inferior sparing of OARs using.

The workload associated with these strategies regarding image acquisition and evaluation, plan generation or selection, and quality control are intensive and limit their use especially in resource limited departments. Adaptive strategies proposed in this study is based on a single planning CT scan which requires less workload than the ITV approach where 2-3 pre-treatment CT scans are required. However, the planning workload to generate a library containing at least 4 plans will be more. To reduce the workload plans tools to automate delineation and planning can be used which will render these strategies clinically more feasible. Fixed margin strategies and the VBM approach also use a single planning CT with no additional treatment plans and therefore are the least resource intensive. The 10- and 15 mm FM strategies ranked higher than the VBM approach and would consequently be favored. Although better OAR sparing is achieved using a 10 mm FM, the suggestion would be to rather opt for a 15 mm margin minimizing the chance of underdosing the target. This is in agreement with recommendations from literature [21,53].

Limitations of this study include the number of plans in the library for adaptive strategies. We anticipate using smaller increments between margins sizes will result in a different outcome especially with regards to OAR sparing. The VBM strategy can be based on lower occupancy probabilities which would result in smaller margins and most probably increase the ranking of this strategy. Lastly, more patients should be included in the FB group to draw firm conclusions.

4.5 Conclusion

The EUD can be used as a quick and reliable way of scoring treatment plans. Based on EUD metrics this study demonstrated that a personalized on-line adaptive strategy is most effective to account for target motion and deformation, yielding sufficient target coverage with adequate OAR sparing. ART is a resource intensive strategy and the use thereof should be prioritized for patients that would benefit from corrections. Tools to automate the process can be used to reduce the associated workload and yield a clinical feasible strategy. The use of a 15 mm FM as suggested by various groups was also confirmed.

4.6 References

1. Mundt AJ, Lujan AE, Rotmensch J, et al. Intensity-modulated whole pelvic radiotherapy in women with gynecologic malignancies. *Int J Radiat Oncol Biol Phys*. 2002;52(5):1330-1337. doi:10.1016/S0360-3016(01)02785-7
2. van de Bunt L, van der Heide UA, Ketelaars M, de Kort GAP, Jürgenliemk-Schulz IM. Conventional, conformal, and intensity-modulated radiation therapy treatment planning of external beam radiotherapy for cervical cancer: {The} impact of tumor regression. *Int J Radiat Oncol*. 2006;64(1):189-196. doi:10.1016/j.ijrobp.2005.04.025
3. Bondar L, Hoogeman M, Mens JW, et al. Toward an individualized target motion management for IMRT of cervical cancer based on model-predicted cervix-uterus shape and position. *Radiother Oncol*. 2011;99(2):240-245. doi:10.1016/j.radonc.2011.03.013
4. Wagner A, Jhingran A, Gaffney D. Intensity modulated radiotherapy in gynecologic cancers: Hope, hype or hyperbole? *Gynecol Oncol*. 2013;130(1):229-236. doi:10.1016/j.ygyno.2013.04.052
5. Brixey CJ, Roeske JC, Lujan AE, Yamada SD, Rotmensch J, Mundt AJ. Impact of intensity-modulated radiotherapy on acute hematologic toxicity in women with gynecologic malignancies. *Int J Radiat Oncol Biol Phys*. 2002;54(5):1388-1396. doi:10.1016/S0360-3016(02)03801-4
6. Rigaud B, Simon A, Gobeli M, et al. CBCT-guided evolutive library for cervical adaptive IMRT. *Med Phys*. 2018;45(4):1379-1390. doi:10.1002/mp.12818
7. Buchali Â, Koswig S, Dinges S, et al. Impact of the filling status of the bladder and rectum on their integral dose distribution and the movement of the uterus in the treatment planning of gynaecological cancer. *Radiother Oncol*. 1999;52:7-12.
8. van de Bunt L, Jürgenliemk-Schulz IM, de Kort GAP, Roesink JM, Tersteeg RJHA, van der Heide UA. Motion and deformation of the target volumes during {IMRT} for cervical cancer: {What} margins do we need? *Radiother Oncol*. 2008;88(2):233-240. doi:10.1016/j.radonc.2007.12.017
9. Beadle BM, Jhingran A, Salehpour M, Sam M, Iyer RB, Eifel PJ. Cervix Regression and Motion During the Course of External Beam Chemoradiation for Cervical Cancer. *Int J*

Radiat Oncol Biol Phys. 2009;73(1):235-241. doi:10.1016/j.ijrobp.2008.03.064

10. Chan P, Dinniwell R, Haider MA, et al. Inter- and Intrafractional Tumor and Organ Movement in Patients With Cervical Cancer Undergoing Radiotherapy: A Cinematic-MRI Point-of-Interest Study. *Int J Radiat Oncol Biol Phys*. 2008;70(5):1507-1515. doi:10.1016/j.ijrobp.2007.08.055
11. van de Bunt L, Jürgenliemk-Schulz IM, de Kort GAP, Roesink JM, Tersteeg RJHA, van der Heide UA. Motion and deformation of the target volumes during IMRT for cervical cancer: What margins do we need? *Radiother Oncol*. 2008;88(2):233-240. doi:10.1016/j.radonc.2007.12.017
12. Taylor A, Powell MEB. An assessment of interfractional uterine and cervical motion: {Implications} for radiotherapy target volume definition in gynaecological cancer. *Radiother Oncol*. 2008;88(2):250-257. doi:10.1016/j.radonc.2008.04.016
13. Ahmad R, Hoogeman MS, Bondar M, et al. Increasing treatment accuracy for cervical cancer patients using correlations between bladder-filling change and cervix–uterus displacements: {Proof} of principle. *Radiother Oncol*. 2011;98(3):340-346. doi:10.1016/j.radonc.2010.11.010
14. Quantification of intra-fraction changes during radiotherapy of cervical cancer assessed with pre- and post-fraction Cone Beam CT scans. *Radiother Oncol*. 2015;117(3):536-541. doi:10.1016/J.RADONC.2015.08.034
15. Taylor A, Powell MEB. An assessment of interfractional uterine and cervical motion: Implications for radiotherapy target volume definition in gynaecological cancer. *Radiother Oncol*. 2008;88(2):250-257. doi:10.1016/j.radonc.2008.04.016
16. Nováková E, Heijkoop ST, Quint S, et al. What is the optimal number of library plans in ART for locally advanced cervical cancer? *Radiother Oncol*. 2017;125(3):470-477. doi:10.1016/j.radonc.2017.08.033
17. Ríos I, Vásquez I, Cuervo E, Garzón Ó, Burbano J. Problems and solutions in IGRT for cervical cancer. *Reports Pract Oncol Radiother*. 2018;23(6):517-527. doi:10.1016/j.rpor.2018.05.002
18. Yan D, Vicini F, Wong J, Martinez A. Adaptive radiation therapy. *Phys Med Biol*.

1997;42(1):123-132.

19. Rigaud B, Simon A, Gobeli M, et al. CBCT-guided evolutive library for cervical adaptive IMRT. *Med Phys*. 2018;45(4):1379-1390. doi:10.1002/mp.12818
20. Stewart J, Lim K, Kelly V, et al. Automated {Weekly} {Replanning} for {Intensity}-{Modulated} {Radiotherapy} of {Cervix} {Cancer}. *Int J Radiat Oncol*. 2010;78(2):350-358. doi:10.1016/j.ijrobp.2009.07.1699
21. Ahmad R, Bondar L, Voet P, et al. A margin-of-the-day online adaptive intensity-modulated radiotherapy strategy for cervical cancer provides superior treatment accuracy compared to clinically recommended margins: {A} dosimetric evaluation. *Acta Oncol*. 2013;52(7):1430-1436. doi:10.3109/0284186X.2013.813640
22. Lim K, Stewart J, Kelly V, et al. Dosimetrically triggered adaptive intensity modulated radiation therapy for cervical cancer. *Int J Radiat Oncol Biol Phys*. 2014;90(1):147-154. doi:10.1016/j.ijrobp.2014.05.039
23. Buschmann M, Majercakova K, Sturdza A, et al. Image guided adaptive external beam radiation therapy for cervix cancer: Evaluation of a clinically implemented plan-of-the-day technique. *Z Med Phys*. 2018;28(3):184-195. doi:10.1016/j.zemedi.2017.09.004
24. Lim K, Small Jr. W, Portelance L, et al. Consensus {Guidelines} for {Delineation} of {Clinical} {Target} {Volume} for {Intensity}-{Modulated} {Pelvic} {Radiotherapy} for the {Definitive} {Treatment} of {Cervix} {Cancer}. *Int J Radiat Oncol*. 2011;79(2):348-355. doi:10.1016/j.ijrobp.2009.10.075
25. Gay HA, Barthold HJ, O'Meara E, et al. Pelvic normal tissue contouring guidelines for radiation therapy: A radiation therapy oncology group consensus panel atlas. *Int J Radiat Oncol Biol Phys*. 2012;83(3):e353-e362. doi:10.1016/j.ijrobp.2012.01.023
26. Bondar L, Hoogeman M, Mens JW, et al. Toward an individualized target motion management for {IMRT} of cervical cancer based on model-predicted cervix–uterus shape and position. *Radiother Oncol*. 2011;99(2):240-245. doi:10.1016/j.radonc.2011.03.013
27. Alber M, Nüsslin F. An objective function for radiation treatment optimization based on local biological measures. *Phys Med Biol*. 1999;44(2):479-493.
28. Laub W, Alber M, Birkner M, Nüsslin F. Monte Carlo dose computation for IMRT

optimization. *Phys Med Biol*. 2000;45(7):1741-1754. doi:10.1088/0031-9155/45/7/303

29. Söhn M, Yan D, Liang J, Meldolesi E, Vargas C, Alber M. Incidence of late rectal bleeding in high-dose conformal radiotherapy of prostate cancer using equivalent uniform dose-based and dose-volume-based normal tissue complication probability models. *Int J Radiat Oncol Biol Phys*. 2007;67(4):1066-1073. doi:10.1016/j.ijrobp.2006.10.014
30. Kavanagh BD, Pan CC, Dawson LA, et al. Radiation dose-volume effects in the stomach and small bowel. *Int J Radiat Oncol Biol Phys*. 2010;76(3 Suppl):S101--107. doi:10.1016/j.ijrobp.2009.05.071
31. Michalski JM, Gay H, Jackson A, Tucker SL, Deasy JO. Radiation dose-volume effects in radiation-induced rectal injury. *Int J Radiat Oncol Biol Phys*. 2010;76(3 Suppl):S123--129. doi:10.1016/j.ijrobp.2009.03.078
32. Viswanathan AN, Yorke ED, Marks LB, Eifel PJ, Shipley WU. Radiation {Dose}–{Volume} {Effects} of the {Urinary} {Bladder}. *Int J Radiat Oncol*. 2010;76(3, Supplement):S116--S122. doi:10.1016/j.ijrobp.2009.02.090
33. Tanderup K, Pötter R, Lindegaard J, et al. Image guided intensity modulated External beam radiochemotherapy and MRI based adaptive brachytherapy in locally advanced cervical cancer EMBRACE-II. *EMBRACE II study Protoc v10*. 2015:0-132. https://www.embracestudy.dk/UserUpload/PublicDocuments/EMBRACE II Protocol.pdf.
34. Jhingran A, Oncologist R, Co-Chair /, Portelance L, Miller BE, Salehpour MR. RTOG 0418 A Phase II Study of Intensity Modulated Radiation Therapy (IMRT) to the Pelvis +/- Chemotherapy for Post-operative Patients with either Endometrial or Cervical Carcinoma Study Chair/Radiation Oncologist. *org Gynecol Oncol*. 2006;(7138).
35. Bertelsen A, Hansen CR, Johansen J, Brink C. Single Arc Volumetric Modulated Arc Therapy of head and neck cancer. *Radiother Oncol*. 2010;95(2):142-148. doi:10.1016/j.radonc.2010.01.011
36. Niemierko A. Reporting and analyzing dose distributions: {A} concept of equivalent uniform dose. *Med Phys*. 1997;24(1):103-110. doi:10.1118/1.598063
37. Niemierko A. A generalized concept of equivalent uniform dose ({EUD}) [abstract]. *Med Phys*. 1999;26:1100.

38. Hysing LB, Skorpen TN, Alber M, Fjellsbø LB, Helle SI, Muren LP. Influence of Organ Motion on Conformal vs. Intensity-Modulated Pelvic Radiotherapy for Prostate Cancer. *Int J Radiat Oncol Biol Phys*. 2008;71(5):1496-1503. doi:10.1016/j.ijrobp.2008.04.011
39. Roeske JC, Bonta D, Mell LK, Lujan AE, Mundt AJ. A dosimetric analysis of acute gastrointestinal toxicity in women receiving intensity-modulated whole-pelvic radiation therapy. *Radiother Oncol*. 2003;69(2):201-207.
40. Wu Q, Mohan R, Niemierko A, Schmidt-Ullrich R. Optimization of Intensity-Modulated Radiotherapy plans based on the Equivalent Uniform Dose. *Int J Radiat Oncol * Biol * Phys*. 2002;53(1):224-235.
41. Niemierko A. Reporting and analyzing dose distributions: {A} concept of equivalent uniform dose. *Med Phys*. 1997;24(1):103-110. doi:10.1118/1.598063
42. Jadon R, Pembroke CA, Hanna CL, et al. A {Systematic} {Review} of {Organ} {Motion} and {Image}-guided {Strategies} in {External} {Beam} {Radiotherapy} for {Cervical} {Cancer}. *Clin Oncol*. 2014;26(4):185-196. doi:10.1016/j.clon.2013.11.031
43. Chan P, Dinniwell R, Haider MA, et al. Inter- and Intrafractional Tumor and Organ Movement in Patients With Cervical Cancer Undergoing Radiotherapy: A Cinematic-MRI Point-of-Interest Study. *Int J Radiat Oncol Biol Phys*. 2008;70(5):1507-1515. doi:10.1016/j.ijrobp.2007.08.055
44. Gordon JJ, Weiss E, Abayomi OK, Siebers J V, Dogan N. The Effect of Uterine Motion and Uterine Margins on Target and Normal Tissue Doses in Intensity Modulated Radiation Therapy of Cervical Cancer. doi:10.1088/0031-9155/56/10/001
45. Pötter R, Tanderup K, Kirisits C, et al. The EMBRACE II study: The outcome and prospect of two decades of evolution within the GEC-ESTRO GYN working group and the EMBRACE studies. *Clin Transl Radiat Oncol*. 2018;9:48-60. doi:10.1016/j.ctro.2018.01.001
46. Jensen NBK, Assenholt MS, Fokdal LU, et al. Cone beam computed tomography-based monitoring and management of target and organ motion during external beam radiotherapy in cervical cancer. *Phys Imaging Radiat Oncol*. 2018;9(December 2018):14-20. doi:10.1016/j.phro.2018.12.002
47. Jadon R, Pembroke CA, Hanna CL, et al. A {Systematic} {Review} of {Organ} {Motion} and

{Image}-guided {Strategies} in {External} {Beam} {Radiotherapy} for {Cervical} {Cancer}. *Clin Oncol*. 2014;26(4):185-196. doi:10.1016/j.clon.2013.11.031

48. Eminowicz G, Motlib J, Khan S, Perna C, McCormack M. Pelvic Organ Motion during Radiotherapy for Cervical Cancer: Understanding Patterns and Recommended Patient Preparation. *Clin Oncol*. 2016;28(9):e85-e91. doi:10.1016/j.clon.2016.04.044
49. Sonke JJ, Aznar M, Rasch C. Adaptive Radiotherapy for Anatomical Changes. *Semin Radiat Oncol*. 2019;29(3):245-257. doi:10.1016/j.semradonc.2019.02.007
50. Tanderup K, Georg D, Pötter R, Kirisits C, Grau C, Lindegaard JC. Adaptive Management of Cervical Cancer Radiotherapy. *Semin Radiat Oncol*. 2010;20(2):121-129. doi:10.1016/j.semradonc.2009.11.006
51. Oh S, Stewart J, Moseley J, et al. Hybrid adaptive radiotherapy with on-line {MRI} in cervix cancer {IMRT}. *Radiother Oncol*. 2014;110(2):323-328. doi:10.1016/j.radonc.2013.11.006
52. Sobotta B, Söhn M, Shaw W, Alber M. On expedient properties of common biological score functions for multi-modality, adaptive and 4D dose optimization. *Phys Med Biol*. 2011;56(10):N123--129. doi:10.1088/0031-9155/56/10/N01
53. Lim K, Small Jr. W, Portelance L, et al. Consensus {Guidelines} for {Delineation} of {Clinical} {Target} {Volume} for {Intensity}-{Modulated} {Pelvic} {Radiotherapy} for the {Definitive} {Treatment} of {Cervix} {Cancer}. *Int J Radiat Oncol*. 2011;79(2):348-355. doi:10.1016/j.ijrobp.2009.10.075
54. Bondar ML, Hoogeman MS, Mens JW, et al. Individualized {Nonadaptive} and {Online}-{Adaptive} {Intensity}-{Modulated} {Radiotherapy} {Treatment} {Strategies} for {Cervical} {Cancer} {Patients} {Based} on {Pretreatment} {Acquired} {Variable} {Bladder} {Filling} {Computed} {Tomography} {Scans}. *Int J Radiat Oncol*. 2012;83(5):1617-1623. doi:10.1016/j.ijrobp.2011.10.011
55. Tyagi N, Lewis JH, Yashar CM, et al. Daily {Online} {Cone} {Beam} {Computed} {Tomography} to {Assess} {Interfractional} {Motion} in {Patients} {With} {Intact} {Cervical} {Cancer}. *Int J Radiat Oncol*. 2011;80(1):273-280. doi:10.1016/j.ijrobp.2010.06.003
56. Bondar ML, Hoogeman MS, Mens JW, et al. Individualized {Nonadaptive} and {Online}-{Adaptive} {Intensity}-{Modulated} {Radiotherapy} {Treatment} {Strategies} for {Cervical}

{Cancer} {Patients} {Based} on {Pretreatment} {Acquired} {Variable} {Bladder} {Filling} {Computed} {Tomography} {Scans}. *Int J Radiat Oncol*. 2012;83(5):1617-1623. doi:10.1016/j.ijrobp.2011.10.011

57. Ahmad R, Hoogeman MS, Bondar M, et al. Increasing treatment accuracy for cervical cancer patients using correlations between bladder-filling change and cervix-uterus displacements: Proof of principle. *Radiother Oncol*. 2011;98(3):340-346. doi:10.1016/j.radonc.2010.11.010
58. Leung LHT, Kan MWK, Cheng ACK, Wong WKH, Yau CC. A new dose-volume-based Plan Quality Index for IMRT plan comparison. *Radiother Oncol*. 2007;85(3):407-417. doi:10.1016/j.radonc.2007.10.018
59. Hernandez V, Hansen CR, Widesott L, et al. What is plan quality in radiotherapy? The importance of evaluating dose metrics, complexity, and robustness of treatment plans. *Radiother Oncol*. 2020;153:26-33. doi:10.1016/j.radonc.2020.09.038
60. Hansen CR, Crijns W, Hussein M, et al. Radiotherapy Treatment plannINg study Guidelines (RATING): A framework for setting up and reporting on scientific treatment planning studies. *Radiother Oncol*. 2020;153:67-78. doi:10.1016/j.radonc.2020.09.033
61. Shang H, Pu Y, Wang W, Dai Z, Jin F. Evaluation of plan quality and robustness of IMPT and helical IMRT for cervical cancer. *Radiat Oncol*. 2020;15(1):1-11. doi:10.1186/s13014-020-1483-x
62. Santos T, Ventura T, Lopes M do C. Evaluation of the complexity of treatment plans from a national IMRT/VMAT audit – Towards a plan complexity score. *Phys Medica*. 2020;70(January):75-84. doi:10.1016/j.ejmp.2020.01.015

Appendix: Chapter 4

Table A1: Mean values ± standard deviation of DVH parameters for pCTV of different strategies for the empty- and full bladder patients. Dose values (D_v) are in Gy and V_D in % volume.

	7	10	15	20	ITV	VBM	OFF	ON
	Empty bladder							
D_{98}	42.41 ± 1.43	43.57 ± 0.94	44.17 ± 0.51	44. 32 ± 0.34	44.12 ± 0.7	44.42 ± 0.56	43. 82 ± 0.54	43.73 ± 0.42
D_{95}	43.90 ± 0.70	44.59 ± 0.52	44.62 ± 0.50	44.68 ± 0.29	44.73 ± 0.37	44.89 ± 0.35	44.61 ± 0.41	44.52 ± 0.32
V_{98}	95.05 ± 2.30	97.04 ± 1.84	98.59 ± 1.20	98.61 ± 1.20	98.42 ± 1.48	98.97 ± 1.02	97.30 ± 1.44	96.83 ± 1.38
V_{95}	97.61 ± 1.33	98.81 ± 0.85	99.75 ± 0.28	99.92 ± 0.12	99.46 ± 0.58	99.75 ± 0.39	99.06 ± 0.62	99.05 ± 0.46
	Full bladder							
D_{98}	42.89 ± 1.27	43.82 ± 0.73	44.41 ± 0.23	44.43 ± 0.32	44.43 ± 0.32	44.24 ± 0.76	44.10 ± 0.50	43.82 ± 0.63
D_{95}	43.96 ± 0.84	44.50 ± 0.50	44.72 ± 0.18	44.76 ± 0.19	44.75 ± 0.22	44.72 ± 0.36	44.70 ± 0.30	44.56 ± 0.34
V_{98}	94.90 ± 3.36	98.03 ± 1.81	99.00 ± 0.69	99.03 ± 0.57	99.07 ± 0.84	98.70 ± 1.35	97.84 ± 1.51	97.11 ± 1.74
V_{95}	97.68 ± 1.78	99.07 ± 0.99	99.76 ± 0.34	99.90 ± 0.19	99.64 ± 0.51	99.39 ± 0.98	99.13 ± 0.95	99.04 ± 0.72

Table A2: Mean values ± standard deviation of DVH parameters for OARs of different strategies for the empty- and full bladder patients. Dose values (D_v) are in Gy and V_D in % volume.

	7	10	15	20	ITV	VBM	OFF	ON
	Empty bladder							
Rectum								
V_{30}	82.07 ± 7.06	83.16 ± 6.05	93.61 ± 3.47	97.35 ± 2.51	88.37 ± 6.38	92.97 ± 4.19	85.74 ± 5.04	84.35 ± 4.25
V_{40}	48.58 ± 14.09	56.22 ± 13.44	75.18 ± 10.86	88.19 ± 7.32	62.87 ± 13.15	75.22 ± 11.79	60.56 ± 14.20	55.27 ± 12.51
Bladder								
V_{30}	75.28 ± 7.84	79.65 ± 5.53	89.36 ± 5.76	94.05 ± 5.21	81.53 ± 6.86	90.3 ± 4.77	82.17 ± 7.60	78.76 ± 7.14
V_{40}	44.35 ± 11.79	52.11 ± 11.75	67.48 ± 12.02	78.70 ± 11.54	54.85 ± 12.64	67.77 ± 13.02	57.61 ± 14.35	51.29 ± 12.93
Sigmoid								
V_{30}	96.56 ± 2.95	94.95 ± 5.71	98.15 ± 1.67	98.70 ± 1.94	96.83 ± 3.20	98.37 ± 1.42	94.66 ± 5.34	95.01 ± 5.31
V_{40}	65.20 ± 16.40	69.97 ± 16.71	80.39 ± 11.16	87.63 ± 10.57	83.10 ± 12.26	82.69 ± 14.49	73.01 ± 15.46	69.45 ± 13.72
Small bowel								
V_{15}	83.70 ± 7.74	84.16 ± 7.77	83.88 ± 7.80	84.77 ± 7.12	85.72 ± 7.13	85.44 ± 6.98	83.38 ± 7.39	83.19 ± 7.45
V_{45}	5.73 ± 3.77	7.53 ± 5.33	8.10 ± 4.79	8.66 ± 5.32	8.72 ± 4.70	9.59 ± 5.89	7.60 ± 5.12	6.68 ± 4.32
	Full bladder							
Rectum								
V_{30}	76.65 ± 12.48	79.80 ± 9.33	91.89 ± 5.41	97.92 ± 1.19	90.99 ± 5.52	89.23 ± 6.12	83.94 ± 7.46	79.66 ± 9.30
V_{40}	45.21 ± 12.76	56.14 ± 12.32	74.89 ± 11.84	87.33 ± 6.70	72.85 ± 10.34	72.24 ± 13.45	60.21 ± 9.60	51.69 ± 11.00
Bladder								
V_{30}	69.98 ± 7.71	70.20 ± 4.41	82.93 ± 6.93	88.27 ± 5.09	76.59 ± 5.03	76.30 ± 3.44	76.09 ± 8.54	72.44 ± 5.93
V_{40}	35.31 ± 7.07	42.30 ± 5.94	56.55 ± 6.21	66.64 ± 5.27	51.82 ± 6.41	48.11 ± 5.90	46.93 ± 10.21	40.53 ± 5.74
Sigmoid								
V_{30}	92.42 ± 6.08	93.90 ± 4.89	95.9 ± 6.40	97.72 ± 2.92	94.15 ± 6.18	94.27 ± 3.98	95.59 ± 4.36	93.59 ± 4.99
V_{40}	63.23 ± 21.53	72.06 ± 18.03	79.44 ± 16.16	85.36 ± 12.06	79.97 ± 12.35	72.42 ± 21.93	73.39 ± 20.24	67.27 ± 20.47
Small bowel								
V_{15}	80.48 ± 7.87	81.54 ± 7.95	82.87 ± 9.00	83.81 ± 8.58	82.96 ± 9.09	80.05 ± 7.76	82.47 ± 8.32	81.32 ± 7.90
V_{45}	3.25 ± 2.21	4.45 ± 2.68	5.05 ± 4.24	6.57 ± 4.97	4.97 ± 4.55	3.05 ± 2.50	4.50 ± 3.01	3.88 ± 2.77

Table A3: Average EUD ± standard deviation for the OARs using different planning strategies.

	Bladder		Rectum		Sigmoid		Small bowel	
	EB	FB	EB	FB	EB	FB	EB	FB
7	40.45 ± 1.26	39.25 ± 0.95	41.48 ± 1.20	41.35 ± 1.38	42.43 ± 1.23	42.28 ± 2.03	28.83 ± 3.22	24.39 ± 2.82
10	41.36 ± 1.31	40.42 ± 0.81	42.43 ± 1.10	42.66 ± 1.13	42.84 ± 1.45	43.22 ± 1.80	29.16 ± 3.21	23.62 ± 1.90
15	42.58 ± 0.99	41.66 ± 0.57	43.44 ± 0.77	43.55 ± 0.80	43.69 ± 0.80	43.61 ± 1.80	29.47 ± 3.42	24.94 ± 3.17
20	43.27 ± 0.75	42.48 ± 0.59	44.04 ± 0.46	44.05 ± 0.40	44.10 ± 0.73	43.95 ± 1.30	29.75 ± 3.71	25.20 ± 3.38
ITV	41.54 ± 1.40	41.34 ± 0.75	42.84 ± 0.95	43.65 ± 0.44	44.09 ± 0.95	43.84 ± 1.36	30.20 ± 2.15	24.77 ± 3.04
VBM	42.37 ± 1.76	40.93 ± 0.62	43.48 ± 0.93	43.61 ± 1.02	43.54 ± 1.58	42.36 ± 2.11	30.26 ± 2.27	24.37 ± 2.93
OFF	41.36 ± 1.27	39.99 ± 1.42	42.24 ± 1.38	42.39 ± 1.12	42.95 ± 1.21	41.79 ± 2.10	29.74 ± 2.00	24.71 ± 3.41
ON	40.63 ± 1.63	39.21 ± 1.64	41.31 ± 2.29	41.62 ± 1.06	42.42 ± 1.22	41.25 ± 2.07	29.56 ± 1.98	24.21 ± 3.39

Table A4: Average EUDs (Gy) ± stdev to the nodal groups using an ITV and VBM planning strategy.

	ITV	VBM
Empty bladder		
CIR	46.19 ± 0.67	45.91 ± 0.92
CIL	46.27 ± 0.50	46.98 ± 0.63
EIR	46.00 ± 0.33	45.79 ± 0.42
EIL	45.91 ± 0.34	45.73 ± 0.49
IIR	46.09 ± 0.34	45.97 ± 0.33
IIL	46.13 ± 0.34	45.92 ± 0.40
OBTL	45.76 ± 0.84	45.65 ± 0.85
OBTR	45.89 ± 0.32	45.75 ± 0.37
PreSac	45.76 ± 0.41	45.52 ± 0.56
Full bladder		
CIR	46.39 ± 0.43	45.95 ± 0.28
CIL	46.42 ± 0.33	46.02 ± 0.23
EIR	45.94 ± 0.24	45.45 ± 0.29
EIL	45.80 ± 0.41	45.48 ± 0.28
IIR	46.04 ± 0.32	46.00 ± 0.26
IIL	46.00 ± 0.40	45.87 ± 0.23
OBTL	45.92 ± 0.33	45.68 ± 0.28
OBTR	45.88 ± 0.28	45.67 ± 0.17
PreSac	45.19 ± 1.64	45.75 ± 1.98

**CIR and CIL = common iliac right and left, EIR and EIL = external iliac right and left, IIR and IIL = internal iliac right and left, OBTR and OBTL = obturator right and left, PreSac = Presacral*

Table A5: Sub scores for OARs based on DVH metrics for the EB and FB groups

	Bladder		Rectum		Sigmoid		Small bowel	
	EB	FB	EB	FB	EB	FB	EB	FB
7	0.927	0.980	0.940	0.966	0.645	0.717	0.900	1.000
10	0.817	0.988	0.917	0.952	0.637	0.666	0.848	1.000
15	0.527	0.851	0.680	0.706	0.484	0.514	0.792	0.982
20	0.414	0.687	0.374	0.393	0.346	0.399	0.505	0.817
ITV	0.766	0.908	0.831	0.754	0.455	0.600	0.611	0.954
VBM	0.442	0.953	0.683	0.766	0.404	0.611	0.603	1.000
OFF	0.754	0.929	0.876	0.931	0.613	0.566	0.819	1.000
ON	0.844	0.977	0.927	0.963	0.662	0.686	0.886	1.000

Table A6: Sub scores for OARs based on EUD for the EB and FB groups

	Bladder		Rectum		Sigmoid		Small bowel	
	EB	FB	EB	FB	EB	FB	EB	FB
7	0.829	0.902	0.754	0.761	0.751	0.667	0.909	0.994
10	0.760	0.840	0.666	0.643	0.711	0.578	0.894	0.998
15	0.652	0.747	0.562	0.550	0.641	0.537	0.873	0.989
20	0.581	0.667	0.496	0.495	0.597	0.505	0.849	0.984
ITV	0.761	0.773	0.626	0.540	0.596	0.516	0.863	0.991
VBM	0.658	0.806	0.556	0.543	0.641	0.657	0.854	0.994
OFF	0.761	0.855	0.678	0.671	0.707	0.706	0.894	0.988
ON	0.802	0.893	0.739	0.744	0.751	0.752	0.902	0.993

Chapter 5: Probabilistic planning

5.1 Introduction

High precision techniques in radiotherapy allow the delivery of highly conformal dose distributions adapted to a particular geometry. Geometric uncertainties due to organ motions can lead to a difference between applied and planned dose [1]. Geometrical uncertainties are described by normal distributions which can be acquired from population statistics, multiple patient scans, or a combination of both [2,3]. Information obtained from a low number of CT images is sufficient to estimate organ motion to be used during planning [4]. However, more samples are necessary to determine a reliable estimation when the distribution becomes wide [1]. Conventionally these errors are handled by expanding the clinical target volume (CTV) to generate a planning target volume (PTV). Recipes used to determine these margins are based on certain coverage or minimum dose delivered to the mobile CTV. These margins only address the target volume and do not consider OARs that overlap with the planning volume. Therefore, to further exploit the probabilistic mechanisms of target volume and OAR overlap, a volume trade-off can be found between maximizing target coverage and minimizing OAR dose [2,4].

Incorporating geometric uncertainties in the optimization process employing coverage probability allows a more relaxed planning aim especially near the edge of the PTV in the overlapping regions. Coverage probability planning (CovP) has been shown to improve target dose homogeneity while reducing rectum dose for the same target coverage [5]. Ramlov et al. [6] proved the clinical feasibility for simultaneous integrated boost (SIB) of pathological nodes with a significant reduction in OAR dose.

This study aimed to evaluate a margin-less treatment planning method where coverage probabilities are used in the optimization of intensity-modulated radiotherapy treatment planning. This method was compared to an online and offline adaptive strategy, as well as a 15

mm fixed margin. In addition to this comparison, an investigation of plan adaptation was performed where a loss of CTV dose coverage was evident.

5.2 Materials and Methods

5.2.1 Patient information and imaging

10 patients receiving radical radiotherapy for cervical cancer have been included in this study. This is a subgroup of the 20 patients in Chapter 4. Patients have been randomly selected, 7 from the empty bladder group and 3 from the full bladder group. A detailed description of patient characteristics, imaging, and delineation information is given in Chapter 2.

5.2.2 Treatment planning

The treatment planning process of the two adaptive and 15 mm fixed margin (FM) approaches are explained in detail in Chapters 3 and 4 respectively. For a fair comparison, optimization parameters were kept the same for all strategies.

5.2.2.1 Coverage probability planning (CovP)

Hyperion® (University of Tübingen, Germany) research dose planning software was used to develop planning aims for CovP. The estimation of coverage probabilities (CP) in Hyperion has been described by Baum et al.[4]. For the empty bladder patients, CPs for the primary and nodal CTVs (pCTV and nPTV) were based on the pre-treatment empty bladder scan (CT_{EB}) and cone-beam CT (CBCT) scans acquired on the first two days of treatment. Full bladder scans acquired on three consecutive pre-treatment days were used to estimate CPs for the full bladder group. During optimization, a cut-off value of 10^{-4} for CP was used to avoid numerical problems.
Due to the fact that the first two CBCTs was used as input data for CP estimation their geometries were not included during treatment simulation and dose accumulation. A 15 mm FM was used for the first two treatment fractions.

5.2.3 Comparison of strategies

As described in Chapter 4, planning strategies were compared based on an objective function proposed by Wu et al. [7]. This function consists of sub scores for target and OARs using EUD metrics. Based on these sub scores a final function is calculated which is used to rank strategies

5.3 Results

5.3.1 Coverage probability planning workload

Table 1 summarizes the workload associated with each strategy based on imaging, planning, dose accumulation, quality assurance (QA), and contouring. Daily CBCT image for positional setup verification was acquired for all strategies. Imaging workload mainly depends on the number of pre-treatment images necessary. Planning was done on one pre-treatment image for the online, offline, and 15 mm FM strategy. The workload associated with plan generation depends on the number of plans in the library which may vary between institutions. Four plans were generated for online and offline strategies. Only one plan was generated for CovP and the 15 mm FM. The frequency of adaptation will determine the plan generation workload for any strategy being adapted. The dose was accumulated using the EUD metric for all strategies. Delineation was done on all pre-treatment images acquired. For CovP it will depend on the number of images used for CP estimation. Online, offline, and 15 mm FM strategies only had one pre-treatment images where structures had to be delineated. Continuous contouring is necessary for plan adaptation to monitor dose or organ motion to decide when plan modification is necessary. Quality assurance for all strategies is linked to the number of plans generated for each strategy.

Table 1: Workload associated with each planning strategy.

	CovP	Online	Offline	15 mm	Adapt
Imaging					
Pre-treatment	3	1	1	1	N/A
During treatment	Daily imaging	Daily imaging	Daily imaging	Daily imaging	Daily imaging
Planning	1	5	5	1	Depends on frequency of adaptation
Dose accumulation	EUD	EUD	EUD	EUD	EUD
Quality assurance	Depends on the number of plans				
Contouring	Same as no. of pretreatment datasets	1	1	1	continuous

5.3.2 Coverage probability planning

Figure 1 illustrates the occupancy maps generated for the pCTV throughout treatment. The reference target volume is indicated by the yellow arrows. Turquoise represents 100% occupancy of the structure while orange represents 50%. The advantage of coverage probability information in terms of OAR sparing is clearly demonstrated on the axial image where the rectum overlaps with the target (green arrow). The occupancy of the target in the overlapping region is low which means that lower than prescribed doses can be permitted in that region.

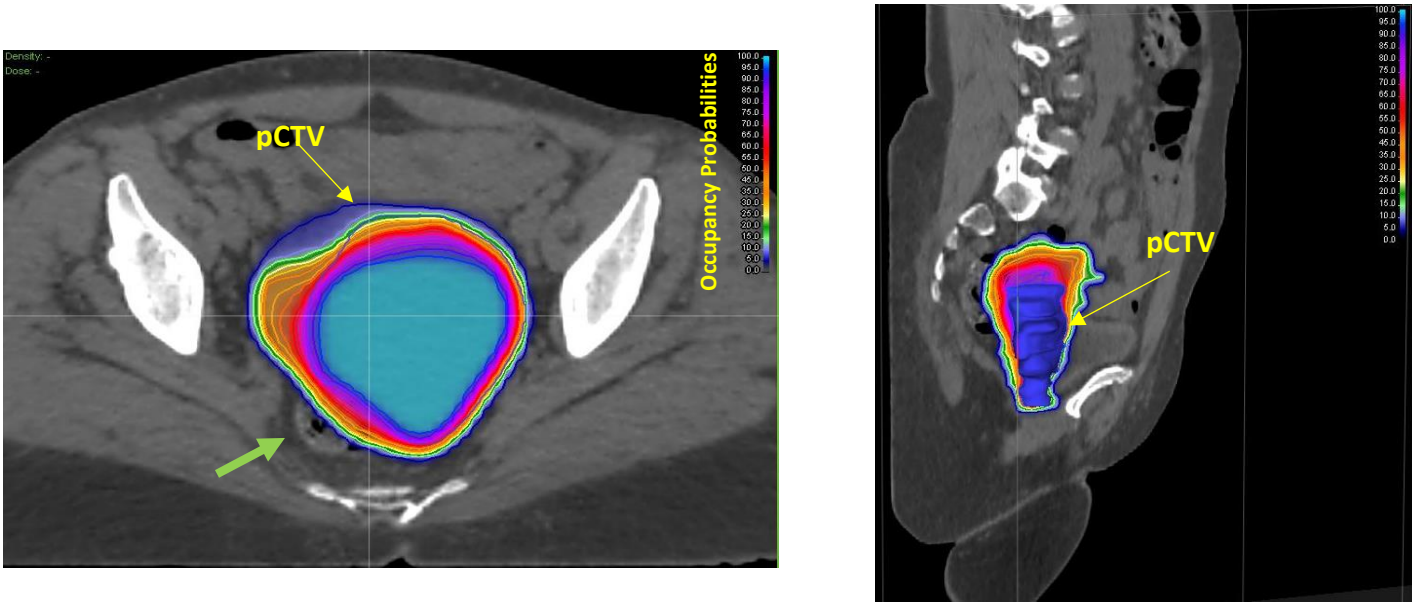

Figure 1: An axial and saggital CT image illustrating occupany maps of the the pCTV throughout treatment. The refernce pCTV are indicated by the arrows.

Figure 2 illustrates the advantage of plan adaptation during treatment for one patient. A gradual reduction in the pCTV EUD values can be seen in Figure 2a (green dots). Plan adaptation was performed at the end of the third week of treatment. The CBCT images of fraction 13, 14, and 15 were used to estimate CPs and optimize the new plan. EUDs scored with the adapted plan are indicated by the blue dots. The average EUD for the CovP plan without adaptation was 44.84 Gy and after adaptation it was 44.91 Gy. Dose to the rectum and sigmoid (Figure 2b and c) was

reduced after adaptation while a slight increase in bladder and small bowel EUD were noted (Figure 2d and e). The outlier seen at fraction 19 is typically seen in other treatment strategies as well. None of the other strategies were able to avoid the under dosage in that specific fraction.

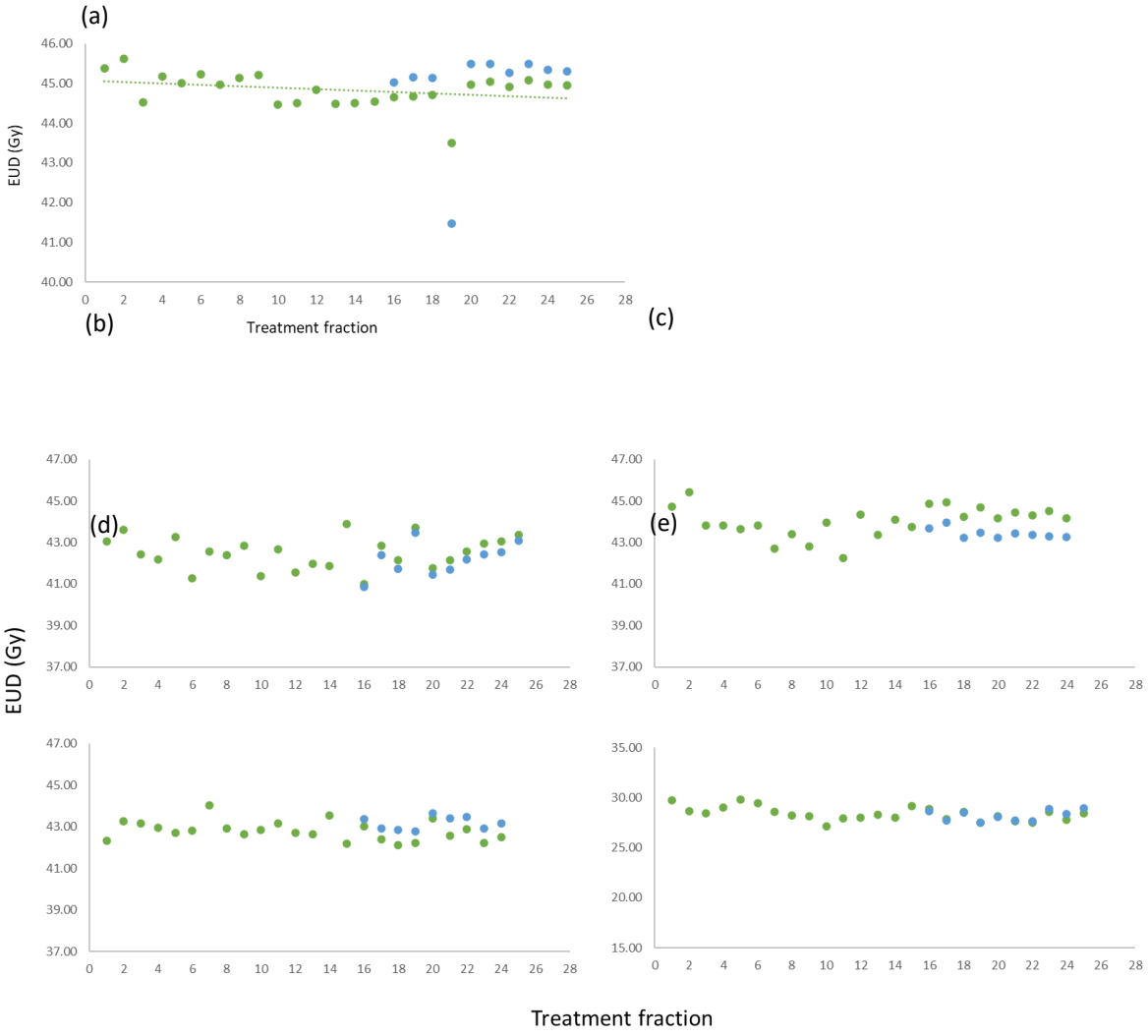

Figure 2: EUD (Gy) values scored for all treatment fractions of one patient for the (a) pCTV, (b) rectum, (c) sigmoid, (d) bladder, and (e) small bowel.

5.3.3 Comparison of strategies

The median EUD for all strategies were higher than the minimum planning requirement (44.9 Gy) as seen in Figure 3. No under dosages were seen in the CoVP and online strategies while one patient in the offline and 15 mm fixed margin strategies was underdosed. This was not the same patient. The average EUDs (EUD_{ave}) for all strategies were comparable and ≥ 45 Gy with the lowest EUD_{ave} (45.16 ± 0.09 Gy) noted for the CoVP strategy (Table 2).

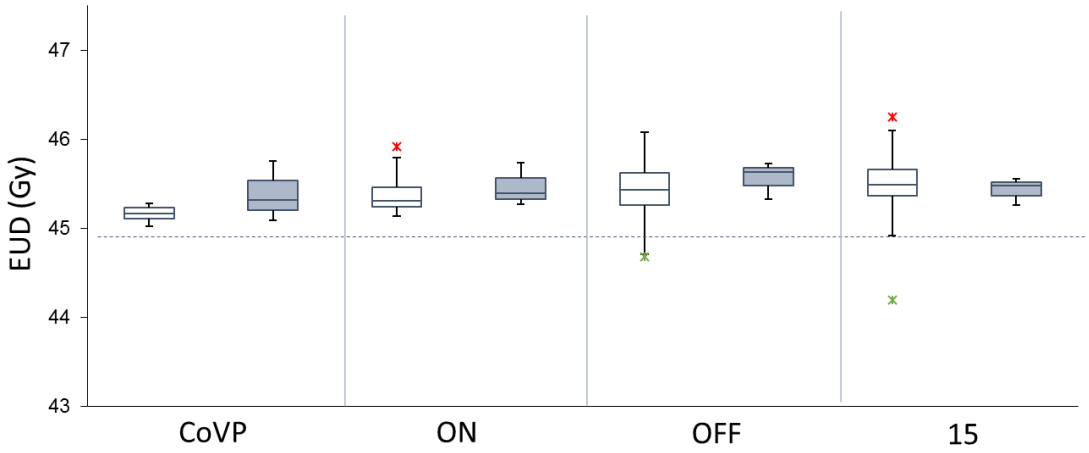

Figure 3: Box-whisker plots of the EUD_{ave} for the pCTV using different strategies. The deviation for the population of empty- (open) and full bladder (solid) patients around the median is shown. The planning objective (44.9 Gy) is indicated by the dashed line.

Table 2: Average EUD ± standard deviation for the pCTV using different planning strategies.

EUD_{avg} (Gy)		
	EB	FB
CoVP	45.16 ± 0.09	45.39 ± 0.34
ON	45.40 ± 0.26	45.47 ± 0.24
OFF	45.42 ± 0.44	45.56 ± 0.21
15	45.43 ± 0.62	45.43 ± 0.15

The average EUDs for all OARs and different strategies are shown in Figure 4. The lowest average EUDs for all OARs, except the small bowel, were obtained with the online adaptive strategy. The CoVP strategy had the lowest EUD_{ave} for the small bowel in the EB group. The highest EUD_{ave} values were scored for all OARs when a 15 mm FM strategy was used. Compared to the CoVP strategy, the average EUD for the bladder was lower in both adaptive strategies. For the EB patients the EUD_{ave} for the rectum was lower using CoVP planning compared to offline adaptation. The values were comparable in the FB group. For the sigmoid the EUD_{ave} of the CoVP and offline strategy were comparable for both EB and FB patients. Table 3 summarizes the average EUDs and standard deviations for all OARS and strategies.

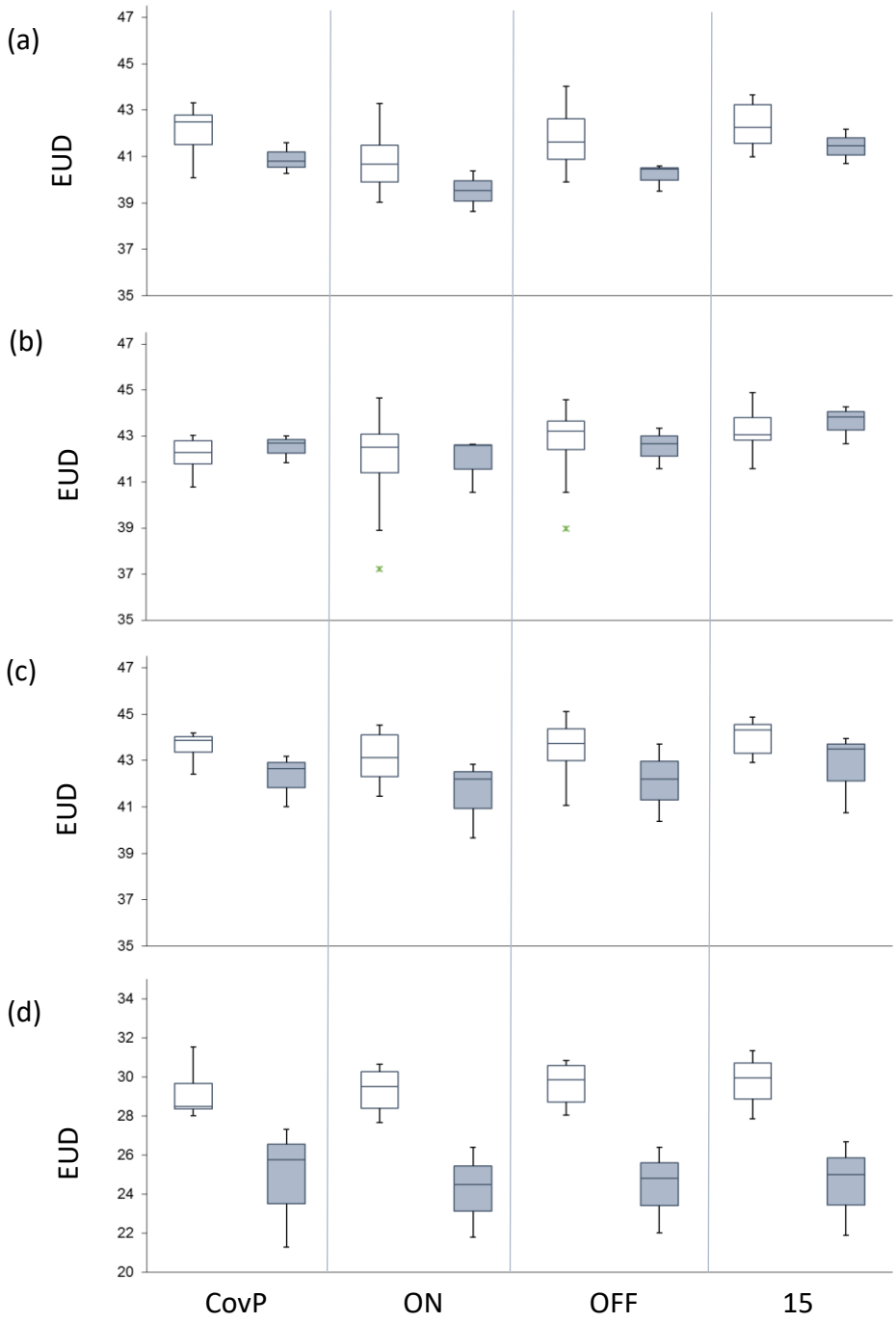

Figure 4: Box-whisker plots of the EUD_{ave} for the (a) bladder, (b) rectum, (c) sigmoid using, and (d) small bowel using different strategies. The deviation for the population of empty- (open) and full bladder (solid) patients around the median is shown.

Table 3: Average EUD ± standard deviation for the OARs using different planning strategies.

	Bladder		Rectum		Sigmoid		Small bowel	
	EB	FB	EB	FB	EB	FB	EB	FB
CoVP	42.08 ± 1.13	40.90 ± 0.67	42.17 ± 0.83	42.51 ± 0.60	43.62 ± 0.62	42.28 ± 1.13	29.15 ± 1.26	24.79 ± 3.13
ON	40.84 ± 1.48	39.52 ± 0.87	41.91 ± 2.37	41.93 ± 1.19	43.14 ± 1.19	41.56 ± 1.67	29.30 ± 1.19	24.22 ± 2.31
OFF	41.80 ± 1.47	40.19 ± 0.59	42.70 ± 1.82	42.53 ± 0.89	43.53 ± 1.37	42.10 ± 1.66	29.62 ± 1.16	24.41 ± 2.22
15	42.36 ± 1.05	41.44 ± 0.74	43.26 ± 1.04	43.59 ± 0.83	43.99 ± 0.78	42.73 ± 1.73	29.76 ± 1.29	24.53 ± 2.43

5.3.4 Scoring of strategies

All strategies resulted in target sub scores higher than 0.5 indicating adequate target coverage (Table 4a). The highest scores were obtained with the offline and 15 mm FM strategy for EB patients and the offline strategy for FB patients. CoVP scored the lowest in terms of target coverage. The best OAR sparing was achieved with the online strategy for both groups, while CoVP ranked second in the EB group and third in the FB group. The lowest OAR sub scores were achieved with a 15 mm FM strategy. The ranking of strategies based on the *F* scores is given in Table 4b. The results are exactly the same for both groups with the online and offline strategies first and second, CovP third and the fixed margin strategy last.

Table 4: Sub score for targets and OARs using the EUD metric for the EB and FB groups. Strategies are ranked based on the final score, F.

(a)

	$f_{T_{EUD}}$		$f_{OAR_{EUD}}$		F_{EUD}	
	EB	FB	EB	FB	EB	FB
CoVP	0.529	0.554	0.747	0.782	0.395	0.433
ON	0.554	0.562	0.779	0.824	0.432	0.463
OFF	0.557	0.573	0.731	0.797	0.407	0.457
15	0.557	0.558	0.696	0.723	0.388	0.404

(b)

	EB	FB
1	ON	ON
2	OFF	OFF
3	CoVP	CoVP
4	15	15

5.4 Discussion

In our view, the use of daily 3D imaging for patient setup correction is a minimum requirement when advanced strategies delivering highly conformal dose distributions are utilized. The clinical feasibility of any strategy depends on the workload associated with it. The lowest workload with regards to imaging was seen in the online, offline, and 15 mm FM strategies. Patients in this study were treated with bladder protocols, therefore, only one pre-treatment image was used. Imaging workload regarding pre-treatment imaging for the CovP strategy can be reduced by using CBCTs as input for the estimation of CPs. The EUD metric was successfully used as a dose metric for quick scoring of CP treatment plans. EUDs can easily be calculated from dose-volume histograms for any dose distribution obtained in new geometries during adaptive treatment if need be. CovP has a relatively low workload, and is associated with low rate toxicity and high local control rates [8]. In accordance with a study by Tilly et al. [5] improved target coverage and a reduction in rectal dose were observed compared to the 15 mm fixed margin plans.

5.5 Conclusion

Coverage probability planning is a promising strategy that incorporates geometric uncertainties of an individual patient in the optimization process. The underlying properties of CovP allow a more relaxed planning aim resulting in better OAR sparing. Adequate target coverage, comparable to that of online adaptive strategies can be achieved. Adaptation based on CovP yields good results and is robust against significant geometrical changes and daily motion.

5.6 References

1. Sobotta B, Söhn M, Alber M. Robust optimization based upon statistical theory. *Med Phys*. 2010;37(8):4019-4028. doi:10.1118/1.3457333
2. Witte MG, Van Der Geer J, Schneider C, Lebesque J V., Alber M, Van Herk M. IMRT optimization including random and systematic geometric errors based on the expectation of TCP and NTCP. *Med Phys*. 2007;34(9):3544-3555. doi:10.1118/1.2760027
3. Van Herk M, Remeijer P, Lebesque J V. Inclusion of geometric uncertainties in treatment plan evaluation. *Int J Radiat Oncol Biol Phys*. 2002;52(5):1407-1422. doi:10.1016/S0360-3016(01)02805-X
4. Baum C, Alber M, Birkner M, Nüsslin F. Robust treatment planning for intensity modulated radiotherapy of prostate cancer based on coverage probabilities. *Radiother Oncol*. 2006;78(1):27-35. doi:10.1016/j.radonc.2005.09.005
5. Tilly D, Holm Å, Grusell E, Ahnesjö A. Probabilistic optimization of dose coverage in radiotherapy. *Phys Imaging Radiat Oncol*. 2019;10(March):1-6. doi:10.1016/j.phro.2019.03.005
6. Ramlov A, Assenholt MS, Jensen MF, et al. Clinical implementation of coverage probability planning for nodal boosting in locally advanced cervical cancer. *Radiother Oncol*. 2017;123(1):158-163. doi:10.1016/j.radonc.2017.01.015
7. Wu Q, Mohan R, Niemierko A, Schmidt-Ullrich R. Optimization of Intensity-Modulated Radiotherapy plans based on the Equivalent Uniform Dose. *Int J Radiat Oncol * Biol * Phys*. 2002;53(1):224-235.
8. Wegener D, Berger B, Outtagarts Z, et al. Prospective evaluation of probabilistic dose-escalated IMRT in prostate cancer. *Radiol Oncol*. 2020;55(1):88-96. doi:10.2478/raon-2020-0075

Chapter 6: Conclusion

Women diagnosed with locally advanced cervical cancer (LACC) can be cured or effectively palliated even with limited resources. Depending on the stage of disease, the standard care is a multimodality approach including surgery, external beam radiotherapy (EBRT), and brachytherapy (BT). Realizing the goals of treatment largely relies on the efficient delivery of brachytherapy with high doses to the tumour while minimizing the dose to surrounding critical structures. High rates of local control can be achieved for small tumours but significantly decrease for larger tumours. Considerable tumour regression during EBRT is generally seen in some patients but may be less significant for others. The advantage of additional tumour shrinkage through effective delivery of EBRT before BT is irrefutable.

Several strategies aiming at escalating tumour dose with a minor increase in normal tissue doses have been developed with improved outcomes tailoring treatment to the individual patient. Although promising results have been achieved often the workload associated with these strategies detracts from clinical feasibility. Ultimately, a successful treatment strategy should be aimed at achieving the best possible dosimetric benefits while still maintaining a viable clinical workflow in terms of the resources available.

6.1 Treatment preparation

Treatment preparation is a fundamental step in the therapy process. Institutional protocols differ with regards to pre-treatment imaging processes, organ filling protocols, and treatment plan generation. These differences impact geometric uncertainties such as setup errors, inter-and intra-fraction organ movement and have a detrimental effect on treatment outcome. Therefore, they should be carefully considered and quantified using data from the treating institution.

Organs in the pelvic area are prone to substantial and complex movements which renders target and organ motion the most relevant aspect to account for when devising treatment plans. These

movements are caused by several, mostly unpredictable, reasons such as tumour regression during treatment and filling status of organs such as the bladder and rectum. In an attempt to predict these geometrical changes, bladder filling protocols have been suggested to achieve reproducible bladder volumes during treatment and minimize the influence on target shape and position.

Even though this is standard practice in many departments, controversy regarding the efficacy and executability of bladder protocols still exists. In this study, we investigated bladder volume variations and their influence on target motion using both empty- and full-bladder protocols. Considering bladder volumes only, empty bladders were more reproducible than full bladders throughout treatment. Additionally, a full bladder protocol could not maintain reproducible volumes compared to planning bladder volumes. The inability to achieve reproducible full bladder volumes was confirmed by analyzing pre-treatment scans acquired on three consecutive days using the same full bladder protocol. Comparing an expected full bladder volume to that of naturally filling bladder volume further highlighted the fact that the intention of achieving a certain bladder volume through the use of protocols can be hindered by factors such as hydration levels and filling rates which are difficult to predict and control.

In our patient population, the application of an EB protocol was easy to follow patients did not have any reservations. Although there were no difficulties in the execution of the FB protocol some patients complained about discomfort before and during treatment. This was evident from their filling rates, as well as the use of 500 ml of water where other studies used slightly less. In institutions with high patient throughput, keeping within the specified time constraints might be a daunting task. Our results demonstrated that a 20 min treatment delay can have a significant impact on bladder volume and consequently target geometries. Although FB patients in this study were treated on time, delays ($CT_{FB2,4,6}$) could potentially have detrimental effects. Furthermore, we quantified the influence of bladder volumes on target motion through the use of occupancy probability matrices of the primary clinical target volume (pCTV) throughout treatment. The frequency of occupation of the pCTV relative to the reference structure

(delineated structure on planning scan) was determined on vaginal-, cervical-, and uterine level to determine the maximum extent of movement. Although empty bladder volumes were more reproducible no significant difference in movement between EB and FB patients was observed. Other than a stable bladder volume, significant motion on the vaginal and cervix levels indicated that rectal, sigmoid, and even small bowel influences the target geometry and position. However, the prominence of individual organs in this regard cannot be quantified.

Thus, considering bladder volume reproducibility and protocol executability, an empty bladder protocol appears simpler in our department. However, our study confirmed dosimetric advantages in bladder and small bowel sparing when a full bladder protocol is used. Therefore, variations in target shape and position cannot be attributed to bladder filling alone. Uncertainties should in any event be compensated for by daily imaging, adaptive approaches, and individualization of treatment margins.

6.2 Treatment planning

The treatment planning process involves various decision-making aspects such as imaging and setup protocols, margins sizes, and planning strategies. Dosimetric analyses of several treatment planning strategies utilizing the EUD as a dose metric in addition to traditional DVH parameters have been performed. While planning strategies require varying levels of imaging applications, such strategies would directly impact the required planning, imaging, and replanning workload. In our study population-based strategies included (i) fixed margins (7, 10, 15, and 20 mm) and (ii) a variable margin. Individualized treatment planning strategies included offline and online adaptive strategies, as well as an individualized ITV approach.

The use of 7 mm and 10 mm fixed margin is an optimistic approach as reproducible geometries are expected when bladder protocols are used. However, they led to under dosages in a large number of fractions in this study sample. A 15 mm margin was found to be a safe option to achieve adequate tumour coverage, although OAR sparing can be improved. This margin is also frequently suggested in the general literature on appropriate margins for cervix cancer IMRT. A

20 mm fixed margin ensures superior tumour coverage, however, but at the cost of significantly larger OAR volumes receiving high doses.

In an attempt to spare the OARs more, a population-based variable margin is effective and different methods of determining this margin exist. We explored an occupancy probability of 0.05 to derive variable margins representing the required expansion that would encompass the pCTV in 95% of treatment fractions. It could be expected that such margins, especially for the EB group, would be too large with resultant high OAR doses. The reason for this is that the dose outside the PTV is never zero, our average planning dose gradients from the 98% - 90 % isodose lines range from 6 – 8 mm, and the largest (20 – 30 mm) CTV positional deviations are few in frequency. Compared to the ITV approach, as well as the data from the off- and online techniques, a 0.15 occupancy probability would result in adequate target coverage and excellent OAR sparing.
The ITV approach was individualized in the sense that variable bladder filling scans of each patient were used to determine the range of movement. A standard 10 mm isotropic margin was added to the ITVs. Some research groups further differentiate between movers and non-movers and subsequently modify margins based solely on pre-treatment imaging. Our experience is that movers and non-movers are not necessarily always predictable (see Chapter 2) and therefore we did not attempt such predictions and modifications. This method has a reasonably low workload but could potentially lead to tumour under dosage for individuals (as seen in the EB group) and slightly inferior OAR sparing compared to other techniques.

Our results demonstrate the advantage of using individualized adaptive strategies. The online strategy ranked first based on both DVH parameters and EUD metrics. The offline strategy ranked second and third based on the EUD and DVH parameters respectively.

6.3 IGART strategy based on EUD

Online adaptive RT is a resource-intensive procedure and requires several layers of interventions throughout the whole course of RT. Lim-Reinders et al. [1] reviewed this process for online and offline techniques. They concluded daily in-room imaging, deformable image registration (DIR), accelerated replanning, and patient-specific QA can be performed in clinics setup for this but may lead to significant extensions in total treatment time. Considering the deviations in only the bladder volume observed in this study such extensions might be counterproductive.

We have put our patient sample through an investigation of automated contouring and automated treatment planning [2] to show how the automatic generation of multiple treatment plans can be produced with the use of very few resources. Automated contouring and pre-treatment imaging allow quick calculations of EUDs for all contoured structures. This comes at a very low cost, neglecting replanning and DIR, while the worst-case scenario [3] EUD tracking can be used to decide on the selection of appropriate larger/smaller plan of the day margins, adaptation, and total dose evaluation. In this respect, the EUD is a very valuable and priceless metric.

In addition, our clinic has recently implemented online linear accelerator component logging through log file recording during pre-treatment QA runs, as well as during treatment. Implementing fast and accurate MC [4–6], recalculation of dose on the patient CT datasets using log files as input, allows almost an online update of the dose delivered per fraction. Though independent QA will never be neglected, online logging or even transmission detector QA [7,8] measurements, could be used to update the delivered dose, estimate trends, and use recent geometries as input for plan adaptation via automated re-planning.

6.4 Final remarks and future research

The clinical feasibility of any treatment relies on the associated workload even more so in a resource limited department. From the results it was seen that a 15 mm fixed margin would yield sufficient target coverage with satisfactory OAR sparing. Using this strategy with a setup protocol requiring weekly imaging would most definitely be the strategy of choice with regards to

workload. However, the question remains, can we do better and not just for a few can we do better for all patients? The aim should therefore be to find a strategy yielding adequate target coverage with minimal normal tissue toxicities retaining a minimum workload that can be implemented for all patients. Although resource intensive, the use of automated contouring and planning will render adaptive strategies clinically more feasible. Coverage probability planning (CovP) offers a clinically feasible alternative to margin-based planning methods. Coverage probability strategies do not need daily images due to the pre-adaptive planning approach [9]. With a reduced workload, CovP is an appealing alternative to online adaptive strategies yielding similar or even better dosimetric outcomes.

More than half of the bodies bone marrow is located in the area that is included in the treatment volume for conventional RT [10]. Future research will include further optimization of treatment strategies to reduce BM irradiation and therefore improve treatment efficacy

6.5 References

1. Lim-Reinders S, Keller BM, Al-Ward S, Sahgal A, Kim A. Online Adaptive Radiation Therapy. *Int J Radiat Oncol Biol Phys*. 2017;99(4):994-1003. doi:10.1016/j.ijrobp.2017.04.023

2. Rhee DJ, Jhingran A, Rigaud B, et al. Automatic contouring system for cervical cancer using convolutional neural networks. *Med Phys*. 2020;47(11):5648-5658. doi:10.1002/mp.14467

3. Sobotta B, Söhn M, Shaw W, Alber M. On expedient properties of common biological score functions for multi-modality, adaptive and 4D dose optimization. *Phys Med Biol*. 2011;56(10):N123--129. doi:10.1088/0031-9155/56/10/N01

4. Hoffmann L, Alber M, Söhn M, Elstrøm UV. Validation of the Acuros XB dose calculation algorithm versus Monte Carlo for clinical treatment plans. *Med Phys*. 2018;45(8):3909-3915. doi:10.1002/mp.13053

5. Stanhope CW, Drake DG, Liang J, et al. Evaluation of machine log files/MC-based treatment planning and delivery QA as compared to ArcCHECK QA. *Med Phys*. 2018;45(7):2864-2874. doi:10.1002/mp.12926

6. Szeverinski P, Kowatsch M, Künzler T, Meinschad M, Clemens P, DeVries AF. Error sensitivity of a log file analysis tool compared with a helical diode array dosimeter for VMAT delivery quality assurance. *J Appl Clin Med Phys*. 2020;21(11):163-171. doi:10.1002/acm2.13051

7. Sarkar V, Paxton A, Kunz J, et al. A systematic evaluation of the error detection abilities of a new diode transmission detector. *J Appl Clin Med Phys*. 2019;20(9):122-132. doi:10.1002/acm2.12691

8. Giglioli FR, Gallio E, Franco P, Badellino S, Ricardi U, Fiandra C. Clinical evaluation of a transmission detector system and comparison with a homogeneous 3D phantom dosimeter. *Phys Medica*. 2019;58(January):159-164. doi:10.1016/j.ejmp.2019.01.016

9. Wegener D, Berger B, Outtagarts Z, et al. Prospective evaluation of probabilistic dose-escalated IMRT in prostate cancer. *Radiol Oncol*. 2020;55(1):88-96. doi:10.2478/raon-2020-0075

10. Mell LK, Kochanski JD, Roeske JC, et al. Dosimetric predictors of acute hematologic toxicity in cervical cancer patients treated with concurrent cisplatin and intensity-modulated pelvic radiotherapy. *Int J Radiat Oncol Biol Phys*. 2006;66(5):1356-1365. doi:10.1016/j.ijrobp.2006.03.018

Appendix 1

O ’reilly, F. H. J. & Shaw, W. A dosimetric evaluation of IGART strategies for cervix cancer treatment. *Phys. Medica* **32**, 1360–1367 (2016).

Physica Medica 32 (2016) 1360–1367

Contents lists available at ScienceDirect

Physica Medica

journal homepage: http://www.physicamedica.com

Original paper

A dosimetric evaluation of IGART strategies for cervix cancer treatment

Frederika H.J. O'Reilly *, William Shaw

Department of Medical Physics (G68), University of the Free State, Nelson Mandela Drive, Park West, Bloemfontein 9300, South Africa

ARTICLE INFO

Article history:
Received 15 January 2016
Received in Revised form 27 May 2016
Accepted 6 June 2016
Available online 11 June 2016

Keywords:
On-line
Off-line
IGART
Cervix cancer
EUD

ABSTRACT

Purpose: Image guided adaptive radiotherapy (IGART) strategies can be used to include the temporal aspects of radiotherapy treatment. A dosimetric evaluation of on- and off-line adaptive strategies are done in this study.
Methods: A library of equivalent uniform dose (EUD)-based Intensity Modulated Radiotherapy Treatment plans with incrementally increasing clinical target volume (CTV)-to-planning target volume (PTV) margins were developed for 10 patients. Utilizing daily computed tomography (CT) images an on-line strategy using a margin-of-the-day (MOD) concept that selects the best plan from the library was employed. This was compared to an off-line strategy with full analysis of accumulated dose between fractions where dosimetric deviations from the treatment intent triggered plan adaptation. A fixed margin treatment approach was used as benchmark.
Results: Using fixed margins of <15 mm lead to under-dosages of more than 5 Gy in total delivered dose. The average CTV EUD for the off-line and on-line strategy was 50.0 ± 5.0 Gy and 50.4 ± 2.0 Gy respectively and OAR doses were comparable.
Conclusion: A fixed margin treatment approach yields a significant probability of CTV under-dosage. Using EUD dose metrics CTV coverage can be restored in both the off-line and on-line adaptive strategies at acceptable OAR dose levels. Considering the workload and time on the treatment machine, the off-line strategy proves to be sufficient and more practical.

1. Introduction

Treatment of locally advanced cervix cancer is generally a combined modality approach of radiotherapy and chemotherapy [1]. This combination yields an increase of 6% overall and disease free survival at 10 years post treatment compared to radiotherapy alone and in addition reduces the rate of distant metastases occurrence [2,3]. A local control rate, even in advanced disease, of >90–95% is achievable when external beam radiotherapy (EBRT) and chemotherapy is combined with image guided adaptive brachytherapy (IGABT) [4]. While these excellent local control rates can be achieved, the predominant mode of failure for these patients are distant metastases [2,5].

Generally the whole pelvis four-field box technique is used to ensure adequate coverage of the lymphatic drainage system (common-, internal and external iliac nodes) and the primary tumour, consisting of the uterus, cervix and vagina [6,7]. However, the dose that can be delivered in this approach is limited by the incidence and severity of late toxicity of the surrounding organs at risk (OARs) including the bowel, rectum, bladder and vagina of which a considerable volume is included in the treatment fields [8]. Gastrointestinal (GU), genitourinary (GI), and bone marrow toxicities are commonly associated with this technique and is the primary drive for implementation of more conformal and high precision EBRT such as intensity-modulated radiotherapy (IMRT) for OAR sparing [9,10]. Compared to conventional techniques, IMRT offers significant OAR dose sparing with similar or improved tumour control and survival [4]. The improved OAR sparing of IMRT also offers the possibility for the safe and effective use of concomitant boost to the para-aortic lymph node region [5].

These promising results are however inhibited by the potential for underdosing the target due to substantial inter- and intrafraction motion in the female pelvis [11]. In addition, tumour regression may be in the order of 60–80% of the pre-therapeutic tumour volume allowing the OARs to frequently move into the high dose area [12]. To address this complex and patient specific anatomical motion, large planning margins, frequent imaging or plan adaptation would likely be required to ensure adequate EBRT tumour coverage. Several image-guided adaptive radiotherapy (IGART) methods for the treatment of cervical cancer have been proposed [13,14]. Such methods are effective as treatment

* Corresponding author.
E-mail addresses: oreillyfhj@ufs.ac.za (F.H.J. O'Reilly), shaww@ufs.ac.za (W. Shaw).

http://dx.doi.org/10.1016/j.ejmp.2016.06.003
1120-1797/

techniques to address geometrical variations in a large population of patients as they cater for the individual, whereas non-adaptive techniques run the risk of sub-optimal treatment for some patients. In this retrospective planning study we perform a dosimetric evaluation of two IGART strategies utilizing the equivalent uniform dose (EUD) metric for targets and generalized EUD (gEUD) metric for OARs [15,16]. The first strategy utilizes a lower workload off-line 'wait-and-see' concept and adapts the treatment based on what has been delivered in the past, while the second strategy is a higher workload on-line margin of the day (MOD) approach and relies on the current geometrical configuration for selection of an acceptable treatment plan. A fixed margin approach was used as a benchmark to evaluate the effectiveness of these strategies.

2. Materials and methods

2.1. Patient data

A total of 10 patients receiving radical radiotherapy treatment for cervix cancer were included in this retrospective planning study for which ethical approval was obtained by the local ethics committee (ECUFS 28/2014A). They received EBRT in the form of a four-field box technique and treatment plans were generated using planning computed tomography (CT)-based image datasets. The prescribed dose was 50.0 Gy in 25 fractions of 2.0 Gy to the ICRU reference point and the distribution of International Federation of Gynecology and Obstetrics (FIGO) stage classification for local tumour stage was IIB = 3 and IIIB = 7 patients. Concomitant weekly Cisplatin-based chemotherapy (5–6 × 25 mg/m^2 body surface area) was also administered during this time. Patients received an additional 5 fractions brachytherapy boost of at least 15.0 Gy to point A in the third week of EBRT. Overall treatment time was less than 44 days.

2.2. Imaging and delineation

During the course of treatment an additional set of 9 CT scans were acquired of each patient. These datasets consisted of 4 pre-treatment CTs, acquired on a daily basis in the week before treatment commenced, and one consecutive weekly CT during the five weeks of EBRT. The timing of the first 4 CTs was a result of logistical difficulties at the time of these patients' treatment, however it was anticipated that this timing would not influence the validity of our results, similar to other studies [14]. It is assumed that this set of images represent random movement of the tumour and OARs during the stage of treatment planning when tumour regression is slow and conventional planned dose distributions are governed by a single snapshot in time of the tumour and OAR positions. The shrinkage in tumour volume and random movements were recorded in the following five weekly image datasets. No bladder or bowel protocol was followed in this study and the additional 9 CT image datasets played no part in the actual treatment of the patients.

The target volume and organs at risk were manually contoured on all CT scans. Delineation was performed by an experienced Radiation Oncologist using a standardized method of contouring [17]. The primary clinical target volume (pCTV) consisted of the utero-cervix and the upper third of the vagina (depending on the tumour extent). The organs at risk included the bladder-, sigmoid- and rectal wall, as well as the small bowel plus peritoneal cavity. The nodal CTV (nCTV) included involved nodes and relevant draining node groups (common, internal, and external iliac and obturator and pre-sacral lymph nodes).

Each CT dataset was rigidly registered (utilizing mutual information) with the original planning CT based on bony anatomy matching using Monaco Sim software (Monaco® 5, Elekta Oncology Systems). Registration was performed automatically and adjusted manually when required. The above mentioned structures were contoured on each of the CT datasets and copied to the original planning CT for further dose assessments. The relative electron densities of all low density structures and cavities on the first CT dataset were overridden with the density of water to eliminate low density dose artefacts.

2.3. Treatment planning

The Hyperion® (University of Tübingen, Germany) treatment planning system (TPS) was used to construct a library of IMRT treatment plans with uniform incrementally increasing pCTV-to-primary planning target volume (pPTV) margins (5, 7, 10, 15, 20 and 25 mm) based on the delineated structures on the first CT scan. A fixed 7 mm nPTV margin was used for the nodal CTV. HYPERION® utilizes a method of biological optimization employing the equivalent uniform dose (EUD) [18]. The TPS uses Monte Carlo (MC) dose calculations to compute IMRT segments that are modified and weighed during dose optimization [19]. Planning objectives and OAR constraints were derived from the Quantitative Analysis of Normal Tissue Effect in the Clinic (QUANTEC) and published EUD data [20–23]. 6 MV IMRT plans using nine equi-distant beam angles were created to deliver a prescribed dose of 50.0 Gy to the primary and nodal PTVs. Table 1 provides a summary of the most important objectives and constraints employed for plan optimization. For simplicity we refer to both the EUD and gEUD as EUD only. For these calculations, $\alpha = 0.4$ in the case of the Poisson Cell Kill EUD and the volume effect parameters for the gEUD calculations were $a = 12$ for the rectal-, sigmoid wall and small bowel, and $a = 8$ for the bladder wall.

2.4. Treatment simulation

A fixed margin (FM) approach was used as dosimetric benchmark to test the effectiveness of the adaptive treatment strategies. Fixed primary PTV margins were applied to the first fraction ($i = 1$) and CT delineated pCTV ($pCTV_1$) and the rest of the treatment was simulated by scoring the dose to all delineated volumes of the successive delineated CTs as the structures were copied from their respective CTs to the first one. This was repeated for the margin sizes ranging from 5 mm to 25 mm. For the sequential delineated structures the average EUDs could be computed via

$$EUD_{ave} = \frac{1}{n}\sum_{i=1}^{n} EUD_i \quad (1)$$

Here, i is the simulated treatment fraction and n the total CT datasets (and thus treatment fractions) included in the calculation of EUD_{ave} (maximum value of $n = 9$). Dose scoring was done without any intervention or adaptation to the original optimized IMRT plan. The nodal CTV (nCTV) was contained inside a fixed 7 mm nPTV margin regardless of the strategy employed.

Table 1
Summary of the most relevant EUD planning objectives and constraints used for the production of IMRT plans.

	Objectives (Gy)	Constraints (Gy)
pCTV	⩾49.8	
nCTV	⩾49.8	
Rectal wall		⩽48.0
Bladder wall		⩽47.0
Sigmoid wall		⩽48.0
Small Bowel		⩽47.0

Next, an individual offline plan adaptation strategy was simulated with full dosimetric analysis performed *between* treatment fractions i and j, i being the last fraction that was treated and j the fraction to be treated. $pCTV_i$ was contoured offline, disregarding all other contours, and $EUD_{(i,x)}$ calculated for each margin plan in the existing library where $x = marginsize(x \in 5, \ldots 25\ \text{mm})$ and X the margin used for treatment. The first treatment fraction was delivered using a 15 mm pCTV margin plan ($X = 15$ mm). Thus, the actual delivered dose recorded for fraction 1 was $EUD_{(1,15\ \text{mm})}$. The smallest margin size selection with adequate tumour coverage and to obtain OAR dose sparing for the rest of the simulated treatment fractions ($j = 2,\ldots n$), was performed using the following procedure: If j is the fraction to be treated and a margin size (x) needs to be determined for j, we determine x such that after j fractions,

$$EUD_{ave} = \frac{1}{j-1}\sum_{i=1}^{j-1} EUD_{i,X} \tag{2}$$

$$\frac{EUD_{(i,x)} + EUD_{(ave)}}{2} \geqslant C \tag{3}$$

and $\boldsymbol{C}$ = 49.8 Gy EUD. In Eq. (3), $EUD_{(i,x)}$, serves as an estimate of what dose will be delivered in fraction j if the geometry in j is similar to the geometry in the past fraction, i. This method is optimistic in the sense that the most recent pCTV geometry will persist in fraction j. However, as a safety feature to prevent tumour underdosage a minimum margin size for treatment fractions $j \geqslant 3$ were calculated using a moving average approach,

$$x_{min} = \frac{1}{j-2}\sum_{i=2}^{j-1} x_i \tag{4}$$

From our experience, a 0.2 Gy drop from 50 Gy prescribed EUD is mostly comparable to an approximately 5% dose reduction from 50 Gy prescribed dose in the pCTV as recommended by the ICRU in terms of dose volume histogram (DVH) parameters [24]. When Eq. (3) resulted in an under-dosage the margin with the maximum EUD_i was chosen.

Lastly, we investigated an individualized on-line adaptive strategy where the adaptation in the treatment is based on the daily $pCTV_j$ position and geometry that will be treated. Thus, $pCTV_j$ was contoured with the patient in the treatment position and the most appropriate margin-of-the-day (MOD) was selected on-line from the library of plans with the criterion that the $pCTV_j$ will receive an EUD of at least 49.8 Gy, regardless of the OAR dose. In contrast to the off-line strategy, contouring and subsequent plan selection should be performed before treatment. As per the offline strategy the pCTV always has priority when selecting a margin size plan.

2.5. Dose accumulation and data analysis

One method of dose calculation in four dimensions (4D) is to accumulate the dose in a reference geometry through deformation fields, obtained from deformable image registration (DIR). However, this is a largely unsolved problem in the pelvic region. Alternatively, Sobotta et. al. [25] exploited the mathematical properties of concave and convex score functions, like the EUD for tumours and OARs, to calculate a reliable worst case estimate of the accumulated dose in multiple geometry instances. In effect, the accumulated instance EUDs will never be lower than this estimate for a tumour, and never be higher than the estimate for an OAR. These estimates are computed without the need for DIR and is a quick scoring method of a treatment plan at only a fraction of the computational cost of a full dosimetric analysis.

In this study, we promulgate the use of EUD dose metrics for IGART for two reasons: (a) The EUD is a quick, reliable and repeatable cumulative dose scoring method underpinned by the Jensen Inequality [25–27], and (b) it is safe to use in the absence of proper deformation fields and computes upper and lower bounds that err on the safe side [28]. The EUD was used as a dose metric in this study to investigate the effectiveness of these planning strategies while DVH parameters were scored in addition. Tumour EUD_{ave} values were required to be at least at a level of 49.8 Gy for the treatment to be regarded as dosimetrically acceptable. On the other hand, successful OAR sparing required that EUD_{ave} be equal to or lower than the optimization result of the first (planning) CT. In addition to the EUD results, common DVH parameters used in EBRT plan assessment were calculated to describe the fluctuations in dose distributions related to tumour and OAR motion and geometrical changes to be comparable to other published results. They included D98 for the tumour, while D90, D50, and D30 were calculated for the OARs.

2.6. Statistical analysis

The Wilcoxon signed ranked test and paired t-test were used to test statistical differences in CTV and OAR doses for the different strategies. Statistical significance was defined as $p < 0.05$.

3. Results

3.1. Timeline and tumour shrinkage

The group of patients included in this study varied not only in disease stage, but also pCTV volumes at the start of treatment. The median tumour volume on the planning CT was 211 cm^3 and ranged from 175 to 336 cm^3. There were no significant changes in these volumes during the first 4 CT scans before treatment and similarly no changes in the first two weeks of treatment. We noted significant average pCTV volume reductions from the third week of treatment (9% reduction) to the final week (18% reduction, range 5%–54%).

3.2. Fixed margin strategy

When utilizing a fixed pCTV-pPTV planning margin, the EUD_{ave} for the population of patients ranged from 46.9 ± 10.5 Gy to the pCTV and 52.3 ± 1.7 Gy to the nCTV for a 5 mm margin, to 51.1 ± 2.3 Gy to the pCTV and 52.5 ± 2.1 Gy to the nCTV for a 25 mm margin from the 9 treatment simulations. The OAR EUDs ranged from 46.4 ± 3.2 Gy, 46.9 ± 3.9 Gy, 48.9 ± 3.6 Gy, 44.7 ± 3.2 Gy to the rectal wall, bladder wall, sigmoid wall and small bowel respectively in the case of a 5 mm margin, to 50.1 ± 0.9 Gy, 49.7 ± 1.7 Gy, 50.7 ± 2.1 Gy, 45.9 ± 3.0 Gy for the same structures with a 25 mm margin. Table 2 summarizes these results.

The pCTV EUD_{ave} were statistically greater for each incremental increase in margin size with $p < 0.05$ in all cases. The nCTV showed no difference. Fig. 1 provides a graphical presentation of box-whisker plots of the distribution of the EUD_{ave} and DVH parameter metrics for the fixed margin approach. Adequate CTV coverage, $\geqslant$49.8 Gy, were seen for margins $\geqslant$15 mm. Therefore, the 15 mm margin will be used as a benchmark to test other strategies. Significant under-dosages (<49.8 Gy) were seen for margins $\leqslant$10 mm. These results are supported by both the EUD and DVH parameter metrics, while other authors found similar results [17,29].

When smaller margins are applied, the OAR doses are on average much smaller than planning with larger margins due to the larger overlap of PTV and OAR in the case where large margins

Table 2
Summary of average EUDs to the pCTV, nCTV and OAR for the population of patients using a fixed margin approach.

	EUD_{ave} (GY) ± SD					
Margin size (MM)	pCTV	nCTV	Rectal wall	Bladder wall	Sigmoid wall	Small Bowel
5	46.9 ± 10.5	52.3 ± 1.7	46.4 ± 3.2	46.9 ± 3.9	48.9 ± 3.6	44.7 ± 3.2
7	47.9 ± 9.2	52.3 ± 1.5	46.8 ± 2.9	47.1 ± 3.6	49.3 ± 3.3	44.9 ± 3.6
10	49.5 ± 6.3	52.4 ± 1.8	47.6 ± 2.2	47.7 ± 3.1	49.7 ± 3.0	45.0 ± 3.3
15	50.6 ± 3.2	52.4 ± 2.0	48.7 ± 1.5	48.8 ± 2.5	50.2 ± 2.7	45.4 ± 3.3
20	51.0 ± 2.5	52.5 ± 2.0	49.6 ± 1.4	49.4 ± 2.4	50.5 ± 2.3	45.5 ± 3.2
25	51.1 ± 2.3	52.5 ± 2.1	50.1 ± 0.9	49.7 ± 1.7	50.7 ± 2.1	45.9 ± 3.0

SD = standard deviation.

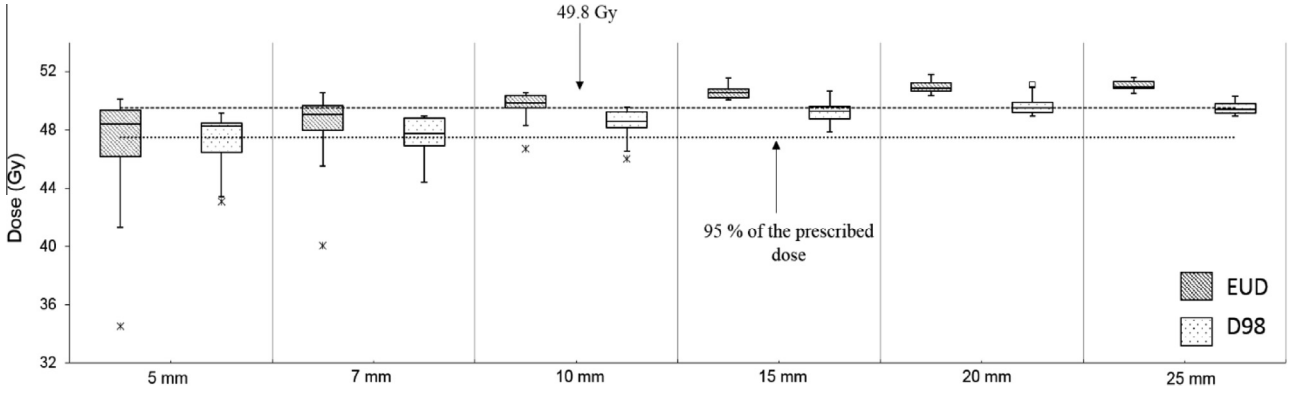

Figure 1. Box-whisker plots of EUD_{ave} and dose to 98% volume (D_{98}) for the pCTV for increasing CTV-PTV margin sizes using a fixed margin approach. The deviation of parameters for the whole population around the median is shown.

are used (OAR EUD and DVH parameter box-whisker plots are provided as Supplementary Data, Fig. S1). Smaller margins thus lead to significant OAR sparing but, too small margins lead to sub-optimal tumour doses due to geometric miss.

When comparing the resultant OAR doses to those used for initial optimization in Table 1, acceptable OAR doses were observed for small margins. Larger volumes of the OAR overlap with the pPTV as the margin increases and at some stage there is no room for OAR sparing anymore as the overlap region is just too big. In such cases there is virtually no difference in terms of OAR dose compared to a conventional four-field box techniques, although non-specified normal tissue dose can still be reduced to some extent with IMRT. Similar trends of dose increases are observed for the rectal-, bladder- and sigmoid walls. These increases were statistically significant for the rectum- and bladder walls. The increase in sigmoid wall doses were statistically significant for small margins but remained relatively constant for margins $\geqslant$15 mm. The small bowel on the other hand exhibited smaller variations in dose as the margins increased. These results are supported by the DVH parameters (see Supplementary Data, Fig. S1).

3.3. Off-line strategy

The EUD_{ave} for the population of patients using the off-line strategy were 50.0 ± 5.0 Gy for the pCTV and 52.1 ± 1.8 Gy for the nCTV. The OAR EUDs were 48.1 ± 3.6 Gy, 48.1 ± 5.3 Gy, 49.8 ± 3.9 Gy and 45.2 ± 3.6 Gy for the rectal-, bladder-, sigmoid wall and the small bowel respectively (Supplementary Data Table S1). As illustrated in Fig. 2a, sufficient CTV coverage was achieved for all patients with only a slight total EUD under-dosage in one patient (49.7 Gy). Under-dosages were found in some fractions, but the adaptation strategy was able to recover the total required dose for all patients except this one. Our results demonstrated that whenever an under-dosage occurred in any particular fraction, it occurred prior to the fourth week of treatment before tumour shrinkage has begun.

When the off-line strategy is compared to a 15 mm FM strategy, the off-line strategy resulted in a distribution of EUD_{ave} that was significantly lower than the FM strategy. However, sufficient coverage was still evident when applying the off-line strategy. Similar results were found in the DVH parameter distributions, except that there were no under-dosage in the D98 parameter (Fig. 2a).

The off-line strategy resulted in frequent use of smaller margins (Fig. 2b). It is expected that the use of smaller margins in this way would result in reduced OAR doses compared to FM. This was indeed the case (see Supplementary Data Figs. S1 and 3) as statistically lower OAR doses were found in this technique for all OARs, supported by EUD and DVH dose metrics. Furthermore, the off-line moving average margin selection procedure acts as a safety feature to prevent future under-dosage by choosing too small a margin based on previous pCTV geometries. This is illustrated in Supplementary Table S1 where the EUD_{ave} for the whole treatment simulation was calculated when each margin in the existing library was chosen as the first plan for fraction 1.

3.4. On-line strategy

Using the most appropriate MOD based on the daily $pCTV_i$ position and geometry yield an EUD_{ave} for the population of 50.4 ± 2.0 Gy for the pCTV and 52.0 ± 1.5 Gy for the nCTV. The OAR EUDs were 48.2 ± 4.5 Gy, 48.0 ± 5.2 Gy, 49.8 ± 4.2 Gy and 45.1 ± 3.4 Gy for the rectal-, bladder-, sigmoid wall and the small bowel respectively. In this strategy none of the patients received a pCTV dose lower than 49.9 Gy which is above the tumour objective (Fig. 4). The D98 parameter support the EUD results with no under-dosage. There were no differences in the distribution of EUD_{ave} when the on-line strategy was compared to FM. Results demonstrated that whenever a fractional under-dosage occurred, it was small in magnitude and occurred towards the latter part

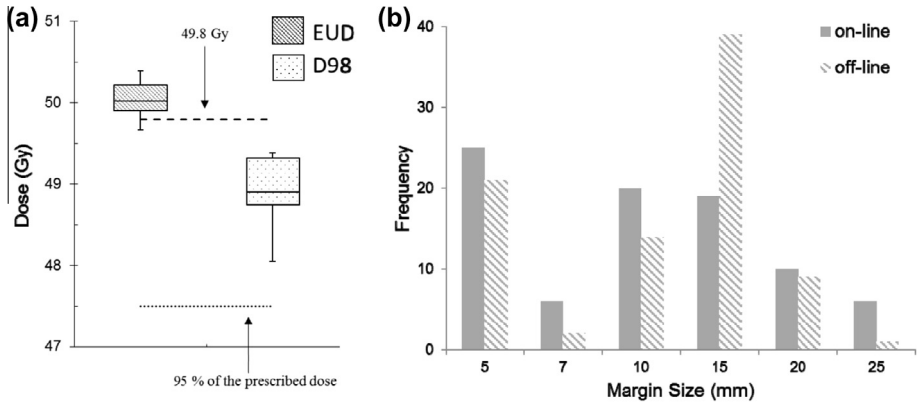

Figure 2. (a) Box-whisker plots of EUD_{ave} and dose to 98% volume (D_{98}) for the pCTV when using an off-line approach. The deviation of parameters for the whole population around the median is displayed. (b) Frequency distribution of margin sizes used for the entire patient population in the on-line and off-line adaptation strategies.

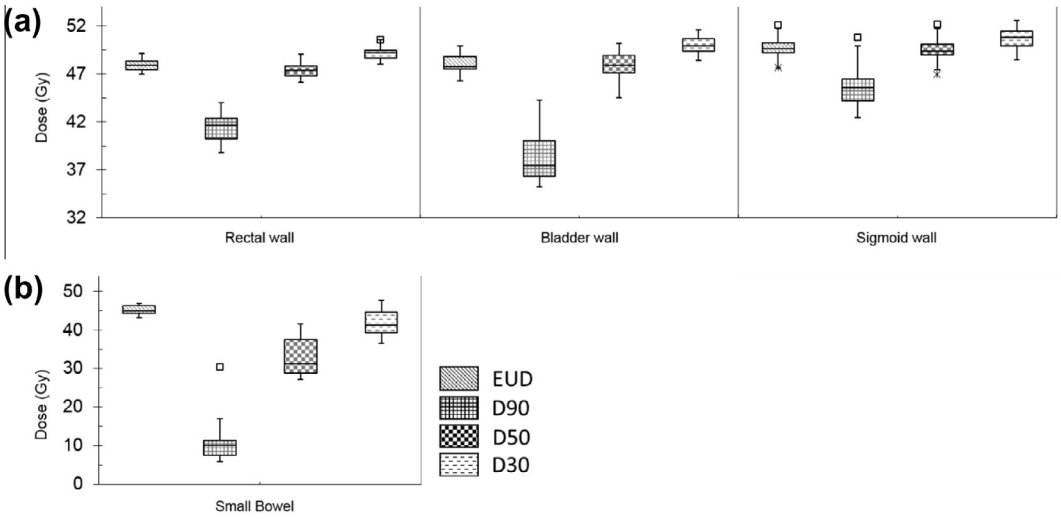

Figure 3. Box-whisker plots of EUD_{ave} and dose to 90%, 50% and 30% (D_{90}, D_{50} and D_{30}) of the (a) rectal wall, bladder wall, sigmoid wall, and (b) small bowel using an off-line approach. The deviation of parameters for the whole population around the median is displayed.

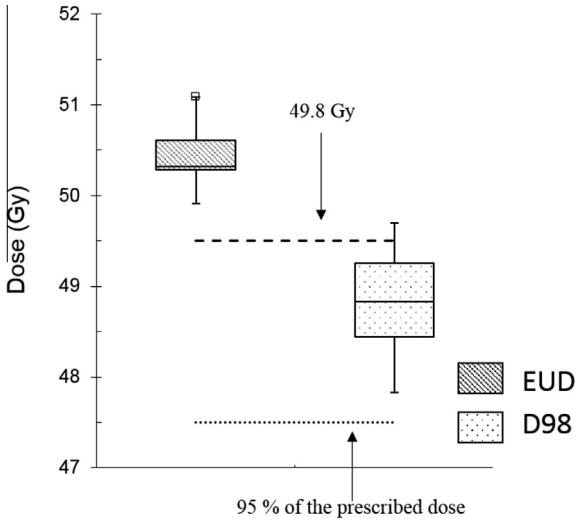

Figure 4. Box-whisker plots of EUD_{ave} and dose to 98% volume (D_{98}) for the pCTV using an on-line approach showing the deviation of parameters for the whole population around the median.

of the treatment schedule as opposed to earlier, as found in the off-line strategy. However, the on-line delivered dose in fractions preceding these under-dosages were large enough in magnitude to offset such small under-dosages.

Ultimately, for the same pCTV dose as in the FM strategy, significant OAR sparing for the bladder wall and small bowel were found (Fig. 5). Although there were no statistical difference for the rectum- and sigmoid wall, the median EUD_{ave} was lower for the on-line strategy demonstrating the advantage of this technique for individuals in a population. The FM strategy does not allow this advantage for individuals.

3.5. Comparison

To summarize the results both adaptive strategies and the 15 mm FM resulted in adequate pCTV coverage. The advantage of the two adaptive strategies is that the MOD resulted in very high tumour dose while some OARs could be spared. The off-line strategy did not achieve the same tumour dose distribution, but the doses still conformed to the prescription while all OAR were spared.

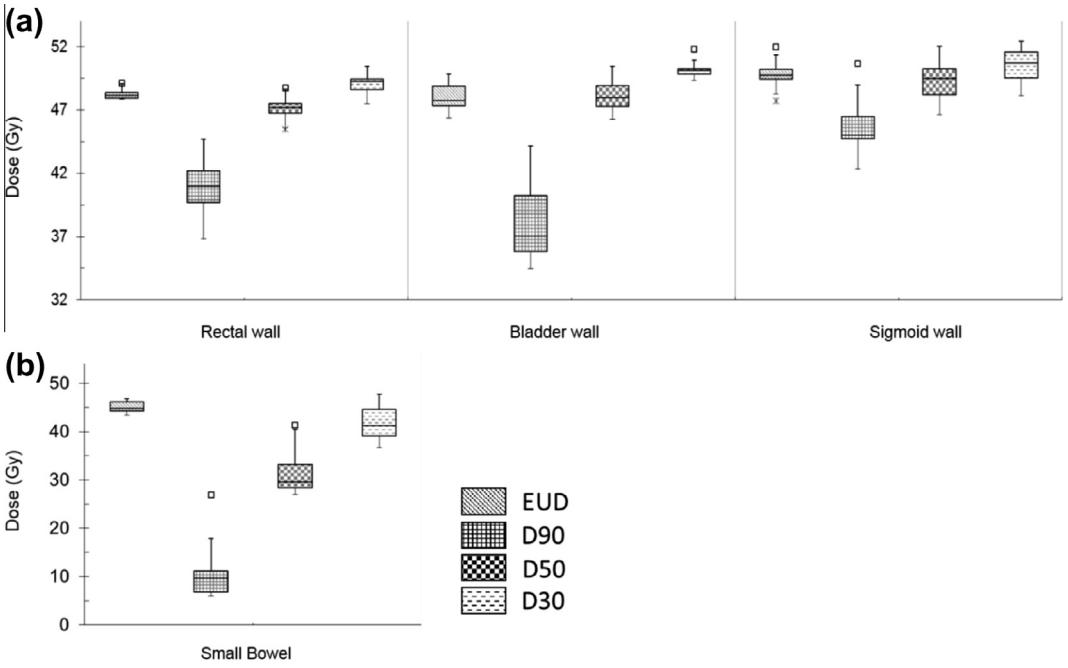

Figure 5. Box-whisker plots of EUD_{ave} and dose to 90%, 50% and 30% (D_{90}, D_{50} and D_{30}) of the (a) rectal-, bladder-, and sigmoid wall and (b) small bowel using an on-line approach.

4. Discussion

Applying the fixed margin strategy three scenarios became evident across the patient population: (I) The planning intent could only be satisfied for margins $\geqslant$15 mm, (II) Small margins (5 mm) yield adequate CTV coverage for patients with very stable organ and tumour geometries, and (III) using margins $\leqslant$10 mm will always lead to under-dosage in a large number of patients. Even with a 10 mm margin, under-dosages can be frequent. The advantage of IMRT treatment plans utilizing smaller CTV-PTV margins is very attractive since OARs can effectively be spared, but this must be offset with adequate tumour coverage. From the results found here, adequate tumour coverage was not achievable with fixed margins smaller than 15 mm, concurrent with previous studies [17,29]. The D98 evaluation supports the EUD results that 10 mm margins would lead to tumour underdosage for some patients and would be classified as risky.

Considering the population a 15 mm FM would yield adequate results as reported by Yilmaz et al. [29]. However, using adaptive strategies treatment can be individualized yielding adequate pCTV coverage with additional OAR dose sparing. This is particularly valuable when considering brachytherapy which will be concomitant or follow external beam treatment.

Overall, adequate tumour coverage was obtained when the off-line strategy was applied. Yet, a large underdosage in one fraction critically influences the rest of the treatment as it is difficult to restore the EUD_{ave} to what was actually intended. Such large under-dosages can be prevented by using past geometries to determine a minimum margin size to be used for the remainder of the treatment. Although the 15 mm margin were used most often in the off-line method, smaller margins were also used offering better OAR sparing compared to the 15 mm FM.

The under-dosage of one patient was caused by a sudden large sigmoid movement. This eludes to the fact that an off-line strategy can only correct for slow changing geometries or systematic deviations as opposed to the on-line strategy that corrects for random deviations as well. Therefore, the off-line pCTV doses in the population will always be slightly lower than those of on-line. However, the selection of a minimum margin size in the off-line approach proved to act to a reasonable extent as a safeguard to prevent future under-dosages.

Application of an on-line strategy prevents geometric misses as it utilizes images of the most recent organ geometries and a MOD that ensures adequate pCTV coverage. This is supported by the results found here, as no patient received a pCTV dose lower than 49.9 Gy when this strategy was applied. Although comparable to the OAR doses of a 15 mm FM, the on-line strategy offers the advantage of significant OAR sparing for some individuals in a population. The nCTV dose was constant and similar for all strategies applied. This emphasizes the fact that there are virtually no interfraction change in nodal geometries and future studies could investigate nPTV margins <7 mm, the margin size we used.

IGART attempts to prevent tumour under-dosage on a per fraction basis. Our results revealed that off-line strategy violations are usually a result of random tumour geometrical changes as they only occurred early on in the treatment schedule. Whereas, later on when tumour shrinkage was at its largest, under-dosages were uncommon. In contrast, the on-line violations were very small and occurred later on in the treatment course after the onset of tumour shrinkage. On-line strategy violations are a direct result of major geometrical changes that require additional larger margin plans in the library. Nevertheless, for this population of patients the on-line strategy never resulted in any total under-dosage.

It was notable that the off-line strategy resulted in more OAR sparing than the on-line strategy. This can be attributed to the fact that OAR doses were disregarded in both strategies and only pCTV contours were used for plan adaptation since tumour dose always had priority. Subsequently, the on-line pCTV doses were higher and the OAR doses were also slightly higher than in the off-line strategy.

The novel use of EUD as a dose metric avoids the use of deformation fields and the associated calculation effort for dose accumulation in both off-line and on-line adaptation strategies. Our results demonstrate that when the target and OAR EUDs are effectively controlled, all DVH parameters are controlled at the

same time, as was found in other studies [31,32]. The use of DIR for dose accumulation requires considerable extension in the already lengthy replan-time [13], while studies that did not employ DIR could make very few assumptions about the accumulated dose [14]. Thus, the EUD method is an excellent way to bypass these limitations.

It is also evident that the EUD is sensitive to pronounced under-dosage in small volumes. This is due to the fact that the EUD considers the entire DVH of the tumour and not just a single point on the DVH. Importantly, we considered the dose to the primary CTV and not PTVs. The under-dosages in the EUD results that at the same time received an adequate D98 supports this. Thus the EUD is an even more sensitive metric to evaluate dose distributions and tumour underdosage compared to DVH parameters as small volumes of the CTV may still receive significantly low doses. Shaw et al. [31] found similar results for OAR overdosages when performing DVH-metric-only analyses in brachytherapy. They specifically considered high doses to small volumes in the OARs that demonstrated the sensitivity of the EUD to high doses in small volumes.

Dose analyses for the off-line strategy was done between fractions with no influence on machine time, offering a lower workload compared to the MOD strategy where plan adaptation was done directly before each fraction considering the most recent organ geometries. Thus, the benefit gained by a somewhat higher CTV dose is defied by a higher workload necessary for an on-line strategy. Based on results found here an off-line strategy offers all the benefits of an on-line strategy and further requires lower workload and less machine time. Therefore, the off-line strategy proves to be clinically more practical and feasible. Other studies had similar conclusions, while hybrid adaptive methods also exist [13]. To further impact the workload associated with adaptive methods, auto-contouring and bladder-filling models have been suggested [13,30]. Any of these methods could benefit from the use of EUD metrics.

Although the actual treatment of cervix cancer patients consist of 25 EBRT fractions, we have used only the 9 CT datasets in addition to the planning CT dataset to represent the full course of treatment. Like other similar studies [13,14], this is a limitation of our study. However, the random nature of organ movement and its influence on the absorbed dose could well be reflected in this limited image dataset: The first 4 CT scans were acquired on a daily basis during the week before treatment commenced. From our results it was evident that there were very little change in CTV volume from CT1 to CT7. Significant differences in CTV volume were only noted from the 8th CT, which in our study represents week 3 of treatment when concomitant brachytherapy starts. The use of the first 4 CTs was an approximation made because dose deviations due to geometric variations in the first three weeks of treatment were expected to be larger than tumour shrinkage. Therefore, the assumption made about slow initial tumour regression seems to have been valid.

Future work on this subject would include daily images of the patients receiving treatment. The limited number of image sets could possibly lead to an over- or under-estimation of some of the metrics scored, but as an approximation, it could be acceptable to cover the influence of tumour and OAR movement and geometrical variations across the total treatment time. Whatever the case may be, these results stress the importance of accounting for tissue movement and geometry variations in the female pelvis. The selection of patients may also be regarded as a limitation to this study as they are representative of a population found in one treatment centre. The results found here may be different to other centres in their magnitude. However, we expect that the principles identified in this study are universal and applicable in similar ways.

5. Conclusion

The dosimetric evaluation of a fixed margin IMRT treatment planning approach was performed in this study and two adaptive treatment strategies were evaluated against this approach. It was found that the use of a fixed primary CTV margin $\leqslant$10 mm for the treatment of cervix cancer would lead to primary tumour under-dosages in some patients. Tumour regression and random organ movement in the female pelvis have an undesirable effect on target coverage and OAR sparing that warrants the implementation of individualized adaptive treatment strategies. On-line and off-line strategies utilizing EUD dose metrics is a fast and safe method through which CTV coverage can be restored at acceptable OAR dose levels. Considering workload and time on the treatment machine, the off-line strategy proves to be sufficient and more practical.

Acknowledgements

This research project was funded by the South African Medical Research Council (MRC) with funds from National Treasury under its Economic Competitiveness and Support Package. Research and any publication thereof is the result of funding provided by the Medical Research Council of South Africa in terms of the MRC's Flagship Awards Project SAMRC-RFA-UFSP-01-2013/HARD.

Appendix A. Supplementary data

Supplementary data associated with this article can be found, in the online version, at http://dx.doi.org/10.1016/j.ejmp.2016.06.003.

References

[1] Portelance L, Chao KSC, Grigsby PW, Bennet H, Low D. Intensity-modulated radiation therapy (IMRT) reduces small bowel, rectum, and bladder doses in patients with cervical cancer receiving pelvic and para-aortic irradiation. Int J Radiat. Oncol. 2001;51(1):261–6.
[2] Schmid MP, Franckena M, Kirchheiner K, Sturdza A, Georg P, Dörr W, et al. Distant metastasis in patients with cervical cancer after primary radiotherapy with or without chemotherapy and image guided adaptive brachytherapy. Gynecol Oncol. 2014;133(2):256–62.
[3] Kirwan JM, Symonds P, Green JA, Tierney J, Collingwood M, Williams CJ. A systematic review of acute and late toxicity of concomitant chemoradiation for cervical cancer. Radiother. Oncol. 2003;68(3):217–26.
[4] Tanderup K, Georg D, Pötter R, Kirisits C, Grau C, Lindegaard JC. Adaptive management of cervical cancer radiotherapy. Semin. Radiat. Oncol. 2010;20(2):121–9.
[5] Vargo JA, Kim H, Choi S, Sukumvanich P, Olawaiye AB, Kelley JL, et al. Extended field intensity modulated radiation therapy with concomitant boost for lymph node-positive cervical cancer: analysis of regional control and recurrence patterns in the positron emission tomography/computed tomography era. Int. J. Radiat. Oncol. 2014;90(5):1091–8.
[6] Zunino S, Rosato O, Lucino S, Jauregui E, Rossi L, Venencia D. Anatomic study of the pelvis in carcinoma of the uterine cervix as related to the box technique. Int J Radiat Oncol. 1999;44(1):53–9.
[7] van de Bunt L, van der Heide UA, Ketelaars M, de Kort GAP, Jürgenliemk-Schulz IM. Conventional, conformal, and intensity-modulated radiation therapy treatment planning of external beam radiotherapy for cervical cancer: the impact of tumor regression. Int. J. Radiat. Oncol. 2006;64(1):189–96.
[8] Roszak A, Wareńczak-Florczak Z, Bratos K, Milecki P. Incidence of radiation toxicity in cervical cancer and endometrial cancer patients treated with radiotherapy alone versus adjuvant radiotherapy. Rep. Pract. Oncol. Radiother. 2012;17(6):332–8.
[9] Hasselle MD, Rose BS, Kochanski JD, Nath SK, Bafana R, Yashar CM, et al. Clinical outcomes of intensity-modulated pelvic radiation therapy for carcinoma of the cervix. Int. J. Radiat. Oncol. 2011;80(5):1436–45.
[10] Mundt AJ, Lujan AE, Rotmensch J, Waggoner SE, Yamada SD, Fleming G, et al. Intensity-modulated whole pelvic radiotherapy in women with gynecologic malignancies1. Int. J. Radiat. Oncol. 2002;52(5):1330–7.
[11] Chan P, Dinniwell R, Haider MA, Cho Y-B, Jaffray D, Lockwood G, et al. Inter- and intrafractional tumor and organ movement in patients with cervical cancer undergoing radiotherapy: a cinematic-mri point-of-interest study. Int. J. Radiat. Oncol. 2008;70(5):1507–15.

[12] van de Bunt L, Jürgenliemk-Schulz IM, de Kort GAP, Roesink JM, Tersteeg RJHA, van der Heide UA. Motion and deformation of the target volumes during IMRT for cervical cancer: what margins do we need? Radiother. Oncol. 2008;88(2):233–40.
[13] Oh S, Stewart J, Moseley J, Kelly V, Lim K, Xie J, et al. Hybrid adaptive radiotherapy with on-line MRI in cervix cancer IMRT. Radiother. Oncol. 2014;110(2):323–8.
[14] Ahmad R, Bondar L, Voet P, Mens J-W, Quint S, Dhawtal G, et al. A margin-of-the-day online adaptive intensity-modulated radiotherapy strategy for cervical cancer provides superior treatment accuracy compared to clinically recommended margins: a dosimetric evaluation. Acta Oncol. Stockholm Swed. 2013;52(7):1430–6.
[15] Niemierko A. Reporting and analyzing dose distributions: a concept of equivalent uniform dose. Med. Phys. 1997;24(1):103–10.
[16] Niemierko A. A generalized concept of equivalent uniform dose (EUD) [abstract]. Med. Phys. 1999;26:1100.
[17] Lim K, Small Jr W, Portelance L, Creutzberg C, Jürgenliemk-Schulz IM, Mundt A, et al. Consensus guidelines for delineation of clinical target volume for intensity-modulated pelvic radiotherapy for the definitive treatment of cervix cancer. Int. J. Radiat. Oncol. 2011;79(2):348–55.
[18] Alber M, Nüsslin F. An objective function for radiation treatment optimization based on local biological measures. Phys. Med. Biol. 1999;44(2):479–93.
[19] Laub W, Alber M, Birkner M, Nüsslin F. Monte Carlo dose computation for IMRT optimization. Phys. Med. Biol. 2000;45(7):1741–54.
[20] Söhn M, Yan D, Liang J, Meldolesi E, Vargas C, Alber M. Incidence of late rectal bleeding in high-dose conformal radiotherapy of prostate cancer using equivalent uniform dose–based and dose–volume–based normal tissue complication probability models. Int. J. Radiat. Oncol. Biol. Phys. 2007;67(4):1066–73.
[21] Kavanagh BD, Pan CC, Dawson LA, Das SK, Li XA, Ten Haken RK, et al. Radiation dose-volume effects in the stomach and small bowel. Int J Radiat Oncol Biol Phys. 2010;76(3 Suppl):S101–7.
[22] Michalski JM, Gay H, Jackson A, Tucker SL, Deasy JO. Radiation dose-volume effects in radiation-induced rectal injury. Int. J. Radiat. Oncol. 2010;76(3, Supplement):S123–9.
[23] Viswanathan AN, Yorke ED, Marks LB, Eifel PJ, Shipley WU. Radiation dose-volume effects of the urinary bladder. Int. J. Radiat. Oncol. 2010;76(3, Supplement):S116–22.
[24] ICRU. International Commission on Radiation Units and Measurements. In: Prescribing, recording and reporting photon beam intensity-modulated therapy (IMRT). 1-106. Report No.: Report 83.
[25] Sobotta B, Söhn M, Shaw W, Alber M. On expedient properties of common biological score functions for multi-modality, adaptive and 4D dose optimization. Phys. Med. Biol. 2011;56(10):N123–9.
[26] Jensen JLWV. Sur les fonctions convexes et les inegalites entre les valeurs moyennes. Acta Math. 1906;30:175–93.
[27] Niyazi M, Karin I, Söhn M, Nachbichler SB, Lang P, Belka C, et al. Analysis of equivalent uniform dose (EUD) and conventional radiation treatment parameters after primary and re-irradiation of malignant glioma. Radiat. Oncol. London Engl. 2013;8:287.
[28] Alber M, Thorwarth D, In reply to M. Witte: Commenting. Multi-modality functional image guided dose escalation in the presence of uncertainties. Radiother. Oncol. J. Eur. Soc. Ther. Radiol. Oncol. 2015;115(1):150.
[29] Yilmaz C, Gultekin M, Eren G, Yuce D, Yildiz F. Determination of optimal planning target volume margins in patients with gynecological cancer. Phys. Med. 2015;31(7):708–13.
[30] Bondar L, Hoogeman M, Mens JW, Dhawtal G, de Pree I, Ahmad R, et al. Toward an individualized target motion management for IMRT of cervical cancer based on model-predicted cervix–uterus shape and position. Radiother. Oncol. 2011;99(2):240–5.
[31] Shaw W, Rae WI, Alber ML. Equivalence of Gyn GEC-ESTRO guidelines for image guided cervical brachytherapy with EUD-based dose prescription. Radiat. Oncol. 2013;8(1):266.
[32] Wu Q, Mohan R, Niemierko A, Schmidt-Ullrich R. Optimization of intensity-modulated radiotherapy plans based on the equivalent uniform dose. Int. J. Radiat. Oncol. Biol. Phys. 2002;52(1):224–35.